PENSOFT

SENCKENBERG
world of biodiversity

Leibniz Association

Two new *Poyntonophrynus* species (Anura: Bufonidae) highlight the importance of Angolan centers of endemism

Ninda L. Baptista[1,2,3,4,5], Pedro Vaz Pinto[1,3,6], Chad Keates[7,8,9], Javier Lobón-Rovira[1,2,3], Shelley Edwards[7], Mark-Oliver Rödel[5,10]

1 *CIBIO-InBIO, Centro de Investigação em Biodiversidade e Recursos Genéticos, Laboratório Associado, Universidade do Porto, Campus Agrário de Vairão, Rua Padre Armando Quintas, 4485-661 Vairão, Portugal*

2 *Departamento de Biologia, Faculdade de Ciências, Universidade do Porto, 4169-007 Porto, Portugal*

3 *BIOPOLIS Program in Genomics, Biodiversity and Land Planning, CIBIO, Campus de Vairão, 4485-661 Vairão, Portugal*

4 *Instituto Superior de Ciências da Educação da Huíla (ISCED-Huíla), Rua Sarmento Rodrigues, Lubango, Angola*

5 *Museum für Naturkunde – Leibniz Institute for Evolution and Biodiversity Science, Invalidenstr. 43, 10115 Berlin, Germany*

6 *Fundação Kissama, Luanda, Angola*

7 *Zoology and Entomology Molecular Lab, Department of Zoology and Entomology, Rhodes University, Makhanda, South Africa*

8 *South African Institute for Aquatic Biodiversity (SAIAB), Makhanda, South Africa*

9 *Department of Nature Conservation Management, Natural Resource Science and Management Cluster, Faculty of Science, George Campus, Nelson Mandela University, George, South Africa*

10 *Berlin-Brandenburg Institute of Advanced Biodiversity Research – BBIB, Altensteinstr. 34, 14195 Berlin, Germany*

https://zoobank.org/7B5494CC-F8F2-46EA-BB73-D28B13D31CB6

Corresponding author: Ninda L. Baptista (nindabaptista@gmail.com)

Academic editors Raffael Ernst, Uwe Fritz | **Received** 23 March 2023 | **Accepted** 10 October 2023 | **Published** 10 November 2023

Citation: Baptista NL, Vaz Pinto P, Keates C, Lobón-Rovira J, Edwards S, Rödel M-O (2023) Two new *Poyntonophrynus* species (Anura: Bufonidae) highlight the importance of Angolan centers of endemism. Vertebrate Zoology 73 991–1031. https://doi.org/10.3897/vz.73.e103935

Abstract

The pygmy toad genus *Poyntonophrynus* is endemic to southern Africa. The morphology of these small toads is conserved. They are usually dully colored, and are predominately adapted to arid conditions. During recent surveys in Angola we found *Poyntonophrynus* specimens that were not assignable to known species. Using an integrative approach, based on mitochondrial and nuclear DNA, morphology, osteology, biogeography and ecology, we identified three new lineages, and describe two of them as new species. All three lineages are closely related to *P. pachnodes*, an Angolan endemic species, but they are geographically isolated from it. The new species are morphologically distinguishable, and are associated with two of the most important Angolan centers of endemism: the western escarpment and the central highlands. In order to get a more comprehensive understanding of the osteology of the genus, we also provide an osteological characterization of *P. dombensis*, which was not available to date. Our findings i) increase the number of earless species in the genus *Poyntonophrynus*, ii) emphasize southwestern Africa as the cradle of diversification in this genus, iii) report the occurrence of *Poyntonophrynus* in humid environments, thus showing that these toads are ecologically more variable than previously thought, and iv) underline the importance of further biodiversity studies in Angolan centers of endemism.

Keywords

Amphibia, Angolan escarpment, Angolan highlands, character displacement, pygmy toad, sexual dichromatism, speciation, syntopy

Resumo

O sapo-pigmeu do género *Poyntonophrynus* é endémico da África Austral. A morfologia destes pequenos sapos é pouco variável. Estes têm uma coloração geralmente parda, e estão predominantemente adaptados a ambientes áridos. Durante pesquisas recentes em Angola, encontrámos *Poyntonophrynu*s que não correspondiam a nenhuma espécie conhecida. Usando uma abordagem integrativa baseada em DNA mitocondrial e nuclear, morfologia, osteologia, biogeografia e ecologia, identificámos três novas linhagens, duas das quais foram descritas como espécies novas. As três linhagens estão geneticamente próximas de *P. pachnodes*, uma espécie endémica de Angola, mas estão geograficamente isoladas desta espécie. As novas espécies são morfologicamente distintas, e estão associadas a dois dos mais importantes centros de endemismo angolanos: a escarpa e as terras altas. Para contribuir para o conhecimento da osteologia do género, fizemos também uma caracterização osteológica de *P. dombensis*, inexistente até à data. Os nossos resultados i) aumentam o número de espécies sem aparelho auditivo no género *Poyntonophrynus*, ii) reforçam o sudoeste de África como o centro de diversificação deste género, iii) relatam a ocorrência de *Poyntonophrynus* em floresta húmida, revelando que estes sapos são ecologicamente mais variáveis do que se pensava, e iv) realçam a importância de estudos mais aprofundados nos centros de endemismo angolanos.

Palavras-chave

Amphibia, deslocamento de caracteres, dicromatismo sexual, escarpa de Angola, especiação, sapo pigmeu, sintopia, terras altas de Angola

Introduction

Angola is the largest African country south of the Equator and, in spite of the relative paucity of scientific studies, holds some of the richest flora and fauna in the continent (Huntley 2019). The heterogeneity of Angolan geomorphology, pedology, and climate is a major contributor to its diversity, well-illustrated by containing seven out of nine African biomes, and a total of 15 global terrestrial ecoregions (Olson et al. 2001; Burgess et al. 2004; Huntley 2019). Within Angola, local diversity is highest across most taxa in two recognized centers of endemism: the western escarpment and the Angolan highlands (Hall 1960; Huntley and Matos 1994; Linder et al. 2012; Cáceres et al. 2017; Huntley 2019). Contrasting to its biological importance, the diversity of the western escarpment is still poorly known (Hall 1960; Huntley 2019). The escarpment corresponds broadly to a transition zone separating the semi-arid coastal plain from the elevated plateau and highlands; it comprises mainly forest and dense woodland (Huntley 2019). The Angolan highlands are mostly situated in central Angola (central highlands) and comprise areas above 1600 m a.s.l., often rising over 2200 m a.s.l. Habitats include relict and highly fragmented patches of Afromontane forests in deep ravines surrounded by montane grasslands, usually bordering mountain peaks. Included within the Angolan highlands are the isolated Humpata plateau further south (southern highlands), and inselbergs on the coastal plain, of which the most notable is Serra da Neve (Huntley 2019), reaching 2489 m a.s.l. These isolated highlands have a complex geomorphology, characterized by rocky substrates with outcrops of different geologic origins (Huntley 2019), features that due to their patchy occurrence can enhance speciation. However, similar to other regions in Angola, these endemism centers are poorly studied, and new endemic species are expected to be found (Clark et al. 2011; Huntley 2019).

Pygmy toads of the genus *Poyntonophrynus* are habitat specialists, with many species being rupicolous, inhabiting granite outcrops in dry and sandy areas (du Preez and Carruthers 2017; Tracy 2021). This genus is morphologically conserved, with small, flattened, and usually dully-colored toads. Species within the genus are thus hard to tell apart by external morphology (Poynton and Broadley 1988; du Preez and Carruthers 2017; Channing and Rödel 2019). Currently, 13 species are recognized (Frost 2023; Rödel et al. 2023); four of which have been recorded from Angola: *P. pachnodes* Ceríaco et al., 2018, endemic to Serra da Neve; *P. dombensis* (Bocage, 1895) and *P. grandisonae* (Poynton & Haacke, 1993), from the arid coastal plains of the Namib Desert in south-western Angola; and *P. kavangensis* (Poynton & Broadley, 1988), from Kalahari sands in the inland plateau. Except for the latter, all species occurring in Angola are strongly associated with rocky environments (Poynton and Haacke 1993; Ceríaco et al. 2018).

Several taxonomic questions are associated with *Poyntonophrynus*. At the genus level, the separation between *Poyntonophrynus* and *Mertensophryne* is not resolved, neither by genetics, nor by osteology or morphology. As far as is currently understood, *Poyntonophrynus* is not monophyletic, with one species, *P. lughensis* (Loveridge, 1932), assignable to *Mertensophryne* (Liedtke et al. 2017; Ceríaco et al. 2018; Tracy 2021). Osteological synapomorphies are also not known for the genus. Some members, such as *P. pachnodes*, have morphological traits that were previously considered characteristic for *Mertensophryne*, e.g. the absence of the tympanic middle ear (Ceríaco et al. 2018). The same applies to qualitative

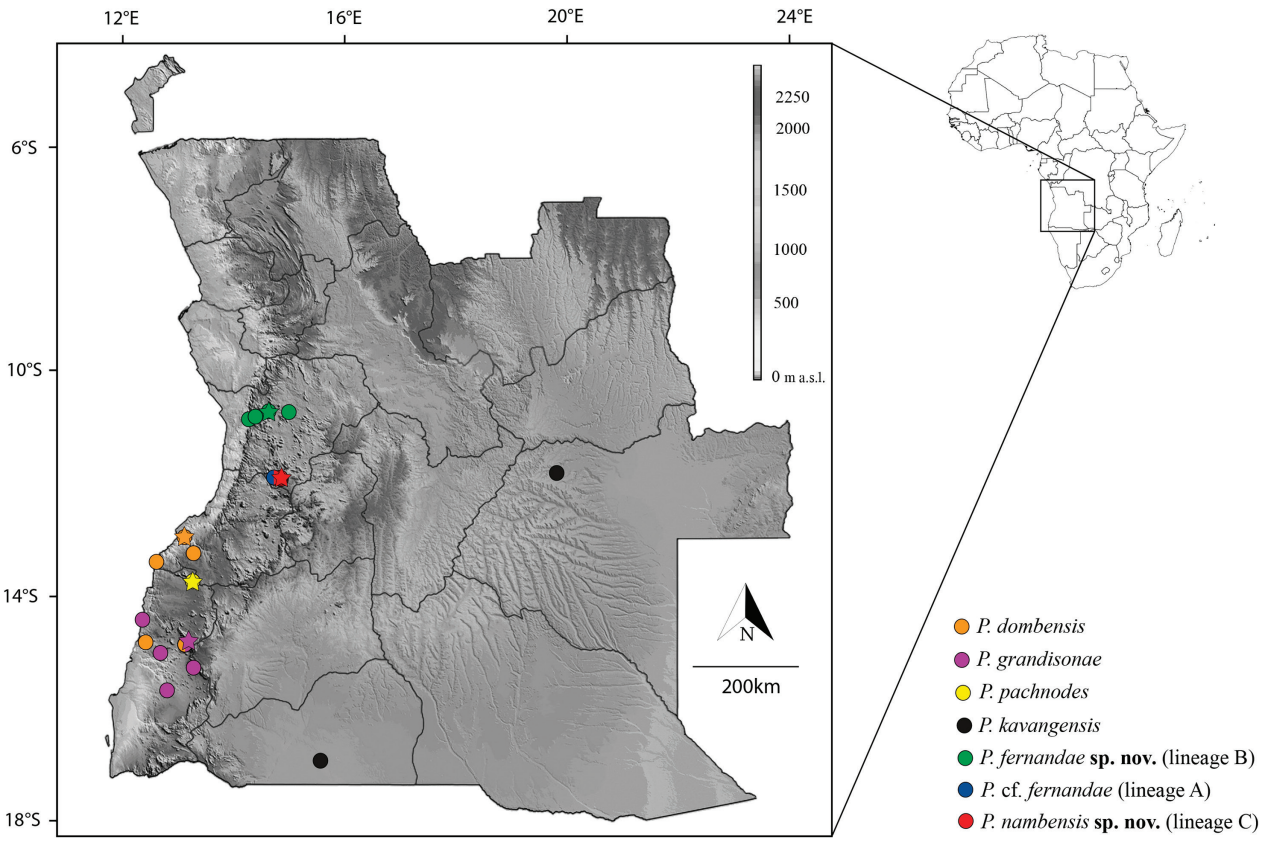

Figure 1. Map of Angola showing records of all known *Poyntonophrynus* taxa from the country, including vouchers examined in this study and historical records. Circles depict recorded sites, stars depict type localities.

morphological characters (e.g., double subarticular tubercles, conspicuousness of tympanum and parotoid glands) defined for *Poyntonophrynus* (Ceríaco et al. 2018; Tracy 2021), but not applicable to all species (e.g., du Preez and Carruthers 2017). At the species level, identification is likewise difficult (Poynton and Broadley 1988), often leading to questioning species' validity (Frost 2023; Rödel et al. 2023).

South-western Africa is considered as the cradle of diversity of *Poyntonophrynus* (Ceríaco et al. 2018; Tracy 2021), consequently being the most important region to study the genus' diversification. In the last decade, surveys in central-western Angola detected *Poyntonophrynus* populations in the Angolan escarpment and central highlands (Fig. 1), not assignable to any known species. To assess their taxonomic status, we herein used an integrative approach based on molecular, morphological, and osteological data.

Methods

Sampling

Between 2016 and 2021, extensive herpetological surveys were conducted on the Angolan highlands and escarpment, targeting amphibians in the rainy season. These efforts led to the detection and collection of 25 specimens from previously unknown populations of *Poyntonophrynus* in both regions. In addition, we collected five pygmy toads from the coastal plain and the inselberg of Serra da Neve (Fig. 1). Specimens were euthanized by being placed in a lethal solution of tricaine methanesulfonate (MS222; American Veterinary Medical Association 2020). Afterwards, the toads were fixed in either 10% formalin, or 96% ethanol, and thereafter transferred to 70% ethanol for permanent storage. Liver or muscle tissue was collected before fixation in 10% formalin and preserved in 96% ethanol. Specimens examined were deposited in the British Museum of Natural History (**BMNH**, London, United Kingdom), the Colecção Herpetológica do Lubango currently in Instituto Superior de Ciências da Educação da Huíla (**CHL**, ISCED – Huíla, Lubango, Angola), the Fundação Kissama-Holísticos collection (**FKH**, Luanda, Angola), and the Museum für Naturkunde (**ZMB**, Berlin, Germany).

Molecular methods

Dataset

The phylogenetic relationships of samples of *Poyntonophrynus* were estimated using genetic information from 45 specimens, covering multiple newly sampled localities across Angola, and other parts of southern Africa (Table 1). Our new tissue samples were supplemented with samples from the herpetological collection of the Port Elizabeth Museum (**PEM**, Port Elizabeth, South Africa). In addition to the new sequences produced for this project, the dataset was supplemented with 11 *Poyntonophrynus* sequences

Table 1. List of *Poyntonophrynus* and other toad genera vouchers examined in this study and their associated metadata. Catalogue numbers of holotypes in bold. NA – not available.

Species	Catalogue number	Field number	Country, locality	Latitude	Longitude	12S	16S	COI	RAG1
Poyntonophrynus fernandae **sp. nov.** (lineage B)	BMNH 2021.7535	EI-0704	Angola, Quibala	–10.7399	14.979755	OR692225	OR692259	OR717565	OR698990
Poyntonophrynus fernandae **sp. nov.** (lineage B)	FKH 1086	EI-0725	Angola, Quibala	–10.7399	14.979755	OR692226	OR692260	OR717566	OR698991
Poyntonophrynus fernandae **sp. nov.** (lineage B)	BMNH 2021.7534	NB0431	Angola, Congulo	–10.883889	14.271667	OR692238	OR692272	OR717578	OR699003
Poyntonophrynus fernandae **sp. nov.** (lineage B)	ZMB 91790	NB0805	Angola, Condé	–10.746667	14.629444	OR692232	OR692266	OR717572	OR698997
Poyntonophrynus fernandae **sp. nov.** (lineage B)	ZMB 91791	NB0806	Angola, Condé	–10.746667	14.629444	OR692233	OR692267	OR717573	OR698998
Poyntonophrynus cf. *fernandae* (lineage A)	BMNH 2021.7536	P0-34	Angola, Chinhundo	–11.914685	14.740552	OR692249	OR692283	OR717589	OR699013
Poyntonophrynus cf. *fernandae* (lineage A)	ZMB 91785	P0-36	Angola, Chinhundo	–11.914685	14.740552	OR692251	OR692285	OR717591	OR699015
Poyntonophrynus cf. *fernandae* (lineage A)	ZMB 91786	NB0454	Angola, Chinhundo	–11.914685	14.740552	OR692229	OR692263	OR717569	OR698994
Poyntonophrynus cf. *fernandae* (lineage A)	FKH-0463	P0-38	Angola, Chinhundo	–11.914685	14.740552	OR692253	OR692287	OR717593	OR699017
Poyntonophrynus nambensis **sp. nov.** (lineage C)	**ZMB 91787**	NB0456	Angola, Fazenda Namba	–11.914167	14.820556	OR692230	OR692264	OR717570	OR698995
Poyntonophrynus nambensis **sp. nov** (lineage C)**.**	ZMB 91788	NB0457	Angola, Fazenda Namba	–11.914167	14.820556	OR692231	OR692265	OR717571	OR698996
Poyntonophrynus nambensis **sp. nov.** (lineage C)	ZMB 91789	P0-35	Angola, Chinhundo	–11.914685	14.740552	OR692250	OR692284	OR717590	OR699014
Poyntonophrynus nambensis **sp. nov.** (lineage C)	FKH-0457	P0-32	Angola, Chinhundo	–11.914685	14.740552	OR692247	OR692281	OR717587	OR699011
Poyntonophrynus nambensis **sp. nov.** (lineage C)	FKH-0458	P0-33	Angola, Chinhundo	–11.914685	14.740552	OR692248	OR692282	OR717588	OR699012
Poyntonophrynus nambensis **sp. nov.** (lineage C)	FKH-0462	P0-37	Angola, Chinhundo	–11.914685	14.740552	OR692252	OR692286	OR717592	OR699016
Poyntonophrynus nambensis **sp. nov.** (lineage C)	FKH-0377	JLRZC0027	Angola, Missão da Namba	–11.922078	14.835542	OR692243	OR692277	OR717583	OR699007
Poyntonophrynus nambensis **sp. nov.** (lineage C)	N/A (not collected)	JLRZC0012	Angola, Missão da Namba	–11.922078	14.835542	OR692242	OR692276	OR717582	OR699006
Poyntonophrynus nambensis **sp. nov.** (lineage C)	FKH-0378	JLRZC0028	Angola, Missão da Namba	–11.922078	14.835542	OR692244	OR692278	OR717584	OR699008
Poyntonophrynus nambensis **sp. nov.** (lineage C)	FKH-0380	JLRZC0030	Angola, Fazenda Namba	–11.914167	14.820556	OR692245	OR692279	OR717585	OR699009
Poyntonophrynus nambensis **sp. nov.** (lineage C)	FKH-0381	JLRZC0031	Angola, Fazenda Namba	–11.914167	14.820556	OR692246	OR692280	OR717586	OR699010
Poyntonophrynus beiranus		HF 30	Mozambique, Taratibu			KY555625	KY555650	KY555665	KY555721
Poyntonophrynus dombensis		AG 117	Angola, Meva Bay	–13.414444	12.579167	OR692222	OR692256	OR717562	OR698988
Poyntonophrynus dombensis		AG 118	Angola, Meva Bay	–13.414444	12.579167	OR692223	OR692257	OR717563	

Species	Catalogue number	Field number	Country, locality	Latitude	Longitude	12S	16S	COI	RAG1
Poyntonophrynus dombensis		AG 120	Angola, Meva Bay	–13.414444	12.579167	OR692224	OR692258	OR717564	OR698989
Poyntonophrynus dombensis	ZMB 91792	JLRZC0086	Angola, Mariquita	–14.853229	12.396146	OR692239	OR692273	OR717579	OR699004
Poyntonophrynus dombensis	FKH-0406	JLRZC0087	Angola, Mariquita	–14.853229	12.396146	OR692240	OR692274	OR717580	OR699005
Poyntonophrynus dombensis	ZMB 91793	JLRZC0088	Angola, Mariquita	–14.853229	12.396146	OR692241	OR692275	OR717581	
Poyntonophrynus dombensis		damaB	Namibia, Brandberg			AF220857	AF220905		
Poyntonophrynus dombensis		damaA	Namibia, Brandberg				AF220906		
Poyntonophrynus fenoulheti		fenoB	South Africa, Kranzkop			OR692227	OR692261	OR717567	OR698992
Poyntonophrynus fenoulheti		fenoC	South Africa, Mashatu			OR692228	OR692262	OR717568	OR698993
Poyntonophrynus fenoulheti	AACRG 1598		South Africa, Phalaborwa			KF664732	KF665265	KF665592	KF666249
Poyntonophrynus fenoulheti	AACRG 1599		South Africa, Phalaborwa			KF664816	KF665081	KF665728	KF666357
Poyntonophrynus fenoulheti		fenoA	South Africa, Mkuze			AF220859	AF220908		
Poyntonophrynus grandisonae	CHL 0903	NB903	Angola, Chapéu Armado	–14.45	12.35	OR692254	OR692288		
Poyntonophrynus grandisonae	FKH-0533	P1-20	Angola, SSW Bibala	–14.856899	13.158968	OR692255	OR692289		OR699018
Poyntonophrynus grandisonae		AMB 10337	Angola, Dolondolo, Serra da Neve	–13.77704	13.25905		MH469716		MH469717
Poyntonophrynus damaranus		BP-001	Namibia, Ondobe			KY555627	KY555648	KY555658	
Poyntonophrynus lughensis		VG001	Kenya, NW of Laisamis, Kaisut Desert			KY555626	KY555641	KY555659	KY555723
Poyntonophrynus pachnodes	**UF 184184**	pachA	Angola, Serra da Neve	–13.77704	13.25905		MH469718		MH469719
Poyntonophrynus pachnodes	FKH-0878	JLRZ0241	Angola, Serra da Neve	–13.758650	13.225194		OR692290		OR699019
Poyntonophrynus pachnodes	FKH-0879	JLRZ0242	Angola, Serra da Neve	–13.758650	13.225194		OR692291		OR699020
Poyntonophrynus vertebralis	PEM A11496	WC-3458	South Africa, Commando Drift Nature Reserve	–32.111944	26.03750	OR692234	OR692268	OR717574	OR698999
Poyntonophrynus vertebralis	PEM A11498	WC-3460	South Africa, Commando Drift Nature Reserve	–32.111944	26.03750	OR692235	OR692269	OR717575	OR699000
Poyntonophrynus vertebralis	PEM A11497	WC-3459	South Africa, Commando Drift Nature Reserve	–32.111944	26.03750	OR692236	OR692270	OR717576	OR699001
Poyntonophrynus vertebralis	PEM A09669	WC-DNA-181	South Africa, 4km on Doornfontein Rd of the R61	–32.025581	25.319722	OR692237	OR692271	OR717577	OR699002
Poyntonophrynus vertebralis		vertA	South Africa, NA			AF220860			
Capensibufo rosei		KTH09-335	South Africa, Silvermine, WC			KF664868	KF665294	KF665706	KF666159
Mertensophryne lindneri	BM 2002.394		Tanzania, Ruvu South			KF664736	KF665426	KF665790	KF666333
Mertensophryne howelli		MTSNT2202	Tanzania, Zanzibar Island, Kiwenga Forest			KF664736	KF665426	KF665790	KF666333
Mertensophryne anotis		HF3	Mozambique, Taributo			KY555630	KY555643	KY555662	KY555712
Vandijkophrynus angusticeps		AC2692	South Africa, Stellenbosch			KF664791	KF665432	KF665693	KF666237
Vandijkophrynus gariepensis		VC178	South Africa, Die Hel Rd			KF664828	KF665376	KF665613	KF666339
Vandijkophrynus robinsoni		AACRG 0068	South Africa, Northern Cape			KF664648	KF665375	KF665788	KF666198
Poyntonophrynus damaranus		FB.Po.D1	Namibia, Okonjima	–20.8592	16.6408		OR692292		OR699021
Poyntonophrynus hoeschi		FB 341	Namibia, Windhoek, Avis Dam	–22.5726	17.1333		ON510295		OR699022
Poyntonophrynus grindleyi	ZMB 90082		Mozambique, Chimanimani Mts	–19.7637	33.0881		ON510296		ON623708
Poyntonophrynus damaranus	NMNW 11200		Namibia, Okonjima	–20.8592	16.6408		OR692293		OR699023
Poyntonophrynus damaranus	NMNW 11187		Namibia, Gobabis dist, Farm Marne	–22.4184	18.854		OR692294		OR699024
Poyntonophrynus hoeschi	NMNW 11197		Namibia, Windhoek, Avis Dam	–22.5726	17.1333		ON510300		ON623709
Poyntonophrynus damaranus	NMNW 11198		Namibia, Okonjima	–20.8592	16.6408		OR692295		
Poyntonophrynus damaranus	NMNW 11188		Namibia, Gobabis dist, Farm Marne	–22.4184	18.854		OR692296		
Poyntonophrynus damaranus	NMNW 11186		Namibia, Gobabis dist, Farm Marne	–22.4184	18.854		ON510304		

Table 2. Primers and PCR protocols used to generate sequences for this study.

Gene	Primer	Length (bp)	Source	Annealing temperature (°C)	Cycles
12S	L1091: 5'-AAAAAGCTTCAAACTGGGATTAGATACCCCACTAT-3' R1478: 5'-TGACTGCAGAGGGTGACGGGCGGTGTGT-3'	367	Kocher et al. (1989); Liedtke et al. (2017)	58	35
16S	L2510: 5'-CGCCTGTTTATCAAAAACAT-3' H3080: 5'-CCGGTCTGAACTCAGATCACG7-3'	542	Palumbi (1996)	50–52	35
COI	P3F: 5'-CAATACCAAACCCCCTTRTTYGTWTGATC-3' P3R: 5'-GCTTCTCARATAATAAATATYAT-3'	771	San Mauro et al. (2004); Liedtke et al. (2017)	42	35
RAG1	RAG1.Mart.FL1: 5'-AGCTGCAGYCARTAYCAYAARATGTA-3' RAG1.AMP.R1: 5'-AACTCAGCTGCATTKCCAATRTCA-3'	867	Páez-Moscoso and Guayasamin (2012); Liedtke et al. (2017)	54–55	35

from GenBank. Sequences from seven closely related taxa were used as outgroups (Table 1).

Extraction, amplification and sequencing

A standard salt extraction (Bruford et al. 1992) was used to isolate DNA from tissues using lysis (Buffer ATL; Qiagen) and elution (Buffer AE; Qiagen) buffers. Standard PCR procedures were utilized to amplify two partial mitochondrial ribosomal genes (12S rRNA [12S] and 16S rRNA [16S]), one partial mitochondrial gene (Cytochrome c Oxidase Subunit I [COI]) and one partial nuclear gene (Recombination Activating Gene 1 [RAG1]) (Table 2). Details about the primer pairs and PCR protocols can be found in Table 2. Amplification was carried out using 20–50 ng/µl extracted genomic DNA with a total PCR mixture volume of 25 µl. Each PCR contained 12.5 µl TopTaq Mastermix (Qiagen; containing 10x PCR buffer, 1.5 mM $MgCl_2$, 0.2 mM dNTPs, and 0.75 U Taq polymerase), 2 µl forward primer (10 µM), 2 µl reverse primer (10 µM), and 8.5 µl of the genomic DNA and de-nucleated water combined. The standard cycling profile comprised of an initial denaturing step at 94°C for 5 min, followed by 35–37 cycles of 94°C for 30 s, 42–58°C for 45 s, and 72°C for 45 s, with a final extension at 72°C for 8 min. The annealing temperature and number of cycles used for the differing primers can be found in Table 2. The final PCR products were sequenced (after purification) by Macrogen Corp. in Amsterdam, Netherlands with the forward primers only.

Phylogenetic analysis

The sequence trace files were checked using BioEdit Sequence Alignment Editor v.7.2.5 (Hall 1999) and aligned with MEGA v.7.0 (Kumar et al. 2016) which currently contains facilities for building sequence alignments, inferring phylogenetic histories, and conducting molecular evolutionary analysis. In version 6.0, MEGA now enables the inference of timetrees, as it implements the RelTime method for estimating divergence times for all branching points in a phylogeny. A new Timetree Wizard in MEGA6 facilitates this timetree inference by providing a graphical user interface (GUI, using ClustalW plugin function, along with the sequences acquired from GenBank. Four individual gene trees were created in MEGA using the Maximum Likelihood (ML) algorithm, 100 bootstrap replicates and the GTR+G+I nucleotide substitution model. Congruency of the different genes was tested using the Congruence Index (de Vienne et al. 2007). However, this approach requires a lot of computational work (human and machine). All gene-tree combinations were found to be congruent and a concatenated dataset of the four genes was created for additional phylogenetic analyses.

The individual, and the first and second combined codon positions, were tested separately for saturation using DAMBE v.6.4.67 (Xia 2013) data analysis for molecular biology and evolution (DAMBE, and saturation was found to be absent. The optimal scheme and best-fitting models of molecular evolution were selected using ModelFinder, implemented in IQ-TREE v.2.1.2 (Minh et al. 2021), with the following settings: -p partition file (each partition has own evolution rate), a greedy strategy and the FreeRate heterogeneity model excluded (only invariable site and Gamma rate heterogeneity considered) (Chernomor et al. 2016; Kalyaanamoorthy et al. 2017). The best-fitting model scheme resulted in three partitions: GTR+I+G (12S, 16S); TPM2+G (COI); GTR+I+G (RAG1). MrBayes v.3.2.7a (Ronquist et al. 2012) was not able to implement TPM2, so the next best alternative (GTR) was used in its place.

Phylogenetic reconstruction

Maximum likelihood (ML) analysis was conducted using IQ-TREE v.2.1.2 (Nguyen et al. 2015)especially for maximum-likelihood (ML. The ML analysis was implemented using a random starting tree and assessed using the ultra-fast bootstrap approximation (UFBoot) method (Hoang et al. 2018) and 1000 bootstrap replicates. Bayesian Inference (BI) analysis was conducted using MrBayes v.3.2.7a (Ronquist et al. 2012) and implemented on the CIPRES Science Gateway XSEDE online resource (http://www.phylo.org; Miller et al. 2010; Tamura et al. 2013). Two parallel runs of 20 million generations were performed, with trees being sampled every 1000 generations, using BEAGLE. *Capensibufo rosei* (Hewitt, 1926) was set as the outgroup. Tracer v.1.6.0. (Rambaut and Drummond 2009) was used to determine the number of generations that should be discarded as burn-in. Using a burn-in of 15%, the effective sample size (ESS) was above 200 for all parameters and the runs reached con-

vergence, indicating that the burn-in was adequate. Both trees were viewed in Figtree v.1.4.2 (Rambaut 2014).

Species delimitation of Poyntonophrynus

Based on the findings from the initial phylogenetic tree, *Poyntonophrynus* was investigated using species delimitation analyses to determine whether the genus harbours unappreciated species diversity. Outgroup taxa were removed, leaving only members of *Poyntonophrynus* [excluding *P. lughensis* (Loveridge, 1932)] for single locus species delimitation. The 16S gene was chosen as it had the best representation across the genus. Automatic Barcode Discovery (ABGD), Assemble Species by Automatic Partitioning (ASAP), Poisson Tree Processes (PTP), and Pairwise Distance Thresholds (PDT) were used to determine whether the topological structuring and novel sequences from previous phylogenies constitute separate species.

Firstly, a 16S alignment was created and uploaded onto the ABGD web interface (abgd web (mnhn.fr), web version 07 July 2022) and the ASAP Web Interface (ASAP web (mnhn.fr), web version 07 July 2022). For ABGD, the following settings were used: standard p-distance metrics, minimum barcode gap width (1.5), intraspecific divergence minima (0.001) and maxima (0.1). For ASAP, the Simple Distance (p-distances) substitution model was used. Secondly, a 16S ML tree was created in IQTREE using the GTR + G substitution model and the same settings implemented in the multi-locus phylogeny. The phylogeny was rendered as a newick file, using Figtree, and uploaded unrooted onto the bPTP web server (http://species.h-its.org/ptp; Zhang et al. 2013) for PTP analysis. Lastly pairwise distance analysis was conducted on the 16S alignment, using MEGA X v.10.1.7. (Kumar et al. 2018). The following settings were used: standard uncorrected p-distance model, uniform rates, pairwise deletion, and 500 bootstraps. The samples were grouped according to specific affiliation and the intra- and interspecific distances separating samples was tabulated. Finally, the results from ABGD, ASAP and PTP were overlaid on the multi-locus phylogeny.

Haplotype Network

A haplotype network was created using the RAG1 marker (785 bp) to elucidate the population structuring of the Angolan *Poyntonophrynus* using all available sequences. Sequences with more than 10% missing data (ambiguous nucleotide positions), were removed from the analysis, resulting in 37 sequences being retained for the analysis, each of which 785 base pairs long. A median-joining haplotype network (Bandelt et al. 1999) was created using the nuclear marker in PopART v.1.7 (http://popart.otago.ac.nz; Leigh and Bryant 2015).

Morphology

Measurements were obtained from a total of 42 *Poyntonophrynus* specimens exclusively collected in Angola. Definitions and terminology were adapted from Ceríaco et al. (2018), and were taken by NLB under a dissecting microscope (Zeiss Stemi SV 6, Jena, Germany) with an electronic calliper (accurate to 0.01 mm, rounded to 0.1 mm). All measurements were performed three times, and the average value was registered. All measurements were performed on the right side of specimens, except when not possible (e.g., damaged finger or toe, tympanum not visible), in which case these measures were taken from the left side. The following measurements were taken: snout–vent length (SVL, from tip of snout to vent); head width (HW, maximum head width); head length (HL, from the maxillary commissure to the snout tip, measured along the jaw (not parallel to the longitudinal axis of the animal); interorbital distance (IOD, shortest distance between the anterior corners of the orbits); eye diameter (ED, horizontally from the anterior to posterior corners of the eye); internarial distance (IND, shortest distance between the inner margins of the nostrils); eye–nostril distance (END, from the anterior corner of the eye to the posterior margin of the naris); horizontal tympanum diameter (TDH, greatest horizontal width of the tympanum); vertical tympanum diameter (TDV, greatest vertical width of the tympanum); upper eyelid width (UEW, greatest width of the upper eyelid margins, measured perpendicular to the anterior-posterior axis); snout length (SL, from the tip of the snout to the anterior corner of the eye); snout-nostril length (NS, from the center of the external nares to the tip of the snout); thigh length (THL, from the vent to the knee); tibiofibula length (TL, from the outer surface of the flexed knee to the heel/tibiotarsal inflection); tarsal length (TaL, from the base of the inner metatarsal tubercle to the tarsal–tibiofibular articulation); foot length (FL, from the base of the inner metatarsal tubercle tip of the longest toe); toe IV length (Toe4L, from the inner metatarsal tubercle to the tip of toe IV); inner metatarsal tubercle (IMTL, maximum length); upper arm length (UAL, from the radioulna–humeral articulation to the trunk, measured along the posterior aspect of the arm); forearm length (FLL, from the flexed elbow to the base of the outer palmar tubercle); hand length (HAL, from the base of the outer palmar tubercle to the tip of the longest finger); finger III length (Fin3L, from the proximal edge of the palmar tubercle to the tip of finger III).

Females were identified based on the presence of eggs, visible through transparent skin, eggs detectable by a hard and rounded belly, or eggs seen after dissection. Males were identified by the presence of nuptial pads consisting of a dense covering of minute, often dark, asperities on upper and inner surfaces of first and second fingers and inner metacarpal tubercle, sometimes only visible under a dissecting microscope. Specimens lacking these obvious male or female features were classified as of 'unidentified sex'. Qualitative features such as conspicuousness of tympanum and parotoid glands may be affected by the preservation of specimens, and classification may differ between observers. Moreover, terminology regarding skin features (e.g. asperities, granules, rosettes, spines, spinose warts, spinules, tubercles, warts), or characterization of skin texture (e.g. granular, leathery, rough, ru-

gose, smooth, warty), varies between authors (e.g. Hewitt 1932; Poynton and Broadley 1988; Poynton and Haacke 1993; du Preez and Carruthers 2017; Ceríaco et al. 2018). For this reason, we compared available information (descriptions and photographs) of several *Poyntonophrynus* species (e.g., Bocage 1895; Poynton and Broadley 1988; Poynton and Haacke 1993; du Preez and Carruthers 2017; Ceríaco et al. 2018; Channing and Rödel 2019) with specimens deposited in the ZMB, BMNH and FKH collections (Tables 1, S1). The description of qualitative features was then adapted as explained below, not always being in agreement with previous classifications (e.g. Ceríaco et al. 2018). Tympanum: i) conspicuous: tympanum and tympanic ring can be clearly seen; ii) visible: tympanum and tympanic ring visible but hard to detect; iii) not visible: tympanum not visible even under dissecting microscope and varying light conditions. Parotoid glands: i) conspicuous: with clear limits, and/or a different coloration when compared to adjacent skin; ii) elevated: considerably protruding in relation to adjacent skin; iii) flattened: not very prominent in relation to adjacent skin. Terminology related to skin and coloration features follows Poynton and Broadley (1988), and Peters (1964): i) spines: minutely spinose surface, conical (on dorsum) or more flattened (on venter); ii) rough skin: skin surface covered in spines; iii) nuptial pads: minute asperities on upper and inner surfaces of first and second fingers and inner palmar tubercle creating a roughened, often dark area in male frogs (presence of character associated with breeding conditions); iv) granular: skin texture resembling tiny grains, characteristic in bufonids (du Preez and Carruthers 2017); v) glandular warts: raised skin glands, similar to parotoid glands, but smaller in size. Numbering of fingers and toes, and nomenclature of hand and feet tubercles follow Peters (1964).

Morphometric analysis

Only data from adult specimens were used for the morphometric analysis. Following Hayek et al. (2001), measurements more prone to vary with preservation status and/or landmark choice were not included in the morphometric analysis (i.e.: ED, IOD, UEW, Fin3L, UAL, Toe4L, TaL, FL, HAL). Small sample sizes precluded tests for statistical significance in some comparisons. Boxplots of relevant body ratios (SVL/FLL, SVL/TL, SVL/HL) were produced. A Principal Components Analysis (PCA) on the residuals of linear regressions of 11 $\log_{10}$-transformed measurements and SVL was conducted, using the *prcomp* function of the *stats*, and visualized using the *autoplot* function of the *ggplot2* package. Analysis and plots were conducted using R v.4.2.1 and R Studio v. 2022.2.3.492 (R Core Team 2021; RStudio Team 2022).

Osteology

Skulls and entire bodies of five females and four males of some of the recently collected *Poyntonophrynus* specimens, including populations from unidentified species and from *P. dombensis*, were analyzed in detail (list of examined vouchers in Table S2). These frogs were compared to the anatomy of *P. pachnodes* (Ceríaco et al. 2018), the only other *Poyntonophrynus* species from Angola, for which there is detailed osteological information. High Resolution X-ray Computed Tomography (HRCT) were performed at the CT Scanner Facility at the Museum für Naturkunde Berlin, using a General Electric Nanotom S system and following the parameters listed in Table S2. 3D segmentation models were generated and colored for the articulated skull and body in Avizo Lite 2020.2 (Thermo Fisher Scientific 2020) and deposited in Morphosource (www.morphosource.org; Project ID 450493; Table S2). Annotations were made in Adobe Illustrator CC 22.0.1 (Adobe Systems Incorporated 2017). Osteological terminology follows Ceríaco et al. (2018), Scherz (2020) for squamosum characterization, and Fabrezi (2001) and Deforel et al. (2021) for prepollex and prehallux characterization.

Results

Phylogenetic relationships and haplotype network analyses

Both the BI and ML algorithm revealed identical topologies for *Poyntonophrynus* with varying levels of nodal support. Whilst the ML algorithm lacked strong support at the deeper nodes, both algorithms found strong support at the inter-species and intra-lineage levels. In addition to the described species, both algorithms recovered three novel lineages: A, B, and C and *Mertensophryne* nested within *Poyntonophrynus*. The phylogenetic tree illustrates that all three novel Angolan lineages (A–C) are closest related to *P. pachnodes* (Fig. 2). Lineages A, B and *P. pachnodes* differed among each other by low 16S pairwise distances (2–3.5%), while lineage C had high 16S pairwise distances compared to these three (8.1–9%) (Table 3). Altogether, lineages A, B and C differed from the other *Poyntonophrynus* species by between 6.1–11.6%. They were more closely related to *P. grindleyi* and *P. hoeschi* (6.1–6.9%), followed by *P. fenoulheti* (7.2–7.8%), *P. vertebralis* (7.9–8.9 %), *P. damaranus* and *P. dombensis* (8.5–9.5%), *P. grandisonae* (9.8–11.6%), and *P. beiranus* (10.5–11.6%).

The network for the RAG1 nuclear marker (Fig. 3) recovered a topology similar to the phylogenetic reconstruction, with each new lineage occupying a distinct haploclade. No haplotype sharing was found between the Angolan lineages. This could indicate a lack of gene flow, but it must be noted that missing data (ambiguous nucleotide positions), especially within the Angolan sequences, may have partially influenced the topology of the haplotype network.

The single-locus species delimitation methods retrieved varying numbers of putative taxa. ABGD, ASAP and PTP analysis recognized 14, 19, 16 species, respectively (Fig. 2). Lineage C was recovered as a potential

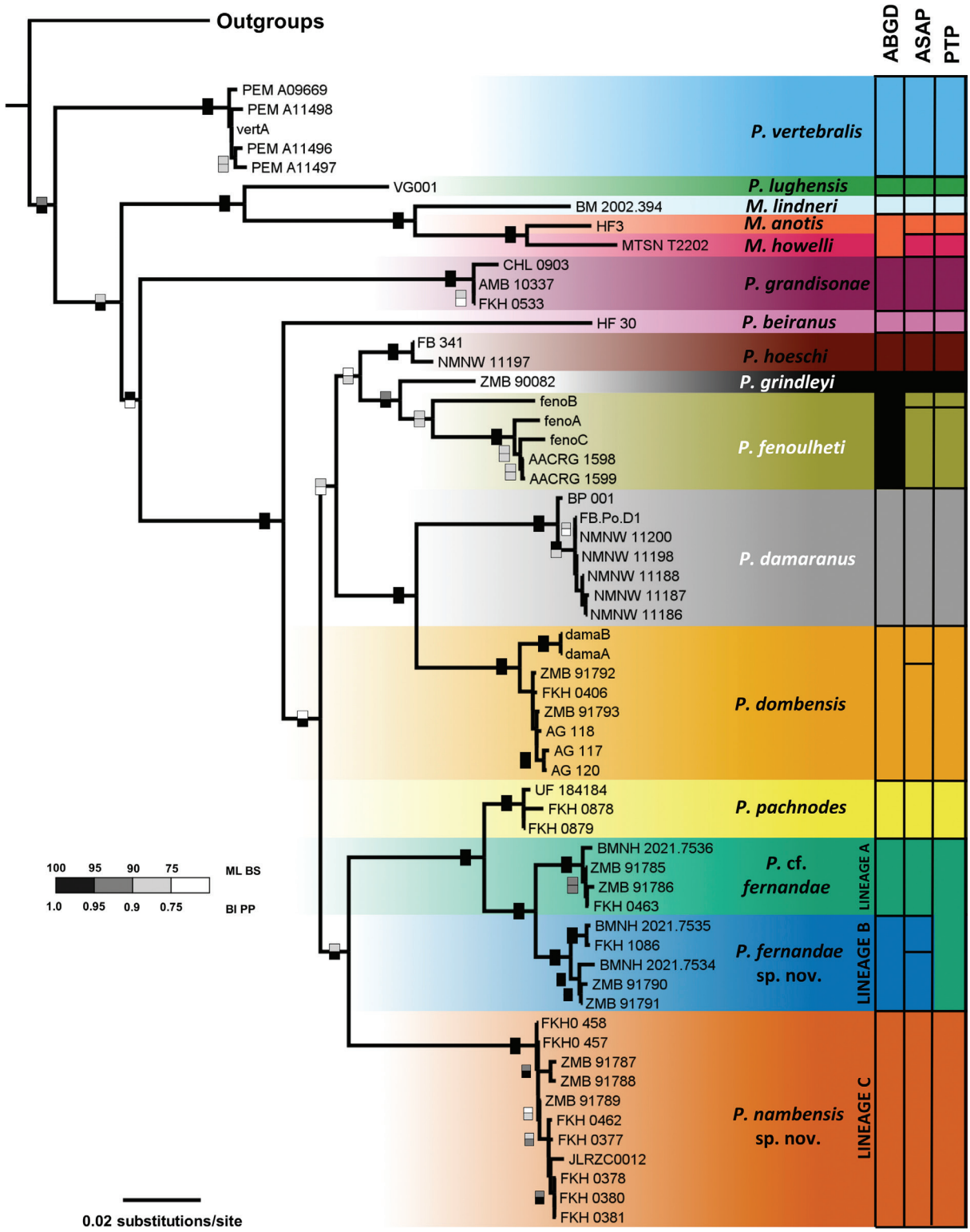

Figure 2. Maximum Likelihood multi-locus (12S, 16S, COI, RAG1) phylogenetic tree of *Poyntonophrynus* and *Mertensophryne* with Bayesian Inference multi-locus support overlaid. The bars to the right of the phylogeny represent the putative taxa assignments from the single locus species delimitation methods employed on the 16S dataset.

species by all three methods, whilst lineages A and B were not recognized as potential species by PTP. ASAP was the most liberal method, recognising all new lineages as potential species.

Throughout the entire genus sampling, the various species delimitation methods highlighted either an under-appreciation or over-appreciation of species diversity as currently understood. Both ASAP and PTP recognized a cryptic species within *P. fenoulheti*, whilst ASAP recovered an unrecognized species within *P. dombensis*. Whilst not the focus of this study, *P. fenoulheti* should be investigated in further detail in future studies to elucidate the most accurate taxonomical structuring of the species.

Table 3. Sequence divergence (uncorrected average pairwise distance values, expressed in percentages) for the examined portion of the mitochondrial 16S gene, for all available *Poyntonophrynus* species and several species of *Mertensophryne*. Numbers in diagonal (in bold) denote intraspecific divergences, numbers below the diagonal denote interspecific divergences, and numbers above the diagonal denote the standard error of the interspecific divergences. NA–Not Available.

		1	2	3	4	5	6	7	8	9	10	11	12	13	14	15
1	*P. beiranus*	**NA**	1.27	1.20	1.21	1.44	1.27	1.24	1.38	1.42	1.43	1.37	1.29	1.35	1.31	1.30
2	*P. damaranus*	9.60	**2.61**	0.81	1.04	1.32	1.04	0.99	1.23	1.24	1.20	1.14	1.24	1.28	1.31	1.37
3	*P. dombensis*	8.90	5.90	**3.54**	0.96	1.26	0.93	0.92	1.16	1.21	1.16	1.15	1.15	1.24	1.23	1.29
4	*P. fenoulheti*	8.60	7.51	7.06	**1.24**	1.14	0.65	0.78	1.06	1.12	1.07	1.10	1.06	1.24	1.23	1.28
5	*P. grandisonae*	12.47	12.02	11.50	8.96	**0.40**	1.16	1.25	1.19	1.26	1.24	1.37	1.15	1.16	1.16	1.26
6	*P. grindleyi*	8.59	6.77	6.20	2.99	8.85	**NA**	0.80	1.12	1.11	1.10	1.09	0.98	1.23	1.24	1.32
7	*P. hoeschi*	8.01	6.57	6.34	4.00	9.65	3.30	**NA**	1.09	1.14	1.10	1.05	1.06	1.24	1.28	1.27
8	*P. pachnodes*	9.97	9.24	8.97	6.43	9.35	6.60	6.01	**0.26**	0.82	0.70	1.20	1.19	1.26	1.25	1.34
9	*P.* cf. *fernandae* (lineage A)	11.07	8.93	9.42	7.35	10.13	6.41	6.75	3.50	**0.19**	0.57	1.20	1.21	1.26	1.27	1.39
10	*P. fernandae* **sp. nov.** (lineage B)	11.64	9.30	9.46	7.15	9.81	6.66	6.86	2.95	2.04	**0.66**	1.23	1.15	1.24	1.23	1.32
11	*P. nambensis* **sp. nov.** (lineage C)	10.47	8.53	9.08	7.75	11.60	6.69	6.11	8.63	8.09	8.95	**0.12**	1.20	1.32	1.36	1.35
12	*P. vertebralis*	9.56	9.79	9.32	7.22	8.59	6.19	6.48	7.34	8.07	7.85	8.90	**0.75**	1.16	1.20	1.21
13	*M. anotis*	12.23	11.35	11.39	10.55	8.80	10.12	10.12	9.70	10.01	9.41	11.18	9.14	**NA**	0.60	0.97
14	*M. howelli*	12.04	11.84	11.31	10.59	8.80	10.51	10.89	9.96	10.40	9.57	11.56	9.93	1.92	**NA**	0.99
15	*M. lindneri*	10.85	11.98	11.27	10.33	9.79	10.49	9.71	9.75	10.97	9.86	11.45	8.77	5.18	5.37	**NA**

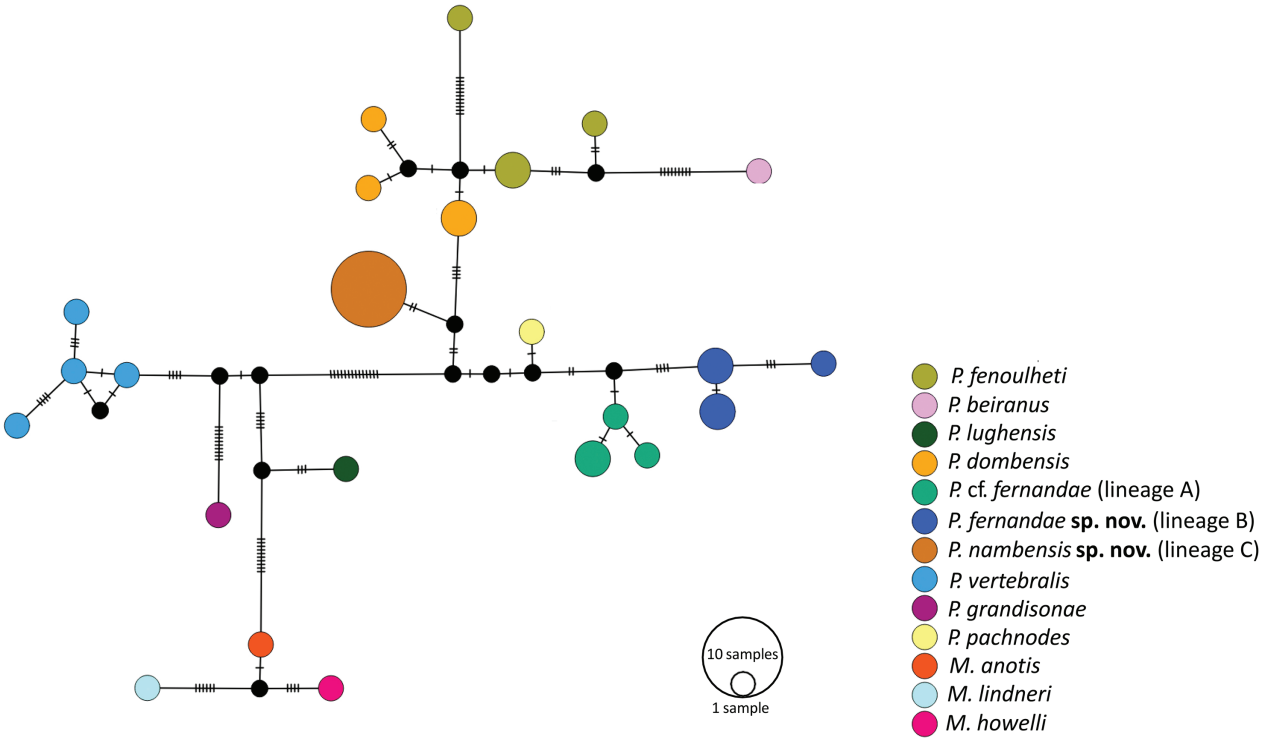

Figure 3. The haplotype network adjacent to the phylogeny illustrates the relationship between *Poyntonophrynus* and several *Mertensophryne* species using the RAG1 marker. Notches between haplotypes represent nucleotide substitutions, and circles' size represents the number of samples sharing the same haplotype.

Morphology

The recently collected Angolan specimens were assignable to the genus *Poyntonophrynus* by being small, having flattened bodies, lacking tarsal folds, and having usually double subarticular tubercles (Poynton 1964; Ceríaco et al. 2018; Tracy 2021). The three new lineages differ from each other and all other examined congeners in morphometry, coloration and qualitative features. We observed that *Poyntonophrynus* toads have body shapes that can broadly be grouped in two types: one with elongate and slender bodies, with relatively shorther limbs

Table 4 – part 1. Compilation of morphology, distribution and ecology of *Poyntonophrynus* taxa. Data from specimens collected for this work and from museums, original descriptions, and additional literature: Poynton and Broadley (1988), Channing (2001), du Preez and Carruthers (2009; 2017), Ceríaco et al. (2018), Rödel and Channing (2019), Tracy (2021), Rödel et al. (2023). M—male, F—female, ⌀—diameter, n/a—information not available, ? — uncertain information.

	***P. fernandae* sp. nov. (lineage B)**	***P.* cf. *fernandae* (lineage A)**	***P. nambensis* sp. nov. (lineage C)**	***P. pachnodes***	***P. grindleyi***	***P. hoeschi***	***P. jordani***	***P. lughensis***
Max SVL (mm)	31.6 (F) 23.9 (M)	29.9 (F) 25.8 (M)	34.9 (F) 26.5 (M)	33.7 (?)	33 (F) 27.7 (M)	37 (F) 32 (M)	30.8 (F) 30.6 (M)	47 (F) 36 (M)
Overall body shape	*dombensis*-like	*dombensis*-like	*dombensis*-like	*dombensis*-like	*dombensis*-like	*dombensis*-like	*dombensis*-like	*vertebralis*-like
Parotoid glands	Conspicuous, flattened, kidney-shaped	Conspicuous, elevated	Conspicuous, elevated, curved outer edge, kidney-shaped, thinner or same width of eye ⌀	Conspicuous, elevated	Conspicuous, elevated	Inconspicuous	Inconspicuous	Inconspicuous, flattenned
Tympanum	Not visible	Not visible	Visible or not visible, less than half eye ⌀	Not visible	Visible, much smaller than eye ⌀	Not visible or visible	Not visible	Visible, ¾ of eye ⌀
Columella	Absent	Absent	Present	Absent	n/a	Present	n/a	Present
Neopalatine	Approaching or synostosed to pterygoid and sphenethmoid	Approaching or synostosed to sphenethmoid, approaching maxilla and pterygoid	Approaching sphenethmoid, maxilla, and pterygoid	Reduced	n/a	Well-developed	n/a	Well-developed
Dorsal skin	Very rough	Rough	Rough	Rough	Very rough, spiny	Leathery	Rough	Rough
Skin on dorsal head	Rough	Rough	Rough	Rough	Rough	Smooth	Rough	Rough
Skin on snout	Rough	Rough	Rough	Rough	Smooth	Smooth	Smooth	Rough
Skin on venter	Granular	Granular	Granular	Granular	Granular	Smooth to slightly granular	Granular	Granular
Vertebral line	Absent	Absent	Absent	Absent	Absent	Usually absent	Absent	Absent
Dorsal coloration	Variation substrate-related. Shades of beige, grey, orange (bright to brick), green (coral to dark), brown on females. Breeding males plain bright yellow. Pale blotches as follows: occipital, mid-dorsal, sacral and above arm insertion.	Shades of beige, brown, grey and dark green. Breeding males with yellowish flanks. Pale blotches as follows: occipital, mid-dorsal, sacral and above arm insertion.	Shades of beige, brown, grey and orange. Pale blotches as follows: occipital, mid-dorsal, sacral and above arm insertion. Occipital and mid-dorsal blotches usually fused, resembling hourglass shape.	Shades of brown (dark to coppery) and grey. Pale blotches as follows: occipital, mid-dorsal, and sacral, and above arm insertion.	Black bands on pale brownish ground color.	Brown to reddish-brown, with light and dark paired markings.	Irregular black and red blotches on a grey background.	Pale-yellowish grey with black speckles, each with a light center, resulting in a pepper-and-salt effect.
Ventral coloration	Pale thin speckles in females, nearly immaculate in males	Dark thick speckles in females, less, paler speckles in males	Nearly immaculate. Median line of black speckles on chest, short black line in front of arms insertion	Immaculate or with speckles	Creamy white, throat yellowish. Interrupted median line of black blotches from chest to hind limbs.	Immaculate, yellowish-white	Creamy white	Cream colored, black speckles in belly
Webbing on toes	Absent or vestigial. Margin not serrated	Ranging between vestigial to first phalange of toe IV free of web. Margin not serrated	Vestigial. Margin not serrated	Toes without margin of web. Webbing vestigial. Margin not serrated	Vestigial. Margin not serrated	Toes with margin of web. Two phalanges of toe III free of web. Margin serrated	Vestigial. Margin not serrated	3 phalanges of toe IV free of webbing. Margin n/a

	***P. fernandae* sp. nov. (lineage B)**	***P.* cf. *fernandae* (lineage A)**	***P. nambensis* sp. nov. (lineage C)**	***P. pachnodes***	***P. grindleyi***	***P. hoeschi***	***P. jordani***	***P. lughensis***
Subarticular tubercles	Usually double at base of finger IV. Usually single at base of digits, usually double or bilobate at joint between phalanges	Always single at base of finger IV. Usually single at base of digits, usually double or bilobate at joint between phalanges	Usually single at base of digits, usually double or bilobate at joint between phalanges	Double	Double	Usually single at base of digits, double or absent at joint between phalanges	Single on fingers, except on finger I, where it is double. Double on toes	Double
Metatarsal tubercles	Oval or diamond-shaped, inner often very pointy. Inner ranging from slightly longer to twice the length of outer	Oval, inner often very pointy. Inner same size to almost twice longer than outer	Both oval, outer between half and two thirds the length of inner	Inner three times larger than outer	Outer about ⅔ the size of inner	Inner same size or smaller than outer	Outer about ⅔ the size of inner	Outer and inner large, smooth and flat
Metacarpal tubercles	Outer larger than inner, inner often absent	Outer larger than inner, inner very reduced, sometimes absent	Outer rounded to triangular, shorter than inner	Inner four times smaller than outer	Outer larger than inner	Inner absent	Two large flat metacarpal tubercles, outer larger than inner	Inner and outer present
Distribution	Angola	Angola	Angola	Angola	Mozambique, Zimbabwe	Namibia	Namibia	Ethiopia, Kenya, Somalia
Habitat	Rocky outcrops in moist forest and secondary Miombo	Rocky outcrops in montane grasslands	Rocky outcrops in montane grasslands	Rocky outcrops in woodlands	Montane grasslands	Rocky outcrops in arid areas	Rocky outcrops in arid areas	Arid savanna

Table 4 – part 2.

	P. damaranus	***P. dombensis***	***P. fenoulheti***	***P. grandisonae***	***P. beiranus***	***P. kavangensis***	***P. parkeri***	***P. vertebralis***
Max SVL (mm)	37.8 (?)	41.1 (F) 39.1 (M)	45 (F) 38 (M)	46 (F) 32.9 (M)	28 (F) 20 (M)	33 (F) 30 (M)	35 (F) 31 (M)	36 (F) 30 (M)
Overall body shape	*dombensis*-like	*dombensis*-like	*dombensis*-like	*dombensis*-like	*vertebralis*-like	*vertebralis*-like	*vertebralis*-like	*vertebralis*-like
Parotoid glands	Conspicuous, flattened, outer edge can be almost straight	Inconspicuous to conspicuous, flattened	Inconspicuous to conspicuous, elevated, wider than eye ⌀	Inconspicuous to hardly discernible	Inconspicuous to conspicuous, curved outline, usually broken into discontinuous patches	Inconspicuous to conspicuous, flattened, outer edge almost straight	Inconspicuous, flattened	Inconspicuous, flattened
Tympanum	Not visible or visible, ⌀ ≤ half eye ⌀	Visible, ⌀ < internarial distance	Visible, more than half eye ⌀, ⌀ < internarial distance	Very conspicuous, ⌀ ≥ internarial distance	Conspicuous to hardly visible	Visible	Not visible to visible, ⌀ half eye ⌀	Conspicuous, ⌀ more than half eye ⌀
Columella	Present	Present	Present	Present	Present	Present	Present	Present
Neopalatine	Well-developed	Approaching but not in contact with sphenethmoid, maxilla, and pterygoid	Not articulated with sphenetmoid or maxilla	Not articulated with maxilla	Well-developed	Well-developed	Well-developed	Sometimes absent. Not articulated with sphenetmoid
Dorsal skin	Rough	Rough	Leathery	Leathery	Rough	Very rough	Rough	Rough
Skin on dorsal head	Rough	Rough	Rough	Smooth	Rough	Rough	Rough	Smooth
Skin on snout	Rough	Smooth	Rough	Smooth	Smooth	Smooth	Smooth	Smooth

	P. damaranus	*P. dombensis*	*P. fenoulheti*	*P. grandisonae*	*P. beiranus*	*P. kavangensis*	*P. parkeri*	*P. vertebralis*
Skin on venter	Granular	Smooth to slightly granular	Smooth to slightly granular	Smooth to slightly granular	Granular	Granular	Smooth to slightly granular	Smooth to slightly granular
Vertebral line	Usually absent	Usually absent	Usually absent	Absent	Usually present	Present	Absent	Usually absent
Dorsal coloration	Green or olive-brown, symmetrical to irregular dark blotches. Pale grey blotches as follows: above snout, occipital, mid-dorsal, above arm insertion.	Shades of brown, grey or green, sometimes with red warts. Pale blotches as follows: occipital, mid-dorsal, and sacral, and above arm insertion.	Variation substrate-related. Light grey to brown, with dark blotches, sometimes red warts. Pale blotches as follows: scapular, sometimes mid-dorsal (single or paired).	Light-grey to brown. Pale blotches as follows: occipital, mid-dorsal, and sacral.	Olive brown, black or reddish-brown blotches. Dark dorsal markings: V-shaped interorbital bar, paired blotches arranged symmetrically.	Grey ground color with black blotches and brick orange warts. Dark interorbital bar, pale scapular patch with projections onto eyelids.	Variation substrate-related. Light grey to dark brown, with scattered dark blotches, and ochraceous to brownish red warts.	Grey to brown with paired dark, orange or reddish markings, pale.
Ventral coloration	Immaculate. Males with yellow throat	Immaculate	Usually immaculate, rarely with dark speckles in midline of pectoral region. Males with yellow or orange throat	Immaculate	Lightly to heavily speckled on grey, tending to merge in midline	Immaculate, cream-colored	Immaculate, white. Males with cream-colored throat	Black blotches that tend to fuse. Males with yellow throat
Webbing on toes	Moderate, 3 to 3.5 phalanges of toe IV free of web. Margin n/a	Toes without or with very narrow web margin. Webbing between toes III and IV beyond base of proximal phalange of toe IV. Margin not to slightly serrated	Broad to vestigial webbing between toes III and IV. Margin not serrated	Toes without web margin. Webbing vestigial. Margin not serrated	Broad webbing between toes III and IV. Margin serrated	Broad webbing between toes III and IV. Margin serrated	Vestigial, reaching the base of toe IV. Margin serrated	Two phalanges of toe III free of web. Margin not serrated
Subarticular tubercles	Usually double	Usually single at base of digits, usually double at joint between finger phalanges. At least distal of toes III and IV are double	Single or double at the base of digits and at joint between phalanges	Single, except distal tubercle of third finger, which is double or bilobed	Usually double	Usually double at base of digits and at joint between phalanges	Usually single at base of digits, usually double at joint between phalanges	Usually single at base of digits, double or absent at joint between phalanges
Metatarsal tubercles	Inner larger than outer	Inner smaller than outer	Inner larger than outer	Inner larger than outer	Inner absent	Inner two to three times larger than outer	Very reduced, rounded. Inner same size or smaller than outer	Inner two to three times larger than outer
Metacarpal tubercles	n/a	Inner smaller than outer	Inner smaller than outer	Outer two thirds to same size of inner	Inner usually absent, small when present	Inner rounded, smaller than outer rounded to triangular-shaped	Inner usually absent, very small when present, outer rounded	Inner much smaller than outer
Distribution	Namibia	Angola, Namibia	Botswana, Mozambique, Namibia, South Africa, Zimbabwe	Angola	Malawi, Mozambique, Zambia	Angola, Botswana, Namibia, Zambia, Zimbabwe	Kenya, Tanzania	South Africa, Botswana
Habitat	Arid grasslands	Rocky outcrops in arid areas	Rocky outcrops in grasslands and woodlands	Rocky outcrops in arid areas	Savanna and grasslands	Grasslands in sandy areas	Open savanna	Rocky outcrops in arid grasslands and savanna

Table 5. Comparative table of measurements of adult males and females of *Poyntonophrynus pachnodes*, *P. fernandae* **sp. nov.**, *P.* cf. *fernandae*, and *P. nambensis* **sp. nov.** Values are average ± standard deviation with range provided in square brackets. For abbreviations of measurements see Methods section. M—male, F—female.

Species	*P. fernandae* sp. nov. (lineage B)	*P. fernandae* sp. nov. (lineage B)	*P.* cf. *fernandae* (lineage A)	*P.* cf. *fernandae* (lineage A)	*P. nambensis* sp. nov. (lineage C)	*P. nambensis* sp. nov. (lineage C)	*P. pachnodes*	*P. pachnodes*
Sex	F	M	F	M	F	M	F	M
n	4	1	3	2	8	6	3	4
SVL	29.2 ± 0.6 [28.5–29.9]	25.8	31.2 ± 0.8 [30.3–31.8]	24.1 ± 0.2 [23.9–24.2]	32.1 ± 1.5 [30.2–34.9]	25.3 ± 1.0 [24.2–26.5]	29.9 ± 1.7 [28–31.4]	30.4 ± 3.0 [26.5–33.7]
HW	9.9 ± 0.5 [9.1–10.3]	9.5	9.9 ± 0.1 [9.8–10]	8.6 ± 0.7 [8.1–9.1]	11.0 ± 0.5 [10.2–11.7]	9.4 ± 0.6 [9–10.6]	9.7 ± 0.4 [9.2–9.9]	9.6 ± 0.7 [8.6–10.3]
HL	7.8 ± 0.4 [7.2–8.1]	7.7	7.7 ± 0.3 [7.4–7.9]	7.3 ± 0.4 [7–7.5]	7.9 ± 0.4 [7.2–8.5]	7.2 ± 0.4 [6.8–7.9]	8.6 ± 0.6 [7.9–9.1]	9.3 ± 2.2 [6.9–11.7]
IOD	3 ± 0.4 [2.5–3.5]	2.6	2.2 ± 0.3 [1.8–2.4]	2.4 ± 0.3 [2.2–2.6]	2.6 ± 0.3 [2–3]	2.4 ± 0.2 [2–2.6]	2.9 ± 0.6 [2.2–3.3]	3.7 ± 0.8 [2.7–4.5]
ED	2.9 ± 0.2 [2.8–3.2]	2.8	2.6 ± 0.1 [2.6–2.7]	2.6 ± 0.3 [2.4–2.8]	3.1 ± 0.3 [2.9–3.5]	2.8 ± 0.2 [2.5–3.1]	2.7 ± 0.2 [2.5–2.9]	2.8 ± 0.3 [2.4–3]
IND	2.1 ± 0.1 [1.9–2.2]	1.9	2.0 ± 0.1 [2–2.1]	2.1 ± 0.0 [2.1–2.1]	2.1 ± 0.1 [1.9–2.3]	1.9 ± 0.2 [1.7–2.2]	2.0 ± 0.1 [1.9–2.1]	2.2 ± 0.3 [1.8–2.5]
END	2.4 ± 0.1 [2.2–2.5]	2.1	2.5 ± 0.2 [2.3–2.6]	2.3 ± 0.1 [2.2–2.3]	2.4 ± 0.2 [2.1–2.8]	2.2 ± 0.1 [2.1–2.4]	2.5 ± 0.2 [2.2–2.6]	2.5 ± 0.3 [2.2–2.8]
UEW	2.4 ± 0.3 [2–2.6]	1.9	2.0 ± 0.1 [1.9–2.1]	2.3 ± 0.4 [2–2.6]	2.4 ± 0.3 [1.9–2.9]	2.2 ± 0.4 [1.7–2.7]	2.6 ± 0.5 [2–2.9]	2.2 ± 0.2 [2–2.4]
SL	3.9 ± 0.3 [3.6–4.2]	3.3	3.7 ± 0.2 [3.6–3.9]	3.4 ± 0.2 [3.2–3.5]	3.7 ± 0.3 [3.2–4.1]	3.3 ± 0.2 [3.1–3.6]	4.0 ± 0.5 [3.5–4.5]	3.8 ± 0.2 [3.6–4]
NS	1.4 ± 0.1 [1.3–1.4]	1.1	1.3 ± 0.1 [1.2–1.4]	1.2 ± 0 [1.2–1.2]	1.4 ± 0.1 [1.3–1.7]	1.2 ± 0.2 [1–1.6]	1.4 ± 0.3 [1.2–1.7]	1.5 ± 0.2 [1.3–1.8]
THL	12.5 ± 0.4 [12.1–13]	11.0	11.3 ± 0.2 [11.2–11.5]	10.4 ± 0.5 [10–10.7]	11.1 ± 0.8 [9.6–12]	10.1 ± 0.6 [9.2–10.9]	11.4 ± 0.2 [11.2–11.6]	11.5 ± 1.3 [10.1–13]
TL	11.8 ± 0.5 [11.1–12.2]	11.4	11.7 ± 0.3 [11.3–11.9]	10.7 ± 0.4 [10.4–10.9]	10.8 ± 0.4 [10.4–11.5]	9.5 ± 0.6 [8.9–10.4]	11.3 ± 0.6 [10.7–11.7]	11.8 ± 1.1 [10.1–12.5]
FL	10.8 ± 1 [10–12.1]	10.1	10.9 ± 0.6 [10.2–11.4]	9.5 ± 0.6 [9–9.9]	10.6 ± 0.5 [9.6–11.1]	9.6 ± 0.7 [8.3–10.3]	11.4 ± 0.6 [10.8–11.8]	11.7 ± 1.0 [10.3–12.5]
Toe4L	5.7 ± 0.2 [5.6–6]	5.1	5.7 ± 0.5 [5.3–6.2]	4.9 ± 0.2 [4.7–5]	5.4 ± 0.5 [4.8–6.1]	4.8 ± 0.3 [4.4–5.2]	5.8 ± 1.0 [4.8–6.7]	6.5 ± 1.2 [5–7.7]
FLL	7.1 ± 0.3 [6.8–7.5]	6.7	6.8 ± 0.4 [6.5–7.2]	5.8 ± 0.3 [5.6–6]	6.5 ± 0.3 [6.1–7]	5.8 ± 0.6 [5.3–6.9]	6.8 ± 0.3 [6.6–7.2]	6.7 ± 0.8 [6–7.8]
HAL	6.4 ± 0.6 [5.5–6.9]	5.6	6.9 ± 0.4 [6.6–7.3]	5.5 ± 0.2 [5.3–5.6]	6.4 ± 0.4 [5.6–6.8]	5.3 ± 0.4 [4.8–5.8]	6.9 ± 0.6 [6.3–7.4]	6.9 ± 0.6 [6–7.4]
Fin3L	3.4 ± 0.4 [3–3.8]	3.4	3.6 ± 0.2 [3.4–3.7]	2.8 ± 0.1 [2.7–2.9]	3.2 ± 0.3 [2.8–3.6]	2.5 ± 0.3 [2.2–3]	4.4 ± 0.2 [4.2–4.6]	4.4 ± 0.6 [3.5–4.9]

compared to body length, and another group with studier, more robust body, and with relatively longer limbs, referred to as 'squat' appearance by Poynton and Broadley (1988). Here we name the first body shape as "*vertebralis*-like", and the latter as "*dombensis*-like". Table 4 comprises morphological, distribution, and ecologic information about all currently known *Poyntonophrynus* taxa. Table 4 was adapted on a table presented by Ceríaco et al. (2018) and supplemented with new data. Qualitative features follow the descriptions of our study, and are therefore not always in agreement with Ceríaco et al. (2018).

Morphometrics

Summarized measurements of Angolan *Poyntonophrynus* specimens examined in this study are provided in Table 5, and detailed measurements from *Poyntonophrynus* from Angola are provided in Tables 6–7, S3. Females were larger than males in all three new lineages (Fig. 4; Table 5), and in all the remaining *Poyntonophrynus* species measured herein (Table S3). According to Ceríaco et al. (2018), *P. pachnodes* does not show a female biased dimorphism in body size, but their work did not mention any criteria for sex and age distinction. As sex identification of these toads was also doubtful based on osteological features (see Osteology section), we suggested reinvestigating the respective vouchers. Indeed, the re-examination of one of the specimens (UF 184183), identified as a male by Ceríaco et al. (2018), was in fact a female (D.C. Blackburn, unpub. Data). The three new lineages differed in SVL and ratios i.e., females of lineages B, A, and C had slightly different mean SVL (29.2 ± 0.6 mm, n = 4; 31.2 ± 0.8 mm, n = 3; and 32.1±1.5 mm, n = 8; respectively), and a similar pattern was found in males (25.8 mm, n = 1; 24.1±0.2 mm, n = 2; and 25.3±1 mm, n = 6; respectively) (Fig. 4; Table 5). Lineages B, A, and C had slightly different relative forelimb length (SVL/FLL ranging between 3.9–4.4, 4.0–4.7, and 3.8–5.1, respectively), hind limb length (SVL/TL ranging between 2.3–2.6, 2.2–2.8, and 2.5–3.2, respectively), and head length (SVL/HL ranging between 3.4–4.0, 3.2–4.1, and 3.4–4.6, respectively), with few overlapping values when comparing males and females separately (Fig. 4). A PCA showed considerable overlap in morphometry of *Poyntonophrynus* spp. (Fig. S1; Table S4), fully reflecting the morphological conservancy reported for the genus.

Coloration and qualitative features

All recently collected specimens showed the typical *Poyntonophrynus* dorsal color pattern, as described by Poynton and Broadley (1988) for the genus: one pale occipital blotch, one pale mid-dorsal blotch, one pale sacral blotch (Fig. 5), and one pale blotch over the arm insertion. Live coloration in lineage B generally exhibited vivid colors, while lineages A and C displayed mostly greyish and brownish color, the latter pattern being more common in the genus. The ventral coloration differed between females of all the three lineages, with very dark and thick speckles in lineage A, small grey speckles in lineage B, and a nearly immaculate venter in lineage C (except for a few dark spots placed in midline of pectoral region, and a dark line curving down in front of insertion of arm). In males we observed a similar pattern, but with less speckles, and less intense pigmentation. Glandular warts were very evident and salient in lineages A and C, but not visible in lineage B. Thus all lineages had a unique combination of coloration features. Parotoid glands were conspicuous, with margins clearly demarcated. They were flattened, and paler than adjacent skin in lineage B, and much more protuberant in lineages A and C. The tympanae were not visible in lineages A and B, and were usually visible in lineage C. For more details see species descriptions.

Osteology

The postcranial skeletons of the recently collected Angolan specimens were very similar to *P. pachnodes*, the only other *Poyntonophrynus* species for which detailed postcranial osteological information is available (Ceríaco et al. 2018). The crania of the new lineages showed the typical *Poyntonophrynus* arrangement (Tracy 2021). However, lineages A–C differed from *P. pachnodes* in having better developed neopalatines, approaching adjacent bones (sphenetmoid and pterygoid) vs. being very reduced in *P. pachnodes* (see Ceríaco et al. 2018). Lineage C differed from lineages A, B and *P. pachnodes* in possessing a columella vs. absent in the other lineages; Fig. 6), and in having a prepollex formed by two elements, instead of a single one in the other two lineages. Lineage A differed from lineage B in having more developed mediolateral processes of the vomer. The otic ramus of the squamosal has been reported as differing among some *Poyntonophrynus* species (Tracy 2021). In our small sample, the otic rami were similar among lineages A–C, *P. pachnodes* and *P. dombensis*: varying from poorly developed to nearly absent. Intra- and inter-specific variation of this character overlapped. Squamosals were present in both CT-scanned *P. dombensis* analyzed herin, thus being different to the results by Tracy (2021), who found no squamosals in *P. dombensis damaranus*. The urostyle of *P. dombensis* had parapophyses on its anterior part, that were apparently absent in all other species. Lineages A–C showed sexual dimorphism in characteristics of the humerus i.e., males bearing medial and lateral crests (Fig. 7) but absent in females. Ceríaco et al. (2018) reported on a male *P. pachnodes* humerus (UF 184183) without crests, but the sex of this specimen was misidentified, being in fact a female (D.C. Blackburn, unpub. Data). We herein added further osteological characters of the new lineages (see species descriptions), and for *P. dombensis* (File S1; Figs S2, S3), for which such data were previously not available.

Distribution of newly collected *Poyntonophrynus*

The three newly recovered lineages were found in association with large boulders (Fig. 8), at mid to high elevations across the Angolan escarpment and central highlands (500 to 1850 m a.s.l.) in the province of Cuanza-Sul (Fig. 1). They are geographically isolated from the closest related taxon, *P. pachnodes* by arid lowlands, and were collected at five localities. These include two sites (Congulo and Condé) in which lineage B was found in or on the edge of moist, dense forest in the central escarpment. At a third site further east (Quibala), lineage B animals were collected near open Miombo woodland. The two remaining localities were in the area of Serra da Namba (Chinhundo and Missão da Namba), central Angolan highlands. In both localities, we recovered lineage C frogs. At Chinhundo, lineage C frogs occurred in syntopy with lineage A individuals. In addition to the collected material, a photographic record from Gabela in the central escarpment could be ascribed to lineage B. No *Poyntonophrynus* specimens were located in other, seemingly suitable habitats in other mountainous regions in the central and southern highlands, suggesting that the genus is patchily distributed in Angola.

Taxonomy

Based on mitochondrial and nuclear DNA, morphological, and osteological differences, and the geographic distribution of the new lineages discussed above, we recognized three distinct lineages. However, as clade A+B has only small distances in the 16S mitochondrial gene between the two lineages that it comprises, we describe two new species, *Poyntonophrynus fernandae* **sp. nov.** (lineage B) and *Poyntonophrynus nambensis* **sp. nov.** (lineage C), and provisionally regard lineage A as conspecific with lineage B. In order to make future use of our data easier, and to avoid potential taxonomic confusion, the type series of *P. fernandae* **sp. nov.** did not include specimens of lineage A, which we refered to as additional material with uncertain species identity (*P.* cf. *fernandae*). We follow the general lineage-based species concept (de Queiroz 1998), and used both criteria of integration by congruence and by accumulation established by Padial et al. (2010).

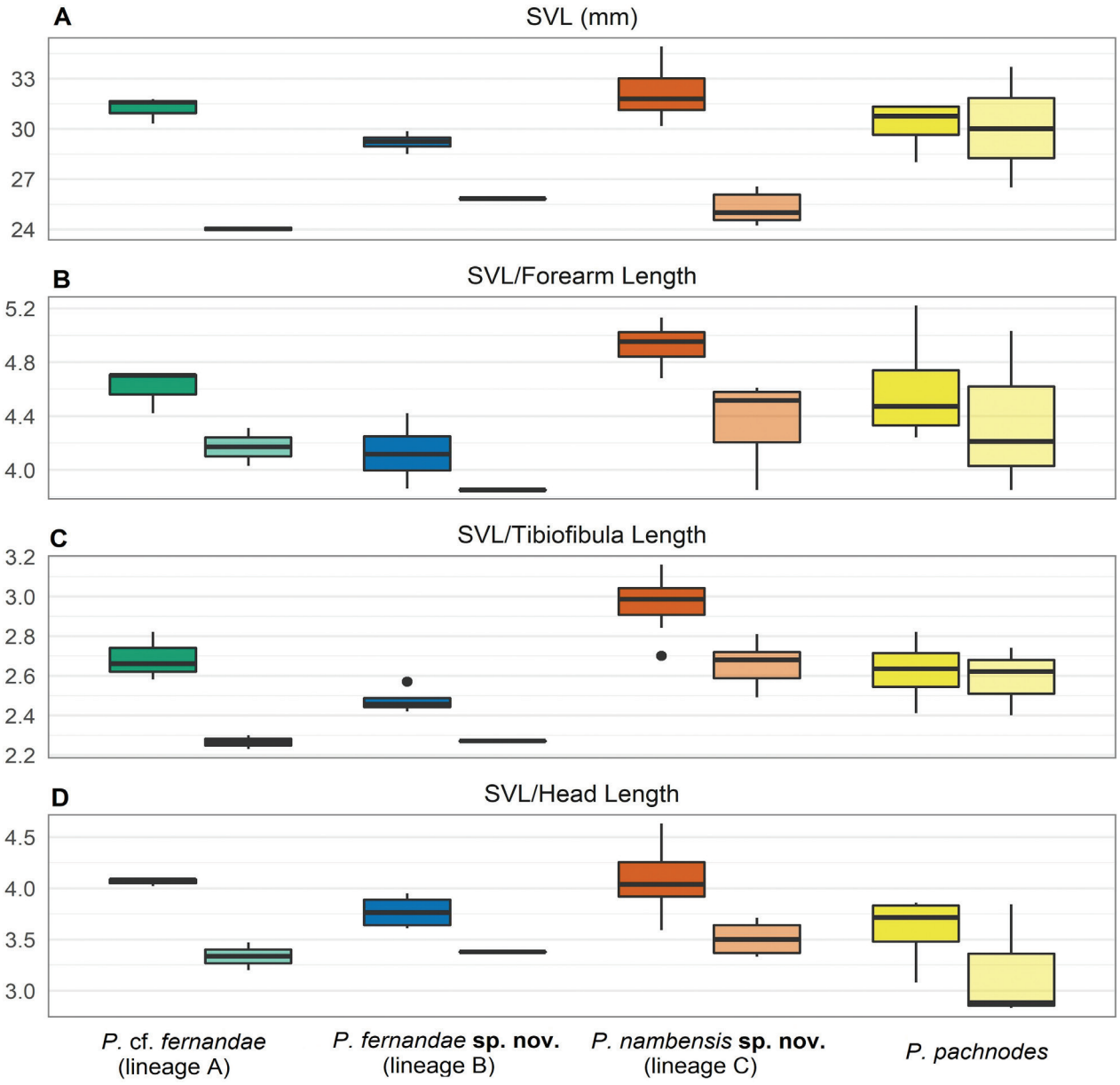

Figure 4. Morphometric comparisons of Angolan *Poyntonophrynus*. Boxplots (top whisker–maximum value; lower whisker–minimum value; dark horizontal line–median; box–1st quartile – 1.5 interquartile range (IQR), and 3rd quartile + 1.5 IQR) comparing morphometric features. **A** SVL, and ratios **B** SVL/TL, **C** SVL/FLL, **D** SVL/HL between *Poyntonophrynus* species, left to right: *P.* cf. *fernandae* (lineage A, green), *P. fernandae* **sp. nov.** (lineage B, blue), *P. nambensis* **sp. nov.** (lineage C, red), and *P. pachnodes* (yellow), the closest related species. For each species, the darker shade (on the left) represents females, and the lighter shade (on the right) represents males. Note sexual size dimorphism in all species, except in *P. pachnodes* (but compare text). SVL = snout–vent length.

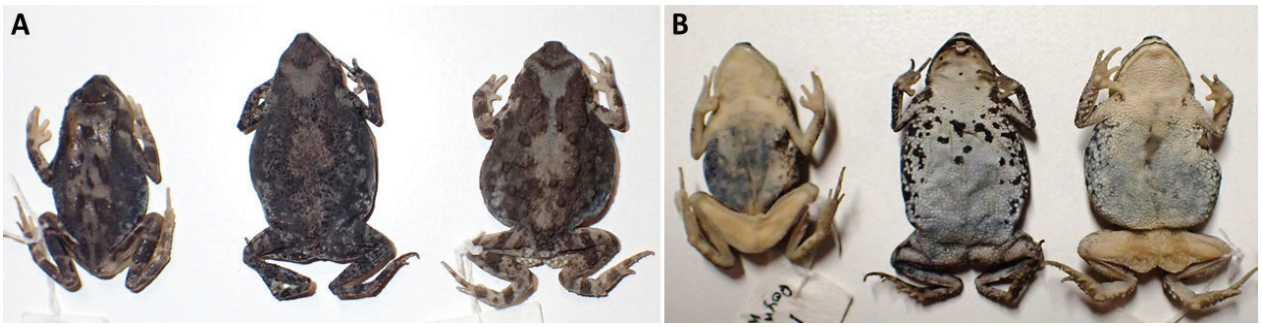

Figure 5. Females of the new Angolan *Poyntonophrynus* lineages detected in this study in (**A)** dorsal, and (**B)** ventral view. Left to right: *P. fernandae* **sp. nov.** (lineage B, ZMB 91791), *P.* cf. *fernandae* (lineage A, ZMB 91785), *P. nambensis* **sp. nov.** (lineage C, ZMB 91787). Note differences in body size, robustness, relative limbs size, dorsal coloration (hourglass shape only in *P. nambensis* **sp. nov.**), and ventral coloration.

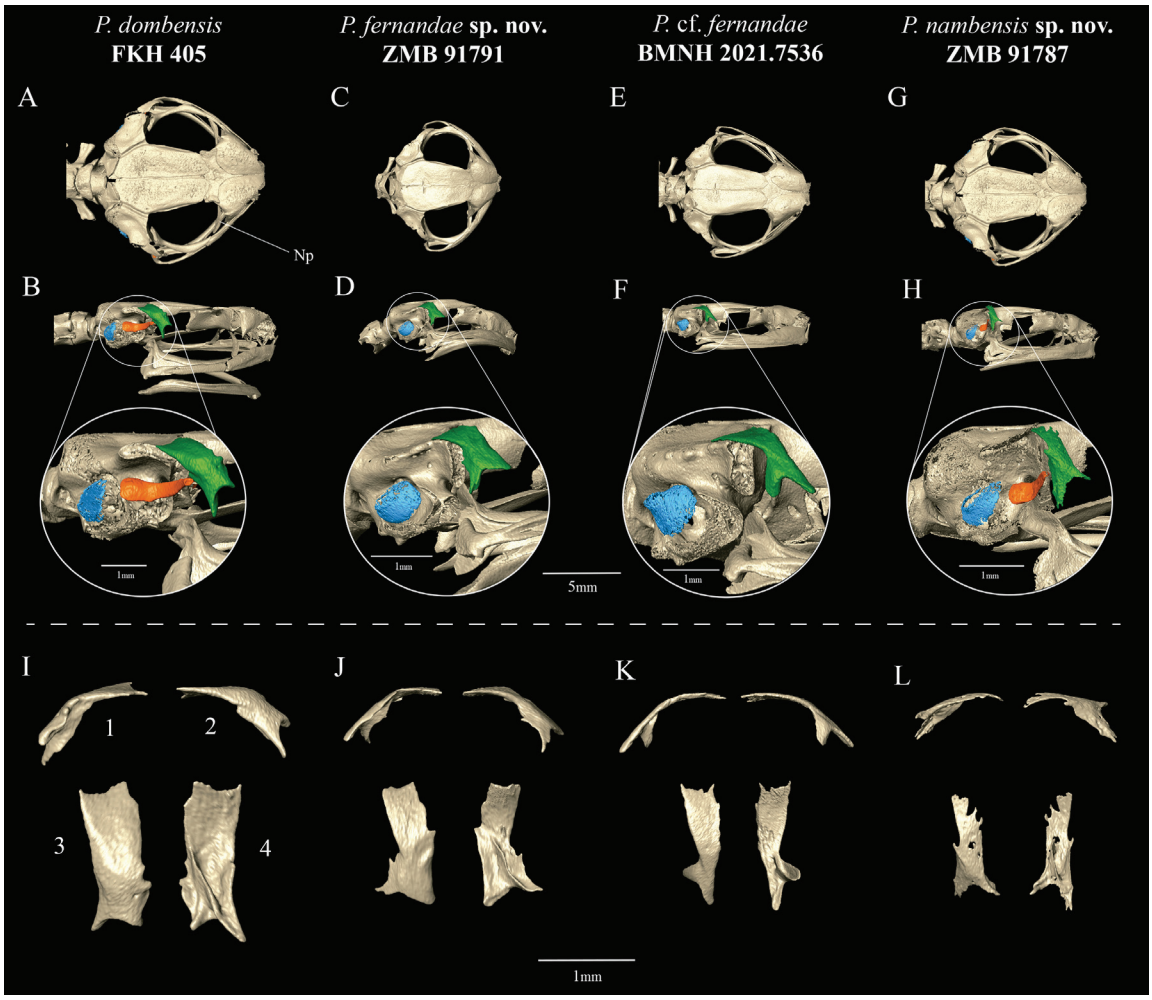

Figure 6. Cranium osteology of Angolan female *Poyntonophrynus*. **A–H** Left to right: skulls of *P. dombensis* (ZMB 91792), *P. fernandae* **sp. nov.** (lineage B) (ZMB 91791), *P.* cf. *fernandae* (lineage A) (BMNH 2021.7536), and *P. nambensis* **sp. nov.** (lineage C) (ZMB 91787), in dorsal view (top row) and lateral view (second row). Green color marks the squamosal, blue indicates the parotic plate, orange indicates the columella, the latter being absent in *P. fernandae* **sp. nov.** and *P.* cf. *fernandae*. Np identifies the neopalatine. **I–L** Left to right: squamosals of *P. dombensis*, *P. fernandae* **sp. nov.**, *P.* cf. *fernandae*, and *P. nambensis* **sp. nov.**, in 1 – posterior, 2 – anterior, 3 – lateral, and 4 – medial views.

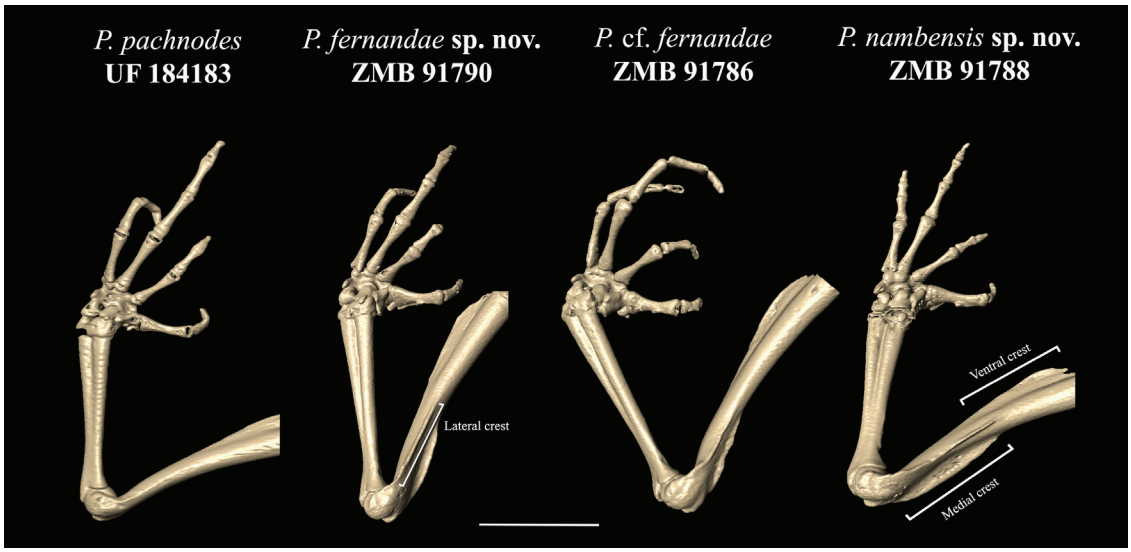

Figure 7. CT-scan reconstructions of arms of male *Poyntonophrynus*. Left to right: *P. pachnodes* (UF 184183), *P.* cf. *fernandae* (lineage A**)** (ZMB 91790), *P. fernandae* **sp. nov.** (lineage B) (ZMB 91786), and *P. nambensis* **sp. nov.** (lineage C) (ZMB 91788), highlighting the humeri. 1 – lateral crest, 2 – ventral crest, 3 – medial crest. Medial and lateral crests on distal part of the humeri, typical of male bufonids, only absent in the reported *P. pachnodes* male (compare text). Scale bar represents 5 mm.

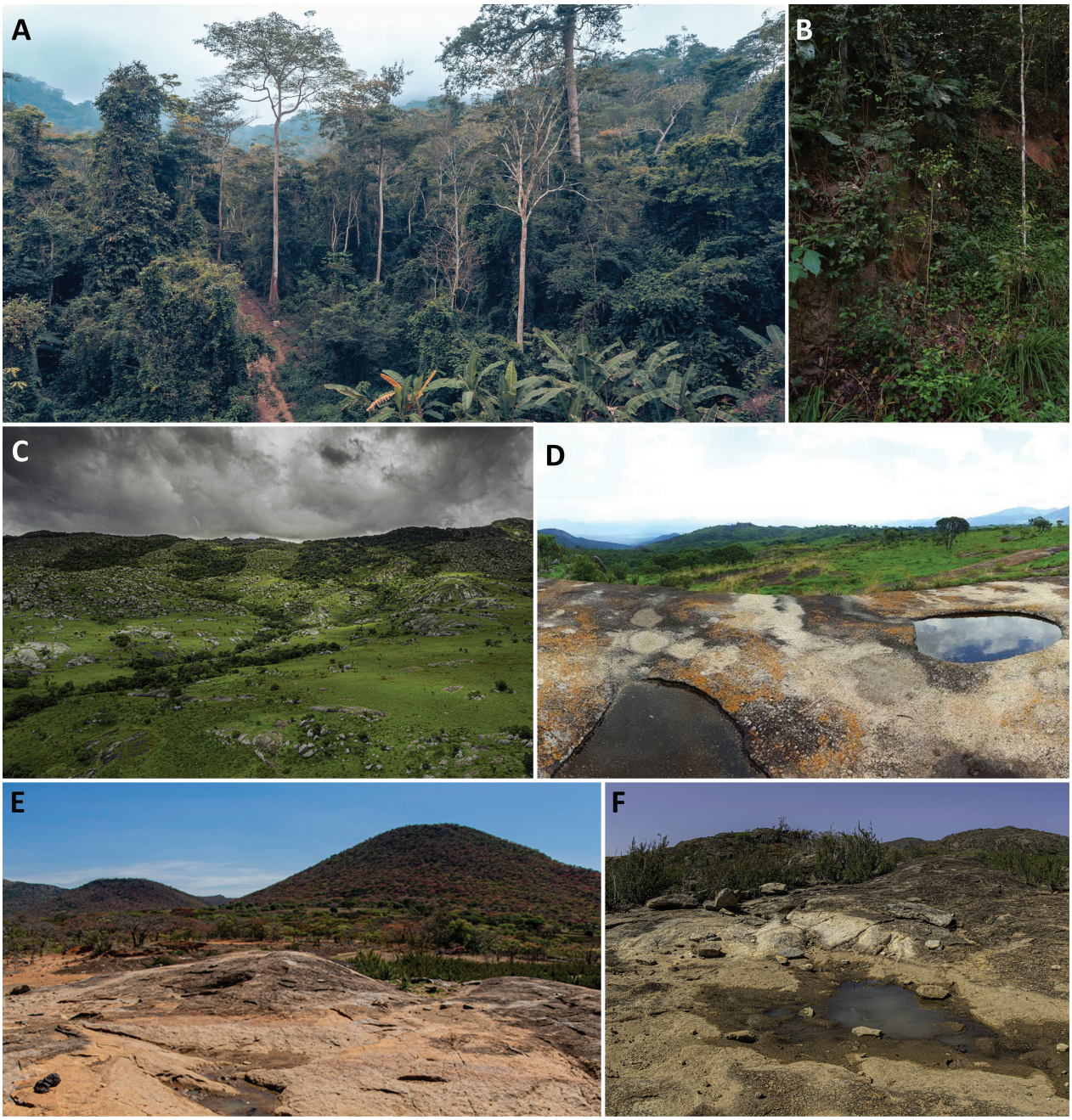

Figure 8. *Poyntonophrynus* habitats. **A**, **B** Habitat of *P. fernandae* **sp. nov.** at Congulo forest, Cuanza-Sul Province. **C**, **D** Habitat of *P.* cf. *fernandae* and *P. nambensis* **sp. nov.** at Namba highlands, Cuanza-Sul Province. **E**, **F** Habitat of *P. pachnodes* at Serra da Neve, Namibe Province. Photos by K. Luchansky (A) and W.R. Branch (D).

Poyntonophrynus fernandae sp. nov.

https://zoobank.org/FD23B293-0F0F-4EF3-80B9-D7D5F4E0FE75

Figures 5–7, 9–11; Tables 5, 6

Holotype. ZMB 91791, adult female, collected 12 km N of Condé on rocky ground at the edge of forest, Cuanza-Sul Province, –10.743744°, 14.631923°, 1260 m a.s.l., 22 November 2017, by Pedro Vaz Pinto (Figs 5–7, 9–11).

Paratypes. ZMB 91790, adult male, same data as holotype; BMNH 2021.7534, adult female, collected on a small plant 30 cm high in Congulo Forest, Cuanza-Sul Province, –10.745881°, 14.630576°, 520 m a.s.l., 21 October 2016, by Ninda L. Baptista, Pedro Vaz Pinto and William R. Branch; BMNH 2021.7535, FKH-1086, two adult females, collected in an accommodation yard at Quibala, in broken rocky foothills of a large granite massif, Cuanza-Sul Province, –10.7399°, 14.979755°, 1303 m a.s.l., 21 September 2018, by Luke Verburgt.

Additional material. Photographic record of lineage B (Fig. 10F). One male and one female (amplectant pair), in Gabela, Cuanza-Sul Province, approx. –10.85°, 14.38°, 1050 m a.s.l., November 2017, by Nguyen Thi Ngan Thanh. Not collected.

We restrict the type series of *P. fernandae* **sp. nov.** to specimens from the escarpment forest and adjacent areas (lineage B). The vouchers from Namba were listed and reported herein as additional referred material of *P.* cf. *fernandae* (lineage A): ZMB 91785, adult female, collected approximately 12 km W of Missão da Namba, Chinhundo, Cuanza-Sul Province, –11.914685°, 14.740552°, 1740 m a.s.l., 16 October 2020, by Pedro Vaz Pinto (Figs 12–14; Tables 5, 6). BMNH 2021.7536, FKH-0463, two adult females, same data as previous specimen; ZMB 91786, BMNH 2021.7537 two adult males, same collecting locality as previous specimen, collected on 03 November 2016, by Ninda L. Baptista, Pedro Vaz Pinto and William R. Branch.

Definition. *Poyntonophrynus fernandae* **sp. nov.** sensu lato are medium-sized pygmy toads with females larger than males, sexual dimorphism in skin texture (females rougher than males), and sexual dichromatism (females with complex dorsal patterns vs. males plain or partially bright yellow; females with speckles ventrally vs. males with nearly immaculate venter). No tarsal fold. Subarticular tubercles at the base of fingers and toes mostly single, and those at the joint between phalanges usually double. Tympanum not visible. Conspicuous parotoid glands, with curved outer edge. Usually two phalanges of toes III and V free of web, webbing between toes III and IV vestigial, not serrated. One or two enlarged palmar tubercles: one large, rounded to triangular-shaped very well developed outer metacarpal tubercle, and one smaller rounded inner metacarpal tubercle sometimes absent. Females with typical *Poyntonophrynus* arrangement of dorsal coloration pattern: pale single occipital, mid-dorsal, sacral and above arm insertion blotches.

Specimens of *P.* cf. *fernandae* (lineage A) differ from those of *P. fernandae* **sp. nov.** (lineage B) in shape of parotoid glands (elevated vs. flattened), conspicuousness of dorsal glandular warts (evident vs. discrete), dorsal coloration (dull vs. complex, colorful, in different shades of orange, green and black), ventral coloration (dark thick speckles vs. pale thin speckles), relative width of dark cross-bands on the limbs (similar width than pale ones and dull vs. much wider than pale ones, and orange on the outer surface of the limbs), inner metacarpal tubercle (conspicuous and always present vs. discrete and sometimes absent), overall sturdiness (sturdy vs. slender), relative limb size (short vs. long). Males differ from males of *P. fernandae* **sp. nov.** (lineage B) in dorsal coloration (dull coloration with similar pattern than females, but partially with yellow on flanks and thighs vs. plain bright yellow).

Diagnosis. *Poyntonophrynus fernandae* **sp. nov.** sensu lato differs from all *Poyntonophrynus* species except *P. pachnodes* in lacking a tympanum and a columella. It differs from *P. pachnodes* in having a better-developed neopalatine. Males differ from *P. pachnodes* and *P. nambensis* **sp. nov.** in dorsal coloration (partially or plain bright yellow vs. complex dull patterns in *P. pachnodes*, and *P. nambensis* **sp. nov.**). It differs from *P. nambensis* **sp. nov.** in being smaller, less sturdy, and having relatively longer fore and hindlimbs, in ventral coloration (speckles vs. nearly immaculate). It differs from *P. beiranus* in parotoid glands conspicuousness (conspicuous, with clearly demarcated margins vs. inconspicuous). It differs from *P. damaranus* in ventral patterning (speckles vs. immaculate). It differs from *P. dombensis* in tympanum (not visible vs. conspicuous), and ventral patterning (speckles vs. immaculate). It differs from *P. fenoulheti* in parotoid glands width (thinner or around same width of eye diameter vs. wider than eye diameter). It differs from *P. grandisonae* in tympanum (not visible vs. conspicuous) and skin texture (rough vs. leathery). It differs from *P. grindleyi* in pale occipital and sacral patches (present vs. absent) and dorsal spines (small vs. large). It differs from *P. hoeschi* in ventral patterning (speckles vs. immaculate). It differs from *P. jordani* in shape of parotoid glands (kidney-shaped vs. a cluster of glands) and pale occipital patch (present vs. absent). It differs from *P. lughensis* in conspicuousness of parotoid glands (conspicuous vs. inconspicuous) and tympanum (not visible vs. conspicuous). It differs from *P. kavangensis* in foot webbing (non-serrated vs. serrated), dorsal patterning (absent vertebral line vs. present), and ventral patterning (speckles vs. immaculate). It differs from *P. parkeri* in ventral patterning (speckles vs. immaculate). It differs from *P. vertebralis* in dorsal patterning (vertebral line absent vs. present), and conspicuousness of parotoid glands (conspicuous vs. inconspicuous).

Holotype description. *External morphology*. Small (SVL 29.4 mm), slender, gravid female (Figs 9, 10, all measurements in Table 6). SVL approximately 2.9 times head width, 3.6 times head length, 2.4 times thigh length, 2.5 times tibiofibula length, and 4.2 times forearm length. Head rounded in dorsal view. Head length approximately 0.8 head width. Rostral tip rounded in dorsal and lateral views, truncate in ventral view. Eyes projecting laterally just beyond eyelids and not beyond margins of head in dorsal view. Eye not projecting above dorsal margin of head in lateral view. Interorbital distance approximately 1.2 times eye diameter, and approximately 1.7 times internarial distance. Eye diameter approximately 1.2 times eye-nostril distance, and 2.2 times naris to rostral tip. Tympanum not visible. Naris small, oval, directed dorsolaterally. Canthus rostralis sharp. Loreal region concave. Limbs and digits slender and well-developed. Tarsal fold absent. Digits of manus and pes elongated. Finger III length approximately 0.5 times hand length. Relative length of fingers: III > IV > II > I. Finger tips rounded, not expanded to discs. Fingers with prominent subarticular tubercles that are always double or bilobate, except under finger IV, which is single, on the right hand; and double or bilobate at the base of fingers I, II, and under finger III, and single at the base of fingers III, IV, and under finger IV, on the left hand. Plants of hands beset with supernumerary tubercles. Digits with subdigital tubercles, often double. Oval outer metacarpal tubercle well developed, larger and much more conspicuous and protuberant than inner metacarpal tubercle (Fig. 9C). Webbing between manual digits absent. Toe IV length approximately 0.6

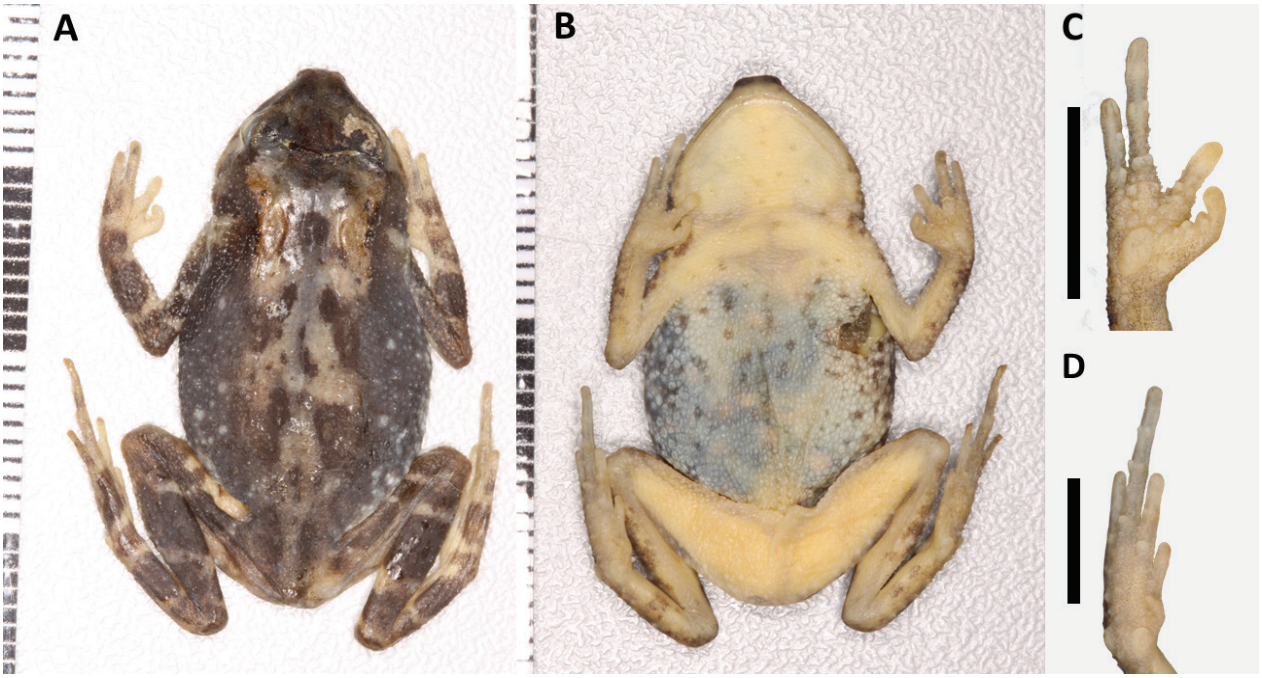

Figure 9. Holotype of *Poyntonophrynus fernandae* **sp. nov.** (ZMB 91791, female) in preservative. **A** Dorsal view. **B** Ventral view. **C** Palm of right hand. **D** Palm of right foot. Photos by F. Tillack. Short scale bars represent 1 mm (A, B), black scale bars represent 5 mm (C, D).

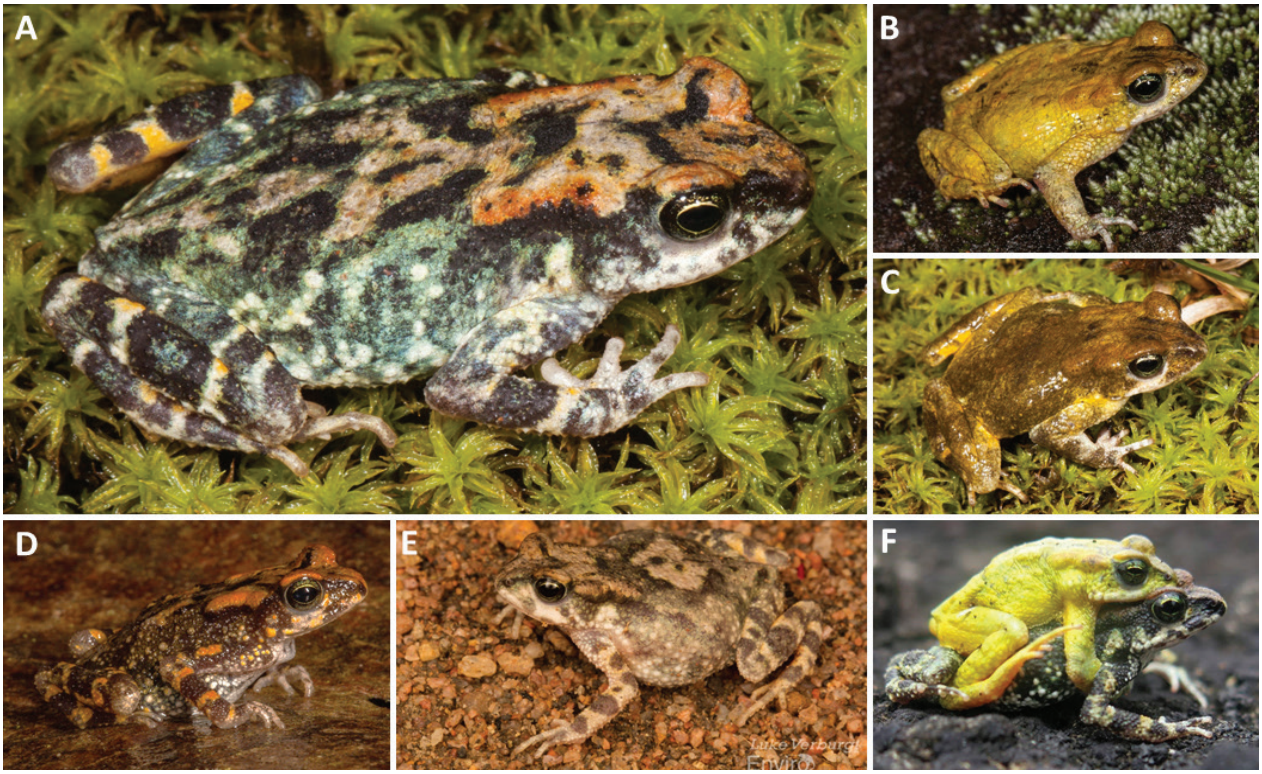

Figure 10. Pictures of live *Poyntonophrynus fernandae* **sp. nov.** **A** Female holotype (ZMB 91791). **B**, **C** Male paratype (ZMB 91790) with yellow color when collected, and with fading coloration after three days. **D** Female paratype (BMNH 2021.7534), darker individual collected in forest. **E** Female paratype (FKH-1086) collected on red gravel, typical of Cuanza-Sul Province ferralitic soils. **F** Pair in axillary amplexus from Gabela (not collected). Photos by L. Verburgt (E) and N.T. Ngan Thanh (F).

times foot length. Relative length of toes IV > III = V > II > I. Toe tips rounded, not expanded to discs. Toes with prominent subarticular tubercles that are always single at toe bases, except for toe I on right foot, which is double, toe I on left foot, which is not visible, and those at the joint between phalanges being all double and elongated, except under finger V on right foot, which is single. Toes without a margin of web. Webbing between toes vestigial,

Table 6. Measurements (in mm) of the type series of *Poyntonophrynus fernandae* **sp. nov.** (lineage B), and the additional vouchers of *P.* cf. *fernandae* (lineage A). For abbreviations see Methods section. M—male, F—female.

Current catalogue number	**ZMB 91791**	**BMNH 2021.7534**	**ZMB 91790**	**BMNH 2021.7535**	**FKH–1086**	**ZMB 91785**	**ZMB 91786**	**CHL 0455**	**BMNH 2021.7536**	**FKH–0463**
Former catalogue number	**CHL 0806**	CHL 0431	CHL 0805	—	—	FKH–0461	CHL 0454	—	FKH–0459	—
Field number	**NB806**	NB431	NB805	EI_704	EI_725	P0–36	NB454	NB455	P0–34	P0–38
Type status	**Holotype**	Paratype	Paratype	Paratype	Paratype	additional voucher	additional voucher	additional voucher	additional voucher	additional voucher
Sex	**F**	F	M	F	F	F	M	M	F	F
SVL	**29.4**	29.1	25.8	29.9	28.5	31.8	24.2	23.9	31.6	30.3
HW	**10.3**	10.0	9.5	10.1	9.1	9.8	8.1	9.1	9.8	10
HL	**8.1**	8.0	7.7	7.7	7.2	7.8	7.0	7.5	7.9	7.4
IOD	**3.5**	3.0	2.6	2.9	2.5	1.8	2.6	2.2	2.4	2.3
ED	**2.9**	2.8	2.8	3.2	2.8	2.6	2.4	2.8	2.7	2.6
IND	**2.1**	1.9	1.9	2.1	2.2	2.0	2.1	2.1	2.1	2.0
END	**2.4**	2.2	2.1	2.5	2.3	2.6	2.2	2.3	2.3	2.5
UEW	**2.0**	2.6	1.9	2.5	2.5	1.9	2.0	2.6	2.0	2.1
SL	**4.1**	3.6	3.3	4.2	3.8	3.7	3.5	3.2	3.9	3.6
NS	**1.3**	1.4	1.1	1.4	1.3	1.2	1.2	1.2	1.4	1.3
THL	**12.4**	12.1	11	13.0	12.4	11.2	10.0	10.7	11.5	11.3
TL	**11.9**	12.0	11.4	12.2	11.1	11.3	10.9	10.4	11.9	11.8
TaL	**5.9**	6.4	5.6	6.8	5.9	6.2	5.4	6.4	6.3	7.0
FL	**11.0**	12.1	10.1	10.0	10.2	10.2	9.0	9.9	11.4	11.2
Toe4L	**6.0**	5.7	5.1	5.6	5.6	5.3	4.7	5.0	6.2	5.7
IMTL	**1.5**	1.3	1.2	1.2	1.3	1.0	1.0	1.0	1.5	1.2
UAL	**5.2**	5.8	5.0	4.8	4.7	5.3	5.2	5.0	4.9	5.4
FLL	**7.0**	7.5	6.7	6.8	7.1	6.8	6.0	5.6	7.2	6.5
HAL	**6.7**	6.9	5.6	6.5	5.5	6.6	5.6	5.3	7.3	6.7
Fin3L	**3.8**	3.6	3.4	3.2	3.0	3.4	2.9	2.7	3.6	3.7

webbing margin not serrated. Inner metatarsal tubercle prominent, nearly diamond shaped, pointy, approximately half the length of toe I, and less than twice longer than outer. Outer metatarsal tubercle prominent, oval. Mid-tarsal tubercle discrete, same size of the remaining tarsal tubercles, near medial edge and positioned at around the middle of the tarsus.

Dorsal skin rough, texture resembling sandpaper, with pale-tipped conical spines on dorsum, arms, legs, and lateral surface of snout. Skin of top of head smooth. Ventral and gular skin, and skin of ventral surface of limbs covered in minuscule spines, less pronounced and pointy than dorsal ones. Skin of venter and gular region granular. Parotoid glands elongated, flattened, conspicuous, with clearly discernible margins, kidney-shaped, with a curved outer margin, placed dorsolaterally and extending from behind the eye to slightly beyond forearm insertion. Poorly developed glandular warts around mid-dorsal pale patch.

***Color*.** In life, dorsal coloration consists of a set of black and paler (mostly beige) blotches, forming a symmetrical pattern (Fig. 10A). From tip of head to sacrum, black blotches are either single or paired, located along the vertebral region. Single black blotches consist of one elongated blotch on top of snout; one continuous interorbital thin chevron directed posteriorly; and small occipital, mid-dorsal, and sacral blotches. Paired black blotches are located anteriorly and posteriorly to the triangular beige mid-dorsal blotch, and on the sides of the sacral beige blotch. From tip of head to sacrum, a series of beige blotches, which have brick orange portions on dorsal part of head and snout. Posterior to that, a triangular mid-dorsal beige blotch pointing forward, followed by an elongated beige blotch resembling a thick half vertebral stripe, outlined in coral green. Side of head cream with black and coral green blotches anterior and posterior to eye. Region below eye cream-colored. Black blotch from anterior corner of eyes to tip of snout. Region on top of lip beige with small black spots. Conspicuous cream roundish blotch above arm insertion. Parotoid glands mostly brick orange, with beige on the medial part, and black outer margins. Eyelid brick orange. Iris golden. Pupil black ellipsoid. Flanks with a reticulate of bright coral green, black, and cream markings. Dorsal surface of forelimbs with thick black cross-bands alternate with much thinner cream inter-spaces. Dorsal surface of fingers I and II cream, and of fingers III and IV cream with black cross-bands. Dorsal surface of hindlimbs (thighs and crus) with three thick black cross-bands, with thin paler inter-spaces that are cream on the inner surface, and bright orange

on the outer surface of the limb (Fig. 10A). Black crossbands on thigh, crus and feet touching when legs flexed. Ventral skin whitish and semi-transparent allowing to see interior of belly, full of eggs. Small grey speckles scattered on chest and belly, as well as on throat, where they are slightly smaller and less densely distributed. Ventral thighs and crus whitish. Ventral tarsus whitish with a grey bar. Plantar surface of pes pale grey, with white tubercles. Ventral surfaces of arm, forearm, hand and fingers whitish. Preserved specimen after 5 years in ethanol, with beige and orange areas now pale grey. Black and coral green areas turned black (Fig. 9). Soles of hands and feet became whitish, tubercles now white.

Osteology (Fig. 11)**.** Skull wider than long, lacking ornamentation on dermal roofing bones. Jaw joint anterior to otic region. Parotic plate incompletely ossified but synostosed to frontoparietal. Premaxillae without teeth, with a robust pars dentalis and a robust alary process taller than wide and widely separated from nasals. Maxillae and mandibles curved and without teeth. Quadratojugals thin and elongate with broad articulation with maxillae. Pterygoids slender, with a long medially curved anterior ramus with broad articulation with adjacent maxilla, short posterior ramus approaching jaw joint, and short medial ramus approaching prootic. Vomers large and plate-like, without teeth, with short pointy mediolateral processes. Neopalatines synostosed (left) or approaching (right) anterior ramus of pterygoid, and synostosed (right) or approaching (left) edge of sphenethmoid. Septomaxillae present at anterior margin of nasal capsule. Prominent sphenethmoid co-ossified across midline and visible in dorsal view between nasals and frontoparietals. Parasphenoid narrows anteriorly and ends in a curve on rostral extent. Squamosals reduced, with dorsalmost otic ramus in contact with frontoparietal dorsally, very reduced zygomatic ramus present, and very poorly developed ventral ramus. Poorly ossified prootic. Columella absent. Posteromedial processes of hyoid ossified and slender.

Eight distinct, procoelous, non-imbricating and not synostosed presacral vertebrae. Atlas without transverse processes, with widely separated cotyles. Sacrum procoelous with laterally expanded transverse processes, bearing expanded diapophyses. Urostyle long and thin, with weakly developed dorsal ridge on proximal half, and bicondylar articulation with sacrum. Firmisternal pectoral girdle, with widely spaced and slender coracoids. Clavicles slender, nearly reaching one another. Scapulae stout, directed laterally but strongly curving dorsally at their lateral extent. No visible ossified sternum or omosternum. Pelvic girdle comprising ilium, pubis, and ischium. Shaft of ilium long and slender, without dorsal crest. Radioulna shorter than humerus. Humerus bearing ventral crest on proximal half, and without medial and lateral crests. Phalangeal formula for manus 2–2–3–3. A single ossified prepollex. Tips of terminal manual phalanges weakly expanded into small knobs. Tibiofibula longer than femur. Phalangeal formula for pes 2–2–3–4–3. A single ossified prehallux. Tips of terminal pedal phalanges weakly expanded as in fingers.

Variation (*P. fernandae* sp. nov. = lineage B). Male (SVL 25.8 mm) smaller than females (28.5–29.9 mm). Male with nuptial pads consisting of a dense cover of minute dark asperities on upper and inner surfaces of finger I and to a lesser extent on the upper medial surface of finger II and inner metacarpal tubercle, absent on females. Male without spines on dorsum or venter, present on females. Male bright plain yellow, different from elaborate dorsal pattern on females.

Measurements of the type series are presented in Table 6, and variation of selected body ratios is summarized in Figure 4. Relative length of toes sometimes IV > III > V > II > I. Subarticular tubercles at the base of fingers: always double on finger I; always double or bilobate on finger II, except for BMNH 2021.7535 on right hand, which is single; always single on fingers III and IV. Subarticular tubercles at the joint between finger phalanges: always double on finger III; always single on finger IV, except for BMNH 2021.7535 on right hand, which is double. Subarticular tubercles at the base of toes: always double on toe I, except for BMNH 2021.7534 on left foot, which is single; always single on toe II, except for ZMB 91790 left foot, which is double; always single on toes III–V, except for BMNH 2021.7534 and BMNH 2021.7535, not visible. Subarticular tubercles at the joint between toe phalanges: when visible, always double on toe III; proximal always double on toe IV, except for ZMB 91790 left foot, which is single; distal always double on toe IV. When single, tubercles are usually rounded, and when double, usually thin and elongated, sometimes extremely pointy. Metatarsal tubercles oval, inner ranging from slightly longer to twice the length of outer. Toes without margin of web. Webbing between base of toes absent or vestigial, not serrated. All female paratypes have spines on top of head. Density of dorsal spines variable (BMNH 2021.7535 > BMNH 2021.7534 > ZMB 91791). Spine tips coloration varies between white, beige and brown. Male (ZMB 91790) with no spines on dorsum or venter, but a few spines on fore and hindlimbs. A few small glandular warts located latero-dorsally, behind parotoid glands.

Dorsal pale markings in life show some differences in shape, extent, and considerable variation in color intensity between type series and holotype. This seems to be at least to some degree substrate-related, and individual toads can apparently change coloration intensity (to darker, brighter, or paler shades of each tone). The shape of the pale dorsal blotches on the paratype females is similar to the typical *Poyntonophrynus* arrangement (e.g. Fig. 10E) (Poynton and Broadley 1988), with the mid-dorsal blotch being roundish or horse-shoe shaped, different from the holotype's, which is triangular. Sections that are bright coral green on the holotype (outlining the black markings) have a paler shade of green in individuals found on reddish gravel ferralitic substrate (BMNH 2021.7535, FKH-1086, Fig. 10E), and very dark (nearly black) green in the specimen collected on a darker substrate in forest (BMNH 2021.7534, Fig. 10D). Pale marking above forearm insertion absent in one female (BMNH 2021.7534), which is generally darker than all others (Fig. 10D). Pale

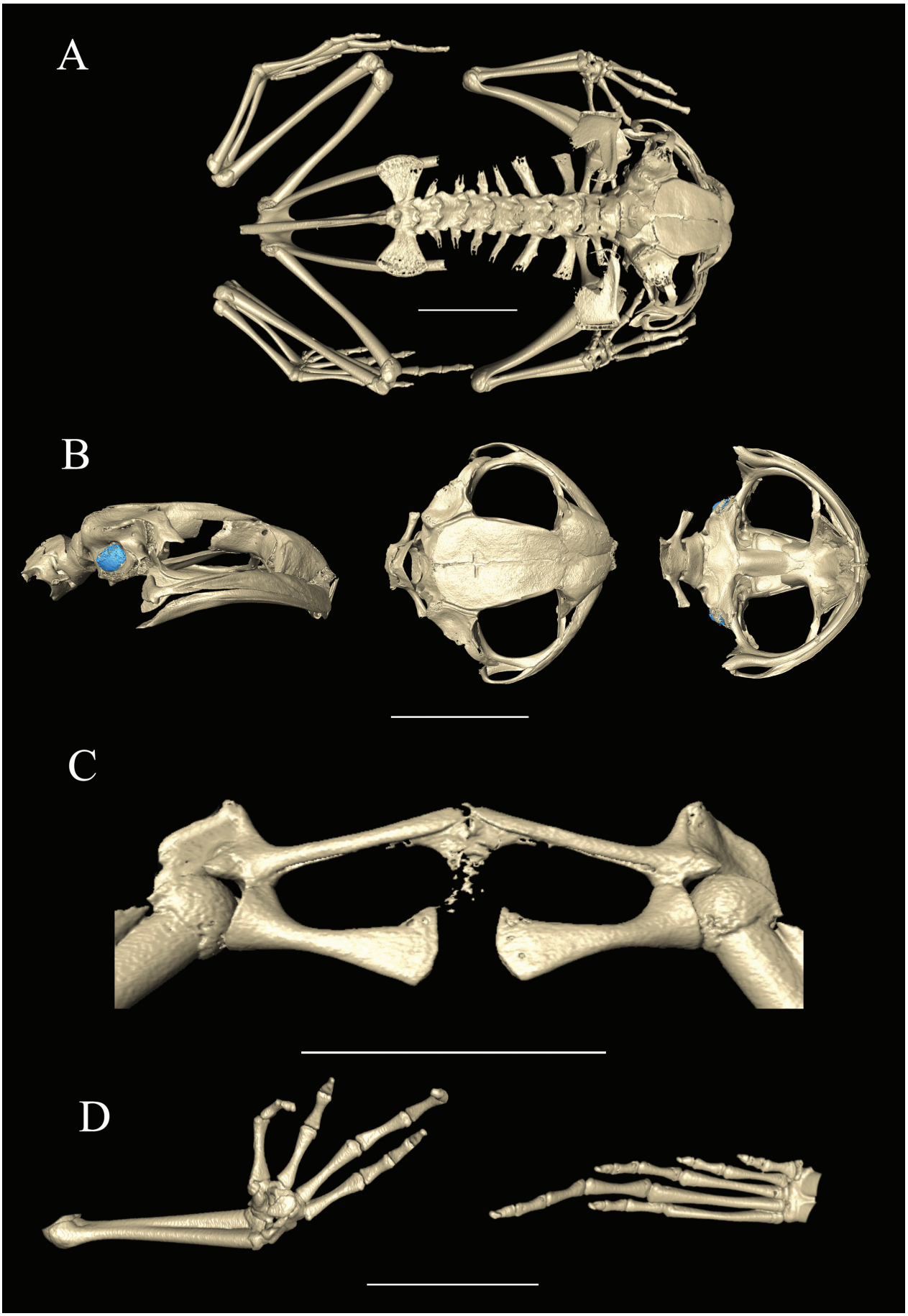

Figure 11. CT-scan of *Poyntonophrynus fernandae* **sp. nov.** female holotype (ZMB 91791). **A** Skeleton in dorsal view. **B** Lateral, dorsal and ventral views of skull (left to right). **C** Pectoral girdle in ventral view. **D** Ventral views of right hand and right foot (left to right). Blue indicates the parotic plate. Scale bars represent 5 mm.

inter-spaces on fore and hindlimbs, that are cream on the holotype, are very bright orange on the specimen found in forest (BMNH 2021.7534, Fig. 10D), and pale beige on individuals found on reddish gravel ferralitic substrate (BMNH 2021.7535, FKH-1086, Fig. 10E). In BMNH 2021.7535 and FKH-1086 all the colors are present (orange, green and beige), but in less intense shades than in holotype, giving a duller aspect that resembles the more common *Poyntonophrynus* coloration. Parotoid glands on females vary from very bright orange (BMNH 2021.7534) to less intense orange (BMNH 2021.7535, FKH-1086), always with a black outer margin, and are lemon yellow on the male (ZMB 91790). The only collected male (ZMB 91790) was uniform lemon yellow in life, that changed to various degrees of yellow-greenish wash after a few days (Fig. 10B, C), and became grey when preserved, with parotoid glands slightly brownish. This plain bright yellow differed completely from all the females' elaborate coloration pattern. Ventral patterning on females varied from immaculate in the male (ZMB 91790), to a sparse speckling of small grey spots placed especially in midline of pectoral region (BMNH 2021.7535, FKH-1086), and similar to holotype (BMNH 2021.7534). Soles of hands and feet whitish or pale grey, tubercles white. Some of the ventral patterning lost intensity or disappeared after preservation.

Male's (ZMB 91790) humerus with medial and lateral distal crests (Fig. 7). Maxillae and mandibles not curved. Neopalatines not synostosed to sphenethmoid, and distant from anterior ramus of pterygoid. Parasphenoid narrowing anteriorly and ending in pointy edge. Ventral rami of squamosals minimally developed, even less than in holotype.

Additional referred specimens. *P.* cf. *fernandae* (lineage A) (Figs 12–14; Tables 5, 6). Males (23.9–24.2 mm, n = 2) smaller than females (30.3–31.8 mm, n = 3). Fewer and less conspicuous ventral speckles in males. Parotoid glands on males more flattened and less conspicuous than on females. Males have the same dorsal coloration pattern than females, but have shades of yellow on the flanks (Fig. 13B, D) (different from *P. fernandae* **sp. nov.** (lineage B), where males are plain yellow). Measurements of the *P.* cf. *fernandae* series are presented in Table 6, and a compilation of selected body ratios in Figure 5. Relative length of fingers sometimes III > IV > II = I. Relative length of toes sometimes IV > III > V > II > I. Subarticular tubercles at the base of finger IV always single. Outer metacarpal tubercle varying between oval and near-triangular, inner metacarpal tubercle always very reduced, sometimes absent. Metatarsal tubercles oval, inner varying between being around the same size to almost two times longer than outer, sometimes being very pointy. Webbing between bases of toes ranging between vestigial to reaching up to the first phalange of toe IV. Conical spines present also on dorsal surface of snout and top of head, with tips being more often white, rarely brown. Parotoid glands elevated, dorsum with glandular warts, located mostly around pale mid-dorsal blotch and dorsolaterally (Fig. 13A). Males sometimes with spines only on fore and hindlimbs, and less conspicuous glandular warts. In life, pale dorsal blotches pale to dark greyish, on a dark brown and dark green ground color (Fig. 13A), distributed along the vertebral region and consisting of a thick conspicuous chevron shaped occipital blotch, extending between the eyes and directed posteriorly, a mid-dorsal horse-shoe shaped blotch, and a small rounded sacral blotch. Glandular warts dark brown. Grey occipital chevron-shaped blotch demarcating dorsal part of head and snout, which are dark brown and dark green. Sides of head grey with dark blotches in front, behind and below the eye. Parotoid glands dark brown. Iris green and golden. Flanks with alternate dark brown, dark green, black and grey thick vermiculation. Dorsal surface of limbs and distal digits grey with dark brown cross-bands with similar width than the pale grey inter-spaces. On females, chest and belly region adjacent to flanks heavily marked with thick black speckles, which sometimes reach throat and belly.

All analyzed specimens (ZMB 91785 (Fig. 14) and BMNH 2021.7536, females; and ZMB 91786, male) had vomers with very elongated, thin, and pointy mediolateral processes, and not curved maxillae and mandibles. ZMB 91785 parasphenoid narrowing anteriorly and arrow shaped at rostral extent. Squamosals of ZMB 91785 reduced, with only dorsalmost otic region, and negligible zygomatic and ventral ramus, which are even more reduced in ZMB 91786. ZMB 91785 neopalatines with small ventral process, in contact with the edges of sphenethmoid, and approaching, but not in contact with, maxillae and anterior ramus of pterygoid distally. BMNH 2021.7536 neopalatines approaching (right) and synostosed (left) to sphenethmoid. ZMB 91786 with ventral process only on left neopalatine. Both ZMB 91786 and BMNH 2021.7536 had single ossified prepollices and prehalluxes, and ossified and slender posteromedial processes of hyoid. In ZMB 91785, prepollex and prehallux not visible due to the resolution of the microCT-scan, and there is also no visible ossification on posteromedial processes of hyoid. Male (ZMB 91786) with short medial and lateral distal humeral crests (Fig. 7).

Natural history and habitat. All specimens were collected in the rainy season. *Poyntonophrynus fernandae* **sp. nov.** (lineage B) ZMB 91790 and ZMB 91791 (male and female) were found during the day, on November 22nd 2017, on a site approximately 12 km northwest of the village of Condé, with the male displaying bright lemon yellow coloration. The female was found on the ground at the base of a hill with many large granite boulders, while the male was found higher up on moist ground with moss near a natural water seepage. These two individuals were kept alive for three days, upon which the coloration in the male faded to a darker yellow-greenish color (Fig. 10B, C), a case of dynamic sexual dichromatism. BMNH 2021.7535, FKH-1086 (two females) were collected shortly after a thunderstorm, near the town of Quibala, in degraded savanna habitat with large granitic boulders. The brightly colored female specimen BMNH 2021.7534 was also collected in November, found on the

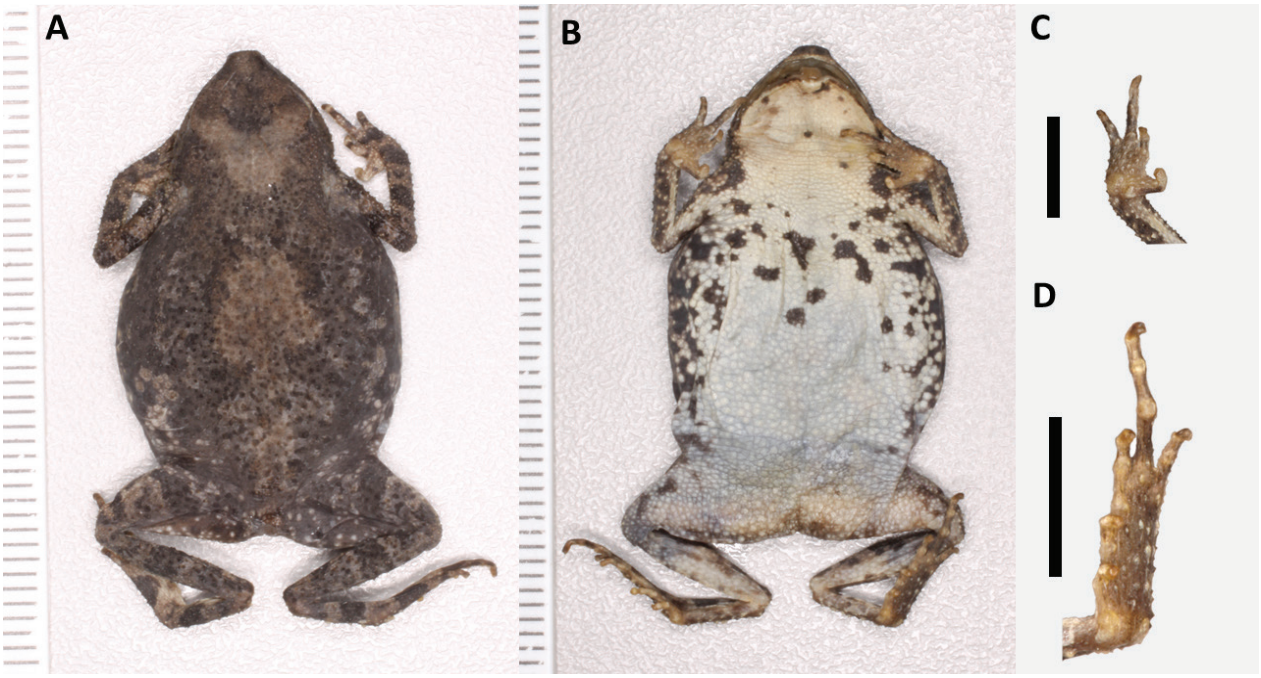

Figure 12. *Poyntonophrynus* cf. *fernandae* (lineage A) (ZMB 91785, female) in preservative. **A** Dorsal view. **B** Ventral view. **C** Palm of right hand. **D** Palm of left foot. Short scale bars represent 1 mm (A, B), black scale bars represent 5 mm (C, D).

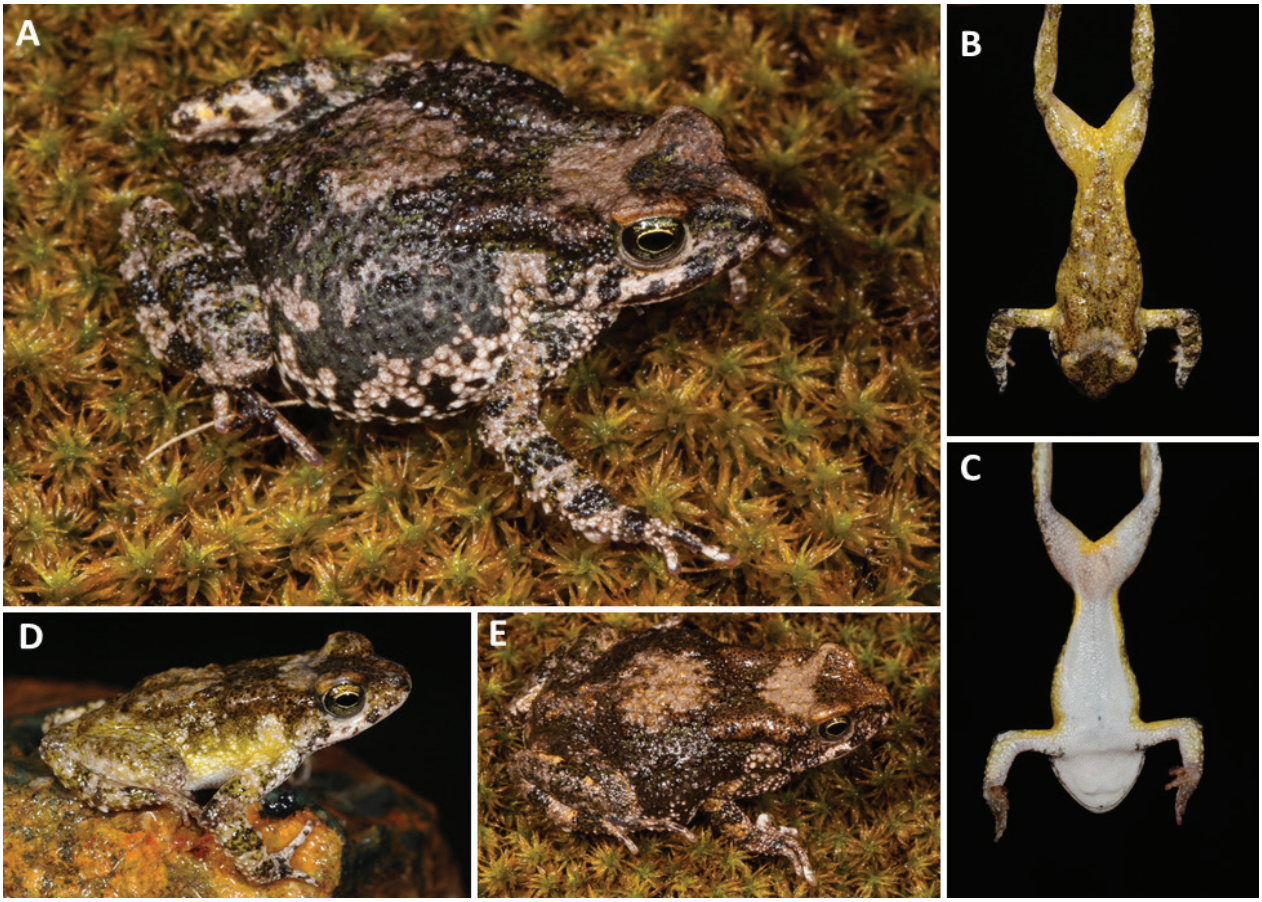

Figure 13. Coloration of live *Poyntonophrynus* cf. *fernandae* (lineage A). **A** Female (ZMB 91785). **B–D** Male (ZMB 91786) with partial yellow coloration. **E** Female (BMNH 2021.7536). Photos by W.R. Branch (B–D).

ground but at night, well inside a moist forest block after rains, and not near water. One amplectant pair ascribed to this species was observed during the day near the town of Gabela (Fig. 10F). The species was always found in close proximity to large granite boulders at elevations from 520 m to 1303 m a.s.l. approximately, but the surround-

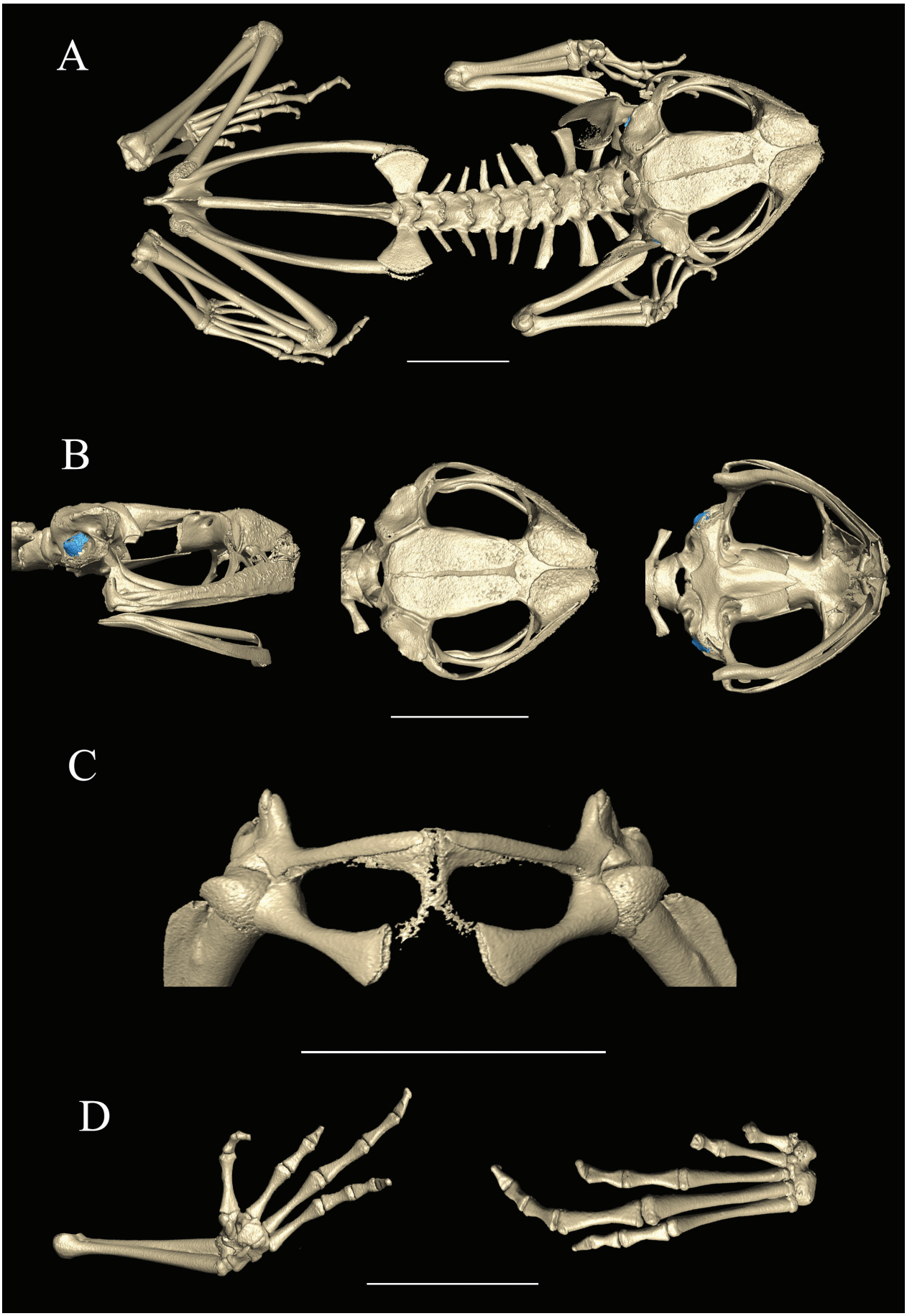

Figure 14. CT-scan of *Poyntonophrynus* cf. *fernandae* (lineage A) (ZMB 91785, female). **A** Skeleton in dorsal view. **B** Lateral, dorsal and ventral views of skull (left to right). **C** Pectoral girdle in ventral view. **D** Ventral views of right hand and right foot (left to right). Blue indicates the parotic plate. Scale bars represent 5 mm.

ing habitat was diverse, including moist escarpment forest at lower elevation (Congulo), secondary coffee forest (plantation of exotic tree species – *Grevillia robusta*) near Condé and degraded Miombo savanna at Quibala (Fig. 8), both the latter at higher elevations. Amphibian species found in sympatry included *Hyperolius cinnamomeoventris* Bocage, 1866, *H. parallelus* Günther, 1858, *H. platyceps* (Boulenger, 1900), *Kassina senegalensis* (Duméril & Bibron, 1841), *Leptopelis* cf. *cynammomeus* (Bocage, 1893), *L.* cf. *jordani* Parker, 1936, *Ptychadena anchietae* (Bocage, 1868), *Sclerophrys pusilla* (Mertens, 1937).

Poyntonophrynus cf. *fernandae* (lineage A) from Chinhundo, in Namba region, differed in some respects from *P. fernandae* **sp. nov.** (lineage B). Two males were collected in November 2016, while active during the day and after heavy rains, showing partially yellow-greenish coloration (Fig. 13B–D), found in syntopy with *P. nambensis* **sp. nov.** On the same location, in October 2020 and also following rains, three gravid lineage A females were collected at night, and again in syntopy with *P. nambensis* **sp. nov.** All *P.* cf. *fernandae* (lineage A) were found on the steep slopes of the same large rock boulder, among moss and water seepages (Fig. 8). The surrounding habitat was montane grasslands with stunted Miombo savanna, and some remnant patches of Afromontane forest in nearby ravines.

Distribution and conservation. *P. fernandae* **sp. nov.** sensu stricto. The species is known from the Angolan central escarpment zone in the region of Gabela, and extending eastwards at least to Quibala, in Cuanza-Sul province, at elevations of 520–1303 m a.s.l. (Fig. 1). It appears to be strongly associated with large granite boulders in moist habitats, and may be more widely distributed along the western escarpment and large rock outcrops in central Cuanza-Sul province. Some of the habitats where it has been recorded were highly threatened by deforestation for wood, agriculture, and encroachment by invasive species (*Inga vera*). From Chinhundo, Namba, at an elevation of 1730 m a.s.l., in southern Cuanza-Sul Province we recorded *P.* cf. *fernandae* (lineage A). This site lies on in the Angolan highlands, on the south-western foothills of Namba mountain chain (Fig. 1). In all other surveyed sites around Namba region we failed to find this toad, including additional places where we retrieved *P. nambensis* **sp. nov.** Currently the conservation status of *P. fernandae* sensu lato needs to remain Data Deficient (DD) as per IUCN Red List Guidelines (IUCN 2022).

Etymology. The specific epithet *fernandae* (Pt.) is a tribute to Fernanda Lages, a researcher and professor of Genetics based in Lubango, Angola. Her continuous investment in capacity building over the last decades and dedication to various research projects and international collaborations gave opportunities and transformed the professional paths of several young Angolan biologists, and thus of research in Biology in the country. The name, built in the feminine singular genitive, also pays homage to women in science. We suggest "Fernanda's pygmy toad" and "sapo pigmeu da Fernanda" as English and Portuguese common names, respectively.

Poyntonophrynus nambensis sp. nov.

https://zoobank.org/D875E1E8-637D-4664-A8EA-E3EAE7D78942

Figures 5–7, 15–17; Tables 5, 7

Holotype. ZMB 91787, adult female, collected in granite bedrock 200 m S of old farm paddock, in Fazenda Namba, Cuanza-Sul Province, –11.914167°, 14.820556°, 1840 m a.s.l., 03 November 2016, by Ninda L. Baptista, Pedro Vaz Pinto and William R. Branch (Figs 5–7, 15–17).

Paratypes. CHL 0326, BMNH 2021.7538, BMNH 2021.7539, 3 females, same data as holotype; BMNH 2021.7540, ZMB 91788, two males, same data as holotype; FKH-0378, FKH-0379, FKH-0380, FKH-0381, four males, collected at night on bedrock near forested stream, in Missão da Namba, Cuanza-Sul Province, –11.922078°, 14.835542°, 1740 m a.s.l., 11 February 2020, by Pedro Vaz Pinto and Javier Lóbon-Rovira; FKH-0377 unconfirmed sex, same data as FKH-0378–0381; FKH-0457, FKH-0458, FKH-0462, ZMB 91789, four females, collected approximately 12 km W of Missão da Namba, Chinhundo, Cuanza-Sul Province, –11.914685°, 14.740552°, 1730 m a.s.l, 16 October 2020, by Pedro Vaz Pinto; CHL 0472, eggs, same data as holotype.

Definition. A medium-sized pygmy toad with females larger and rougher than males. No tarsal fold. Subarticular tubercles at the base of fingers and toes usually single, remaining ones, located at the joint between phalanges, usually double. Tympanum varies between visible and not visible. Conspicuous protuberant parotoid glands, with curved outer edge. Very conspicuous dorsal glandular warts. Usually 1.75 phalanges of toes III and V free of web, webbing between toes III and IV vestigial, not serrated. Two enlarged well-developed palmar tubercles: large, rounded to triangular-shaped outer metacarpal tubercle, and smaller oval inner metacarpal tubercle. Typical *Poyntonophrynus* dorsal coloration: one pale occipital blotch, one mid-dorsal blotch, one sacral blotch, and one pale blotch over arm insertion. In most individuals, the occipital and mid-dorsal pale blotches are connected in the vertebral area, resembling an hourglass shape only observed in this species. Dorsal coloration identical in both sexes, generally dull, varying in shades of grey, beige and brown with some traces of brick orange and dark brown. Dark cross-bands on limbs around the same width as pale interspaces.

Diagnosis. *Poyntonophrynus nambensis* **sp. nov.** differs from *P. pachnodes* and *P. fernandae* **sp. nov.** sensu lato in having a columella. It differs from *P. pachnodes* in having a better-developed neopalatine. Differs from *P. fernandae* **sp. nov.** sensu lato in ventral patterning (few speckles along midline of chest, and dark line in front of arm insertion vs. scattered speckles at least on the chest), and dorsal coloration (dorsal pale hourglass-shaped blotch almost always present vs. absent), and breeding male coloration

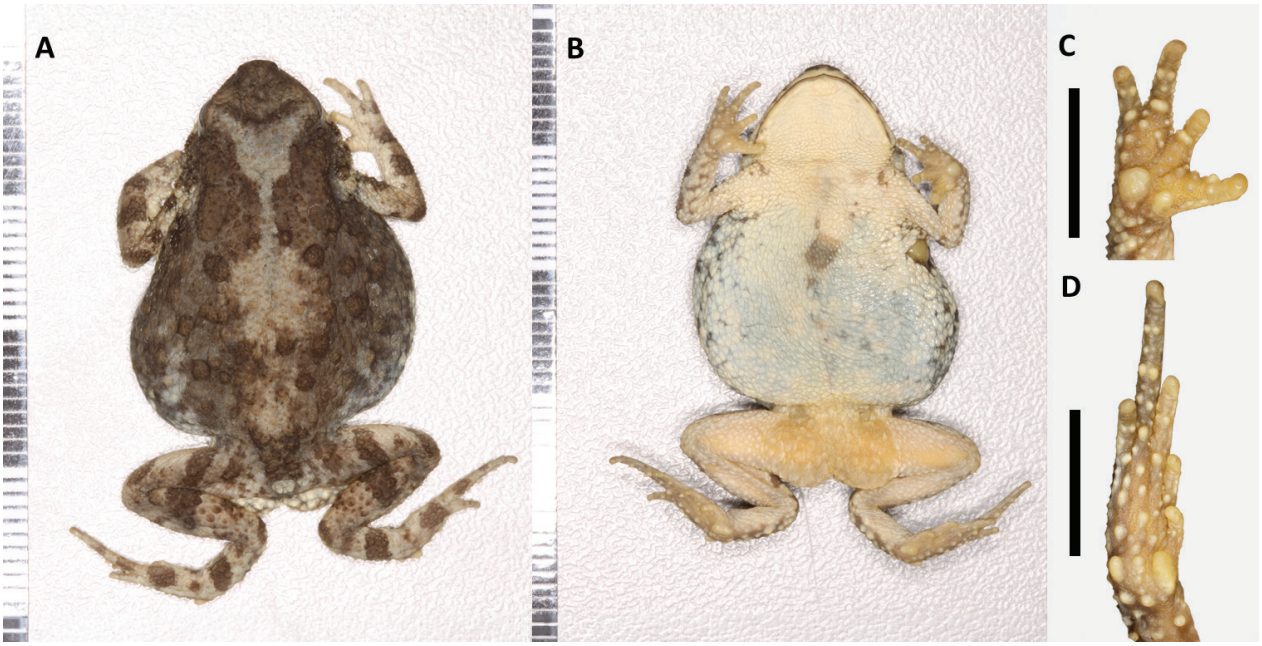

Figure 15. Holotype of *Poyntonophrynus nambensis* **sp. nov.** (ZMB 91787, female) in preservative. **A** Dorsal view. **B** Ventral view. **C** Palm of right hand. **D** Palm of right foot. Photos by F. Tillack. Short scale bars represent 1 mm (A, B), black scale bars represent 5 mm (C, D).

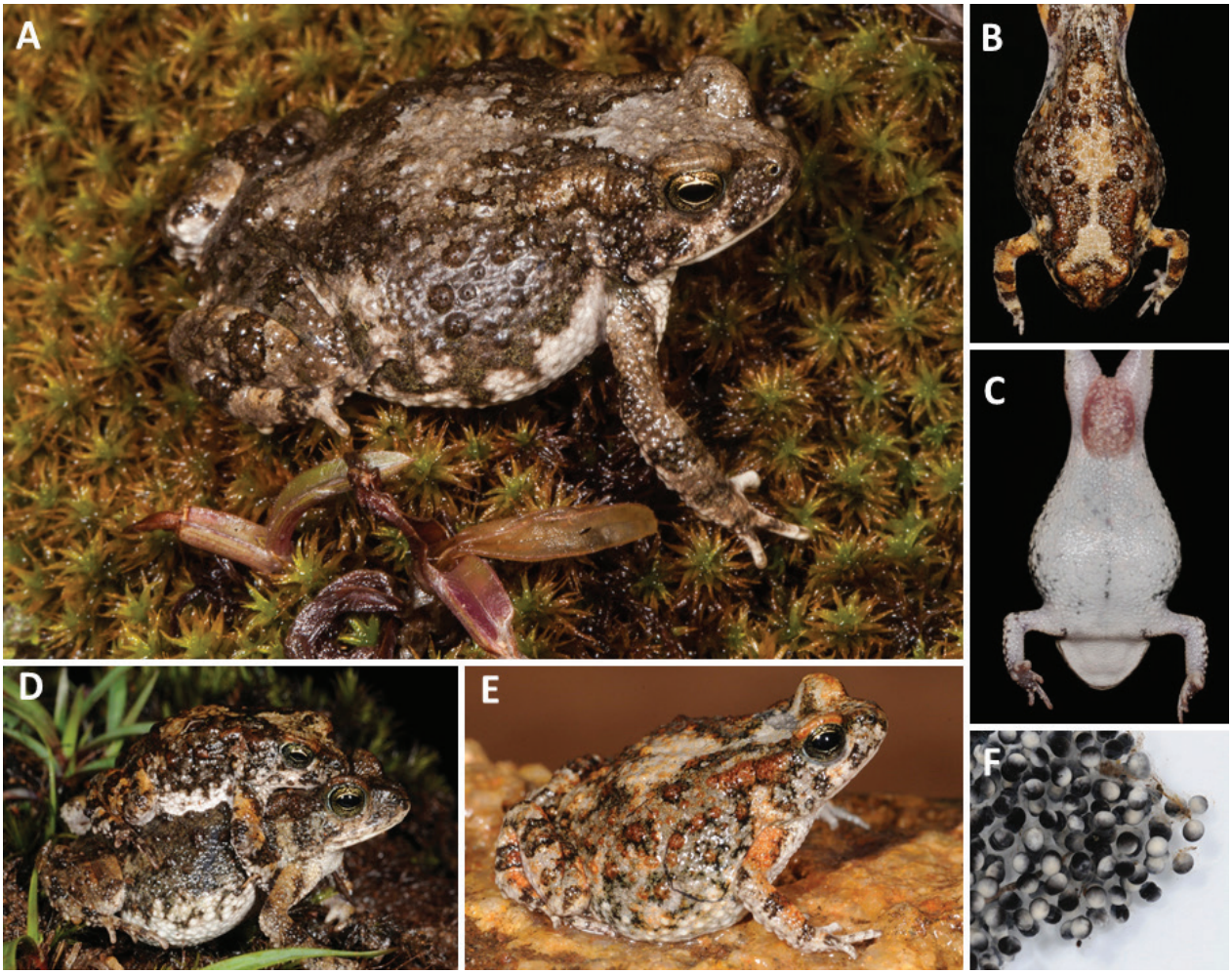

Figure 16. Pictures of live *Poyntonophrynus nambensis* **sp. nov.** **A** Female paratype (FKH-0458) with greyish coloration. **B**, **C** Female holotype (ZMB 91787) with dorsal and ventral coloration, respectively. **D** Pair in axillary amplexus [female (CHL0326), and male (BMNH 2021.7540) paratypes]. **E** Female paratype (BMNH 2021.7539) with brighter shades of brown and orange. **F** Eggs (CHL0472). Photos by W.R. Branch (B–F).

(dulls, similar to females vs. partially or completely bright yellow). It differs from *P. beiranus* in parotoid glands conspicuousness (conspicuous, elevated, with clearly demarcated margins vs. inconspicuous), and dorsal patterning (vertebral line absent vs. present). It differs from *P. damaranus* in ventral patterning (few dark speckles along midline of chest, and dark line in front of arm insertion vs. immaculate). It differs from *P. dombensis* in tympanum size (when visible, between 0.5 and 0.6 times internarial distance, vs. conspicuous and around 0.7 times internarial distance), and ventral patterning (few speckles along midline of chest, and dark line in front of arm insertion vs. immaculate). It differs from *P. fenoulheti* in parotoid glands width (thinner or around same width of eye diameter vs. wider than eye diameter). It differs from *P. grandisonae* in tympanum size (when visible, between 0.5 and 0.6 times internarial distance, vs. same width or wider than internarial distance) and skin texture (rough vs. leathery). It differs from *P. grindleyi* in pale occipital and sacral patches (present vs. absent), dorsal spines (small vs. large), and ventral coloration (few dark speckles along midline of chest, and dark line in front of arm insertion vs. dark thick ventral marbling). It differs from *P. hoeschi* in ventral patterning (few speckles along midline of chest, and dark line in front of arm insertion vs. immaculate). It differs from *P. jordani* in shape of parotoid glands (kidney-shaped vs. a cluster of glands) and pale occipital patch (present vs. absent). It differs from *P. lughensis* in conspicuousness of parotoid glands (conspicuous vs. inconspicuous). It differs from *P. kavangensis* in foot webbing (non-serrated vs. serrated), dorsal patterning (absent vertebral line vs. present), and ventral patterning (few speckles along midline of chest, and dark line in front of arm insertion vs. immaculate). It differs from *P. parkeri* in development of parotoid glands (elevated vs. flattened). It differs from *P. vertebralis* in dorsal patterning (absent vertebral line vs. present), ventral patterning (few speckles along midline of chest, and dark line in front of arm insertion vs. distinct thick dark blotches), and conspicuousness of parotoid glands (conspicuous vs. inconspicuous).

Holotype description. ***External morphology.*** Small (SVL 31.9 mm), robust gravid female (Fig. 15, Fig. 16B, C, all measurements in Table 7). SVL approximately 2.9 times head width, 3.9 times head length, 2.8 times thigh length, 2.9 times tibiofibula length, and 4.8 times forearm length. Head rounded in dorsal view. Head length approximately 0.7 head width. Snout profile rounded, snout projecting slightly beyond upper jaw. Rostral tip rounded in dorsal, ventral and lateral views. Eyes projecting laterally just beyond eyelids and not beyond margins of head in dorsal view. Around a third of the eye projecting above dorsal margin of head in lateral view. Interorbital distance approximately 0.9 times eye diameter and 1.4 times internarial distance. Eye diameter approximately 0.9 times eye-nostril distance, and 2.7 times naris to rostral tip distance. Naris small, oval, directed dorsolaterally. Tympanum visible under dissecting microscope, approximately 0.3 times eye diameter. Canthus rostralis sharp. Loreal region concave. Limbs and digits robust and well-developed. Tarsal fold absent. Digits of manus and pes elongated. Finger III length approximately 0.5 times hand length. Relative length of fingers: III > I > IV = II. Finger tips rounded, not expanded to discs. Fingers with prominent subarticular tubercles that are single at the base of fingers II, III and IV, double at the base of finger I, and bilobate under fingers III and IV, on the right hand; and always double or bilobate, except at the base of fingers III and IV, which are single, on the left hand. Plants of hands beset with supernumerary tubercles. Digits with subdigital tubercles, often double. Inner and outer metacarpal tubercles very well developed (Fig. 15C), approximately oval in shape, the first being around twice as long as the latter. Webbing between manual digits absent. Toe IV length approximately 0.6 times foot length. Relative length of toes IV > III > V > II > I. Toe tips rounded, not expanded to discs. Prominent subarticular tubercles that are single at toe bases, the remaining being double. Double subdigital tubercles. Toes without a margin of web. Webbing between toes vestigial, only at the base of toes, webbing margin not serrated. Prominent oval inner and outer metatarsal tubercles, the first around twice longer than the latter. Inner metatarsal tubercle around half the length of toe I.

Dorsal skin rough, with brown-tipped conical spines on dorsum, arms, legs, dorsal and lateral surface of snout, top of head, and outer ring of tympanum. Ventral, gular skin, and ventral surface of limbs granular with no spines. Dorsum with very prominent rounded glandular warts, located mostly around pale mid-dorsal and sacral blotches, and dorsolaterally towards the flanks (Fig. 16B). Parotoid glands elongated, elevated, with clearly discernible margins, with a curved outer margin, placed dorsolaterally and extending from behind the eye to slightly beyond the forearm insertion. Both kidney-shaped, but the right one consisting of a single mass, and the left broken in the middle, consisting of a junction of two masses.

Color. In life, dorsal coloration consists of a set of pale beige blotches distributed along the vertebral region, forming a symmetrical pattern (Fig. 16B). These include a thick conspicuous chevron-shaped occipital blotch extending between eyes and directed posteriorly, connected to a mid-dorsal roundish blotch (the connection between these two blotches resembling an hourglass shape), and a small rounded sacral blotch. Rest of the dorsum with dark-, coppery- and orangey-brown mottling. Dark brown glandular warts located around the mid-dorsal blotch and towards the flanks. A thin dark brown interorbital bar, forming the anterior border of the beige occipital patch. Anterior to it, one continuous interorbital brown thin chevron directed posteriorly. Brown dorsum of head and snout. A dark brown line extending from anterior corner of eye to tip of snout. A pale beige blotch under both eyes. Conspicuous beige blotch above arm insertion. Parotoid glands brown. Eyelid brick orange. Iris olden. Pupil black ellipsoid. Flanks with dark brown (corresponding to glandular warts) and coppery markings on a pale grey background, becoming faint towards the venter. Dorsal surface of forelimbs and fingers III and IV pale beige, with dark brown cross-bands thinner than the

Table 7. Measurements (in mm) of type series of *Poyntonophrynus nambensis* **sp. nov.** (lineage C). For abbreviations see Methods section. M—male, F—female, U—unidentified.

Current catalogue number	**ZMB 91787**	**CHL 0326**	**BMNH 2021.7538**	**BMNH 2021.7539**	**BMNH 2021.7540**	**ZMB 91788**	**FKH-0377**	**FKH-0378**	**FKH-0379**	**FKH-0380**	**FKH-0381**	**FKH-0457**	**FKH-0458**	**ZMB 91789**	**FKH-0462**
Former catalogue number	**CHL 0456**	—	CHL 0327	CHL 0328	CHL 0329	CHL 0457	—	—	—	—	—	—	—	FKH-0460	—
Field number	**NB456**	NB326	NB327	NB328	NB329	NB457	JLRZC0027	JLRZC0028	JLRZC0029	JLRZC0030	JLRZC0031	P0-32	P0-33	P0-35	P0-37
Type status	**Holotype**	Paratype	Paratype	Paratype	Paratype	Paratype	Paratype	Paratype	Paratype	Paratype	Paratype	Paratype	Paratype	Paratype	Paratype
Sex	**F**	F	F	F	M	M	U	M	M	M	M	F	F	F	F
SVL	**31.9**	30.2	30.7	31.7	24.2	26.5	26.4	24.4	25.0	26.4	25.0	32.9	33.4	34.9	31.3
HW	**11.0**	10.6	11.4	11.1	9.1	10.6	9.2	9.0	9.0	9.6	9.1	10.7	11	11.7	10.2
HL	**8.1**	7.8	8.5	8.1	7.1	7.9	6.7	7.3	6.8	7.1	6.9	7.7	7.2	8.2	7.6
IOD	**3.0**	2.6	2.5	2.7	2.0	2.6	1.9	2.2	2.4	2.6	2.4	2.3	2.5	2.9	2.0
TDH	**1.2**	1.2	1.2	—	1.1	1.1	—	—	—	—	—	1.2	—	—	1.1
ED	**3.5**	3.2	3.5	3.1	2.9	3.1	2.8	2.8	2.8	2.6	2.5	2.9	2.9	3.0	2.9
IND	**2.2**	2.1	2.1	2.1	2.0	2.2	1.7	1.7	1.7	1.9	1.7	2.2	2.1	2.3	1.9
END	**2.7**	2.3	2.3	2.5	2.1	2.4	2.5	2.1	2.2	2.1	2.2	2.1	2.3	2.8	2.4
UEW	**2.3**	2.5	2.9	2.8	2.7	2.7	1.8	2.0	1.7	2.3	2.0	2.2	2.4	1.9	2.3
SL	**3.4**	4.0	4.1	3.8	3.6	3.5	3.2	3.3	3.1	3.2	3.1	3.7	3.5	4.1	3.2
NS	**1.3**	1.6	1.4	1.7	1.4	1.6	1.1	1.1	1.0	1.3	1.0	1.4	1.3	1.4	1.4
THL	**11.3**	12	11.9	11.2	9.9	10.9	9.7	10	10.5	9.9	9.2	9.6	10.8	11.7	10.5
TL	**10.9**	10.6	11.4	10.4	9.7	10.4	9.7	9.0	9.4	9.8	8.9	10.8	10.5	11.5	10.6
TaL	**5.8**	5.8	5.3	5.4	5.3	5.6	4.7	4.5	4.7	5.0	4.9	6.4	6.2	6.1	5.6
FL	**11.1**	11.0	10.4	10.6	9.6	10.3	9.6	8.3	9.5	9.9	9.9	10.7	10.7	10.9	9.6
Toe4L	**6.1**	5.5	5.1	5.3	4.7	5.1	4.9	4.4	4.7	5.2	4.6	5.9	5.4	4.9	4.8
IMTL	**1.6**	1.4	1.4	1.7	1.3	1.2	1.2	1.3	1.2	1.5	1.3	1.2	1.3	1.4	1.2
UAL	**4.7**	4.6	4.9	4.5	4.4	4.9	3.5	3.4	4.2	4.6	3.8	5.0	5.6	5.9	4.8
FLL	**6.6**	6.1	6.6	6.5	5.9	6.9	5.4	5.3	5.5	5.9	5.5	6.5	6.7	7.0	6.1
HAL	**6.3**	6.1	6.5	6.5	4.8	5.8	5.3	5.0	5.4	5.7	4.9	6.6	6.6	6.8	5.6
Fin3L	**3.6**	3.2	3.4	3.4	2.3	2.6	2.5	2.2	2.8	3.0	2.2	2.8	3.4	3.1	2.9

beige inter-spaces. Dorsal surface of fingers I and II pale grey. Dorsal surface of hindlimbs (thighs and crus) beige with two dark brown cross-bands thinner than the beige inter-spaces. Dark cross-bands on thigh, crus and feet touching when legs flexed. Ventral skin almost immaculate white, with dark spots placed in midline of pectoral region, and a dark line curving down in front of insertion of arm (Fig. 16C). Plantar surface of manus and pes grey with white tubercles. Preserved specimen, after six years in ethanol, pale beige and grey blotches turned pale grey, and dark blotches (shades of brown) turned dark grey (Fig. 15). A large grey blotch on mid chest corresponding to area where formalin was injected for preservation, unrelated to natural pigmentation (Fig. 15B).

Osteology (Fig. 17)**.** Skull wider than long, without ornamentation on dermal roofing bones. Jaw joint anterior to otic region. Parotic plate incompletely ossified but synostosed to frontoparietal. Premaxillae lacking teeth, with robust pars dentalis and robust alary process that is taller than wide, and widely separated from nasals. Maxillae and mandibles without teeth. Quadratojugals thin and elongate with broad articulation with maxillae. Pterygoids slender, with long medially curved anterior ramus with broad articulation with adjacent maxilla, short posterior ramus approaching jaw joint, and short medial ramus approaching prootic. Vomers large and plate-like, without teeth, with short and pointy mediolateral processes, and reduced anterior processes. Neopalatines thin flat rods, approaching but not in contact with edges of sphenethmoid, maxillae, and anterior ramus of pterygoid distally. Septomaxillae present at anterior margin of nasal capsule. Prominent sphenethmoid co-ossified across midline and visible in dorsal view between nasals and frontoparietals. Parasphenoid narrowing anteriorly and exhibiting a small bifurcation at its anterior extent. Squamosals reduced, with dorsalmost otic region, reduced zygomatic ramus present, and vestigial ventral ramus separate from main bone. Prootic poorly ossified. Columella well ossified, with pars interna plectri developed as an expanded knob on medial end of pars media plectri, which is antero-posteriorly compressed. Posteromedial processes of hyoid ossified and slender.

Eight distinct, procoelous, non-imbricating, not synostosed presacral vertebrae. Atlas without transverse processes, with widely separated cotyles. Sacrum procoelous with laterally expanded transverse processes, bearing expanded diapophyses. Urostyle long and thin with weakly developed dorsal ridge on proximal half, a small pointy posteriorly directed protrusion on the right side of its right cotyle, and bicondylar articulation with sacrum. Pectoral girdle firmisternal, with widely spaced and slender coracoids. Clavicles slender, nearly reaching one another. Scapulae are stout, directed laterally but strongly curving dorsally at lateral extent. No visible ossified sternum or omosternum. Pelvic girdle comprising ilium, pubis, and ischium. Shaft of ilium long and slender, lacking a dorsal crest. Radioulna shorter than humerus. Humerus bearing a ventral crest on proximal half, and without medial and lateral crest. Phalangeal formula for manus 2–2–3–3. Ossified prepollex formed by two elements, a rounded proximal element, and a thinner, elongated and pointy distal element. Tips of terminal manual phalanges weakly expanded into small knobs. Tibiofibula around same length as femur. Phalangeal formula for pes 2–2–3–4–3. Tips of terminal pedal phalanges weakly expanded as in fingers. A single ossified prehallux.

Variation. Males (SVL 24.4–26.4 mm, n = 6) smaller than females (30.7–34.9 mm, n = 8). Males with a dense covering of minute dark asperities on upper and inner surfaces of finger I and to a lesser extent on the upper medial surface of finger II and inner metacarpal tubercle. Males with smoother skin than females, with few spines on snout, different from females, which have a rough dorsal skin. Parotoid glands on males less conspicuous and more flattened than on females.

Measurements of the type series are presented in Table 7, and variation in selected body ratios is summarized in Figure 4. Relative length of fingers sometimes III > IV > II = I. Relative length of toes sometimes IV > III > V > II > I, rarely IV > V > III > II > I. Variation on subarticular tubercles based on five paratypes (ZMB 91788–9 and BMNH 2021.7538–40). Subarticular tubercles at the base of fingers: always double or bilobate on fingers I and II; always single on finger III except for ZMB 91788 on right hand, which is bilobate, and for BMNH 2021.7540 and ZMB 91788 on both hands, which are double; always single on finger IV except for BMNH 2021.7540 on right hand, and for BMNH 2021.7539 on left hand, which are double. Subarticular tubercles at the joint between finger phalanges: always double on finger III; always single on finger IV, except for BMNH 2021.7538 on right hand, which is double, and for ZMB 91788 on right hand, which is absent. Subarticular tubercles at the base of toes: always double on toe I, except for BMNH 2021.7538 on both feet and for BMNH 2021.7540 on left foot, which are single, and for ZMB 91788 and BMNH 2021.7539 on left feet, which are not visible; always single on toe II, except for BMNH 2021.7539 which are double on both feet; always single on toes III–V. Subarticular tubercles at the joint between toe phalanges: always double on toe III; always double on toe IV except for ZMB 91790, distal one on right foot, which is single; always single on finger V, except for BMNH 2021.7540 on both feet and for ZMB 91788 on right foot which are absent, and ZMB 91789, which is double on both feet. Tympanum's conspicuousness variable, being conspicuous (CHL 0326, FKH-0462), visible (BMNH 2021.7540, FKH-0377, FKH-0380, FKH-0457, ZMB 91788), and not visible in almost half of the collected specimens (BMNH 2021.7538–9, FKH-0378–9, FKH-0381, FKH-0458, ZMB 91789). Metatarsal tubercles oval, outer between half and two thirds the length of inner. Male paratypes usually with no spines, except on snout. Parotoid glands kidney-shaped, but very often in paratypes they look like the holotype's left one, broken in the middle, consisting of two masses. Plants of hands and feet beset with supernumerary tubercles, less densely on feet than on hands. Spine tips vary in coloration between white, beige and brown.

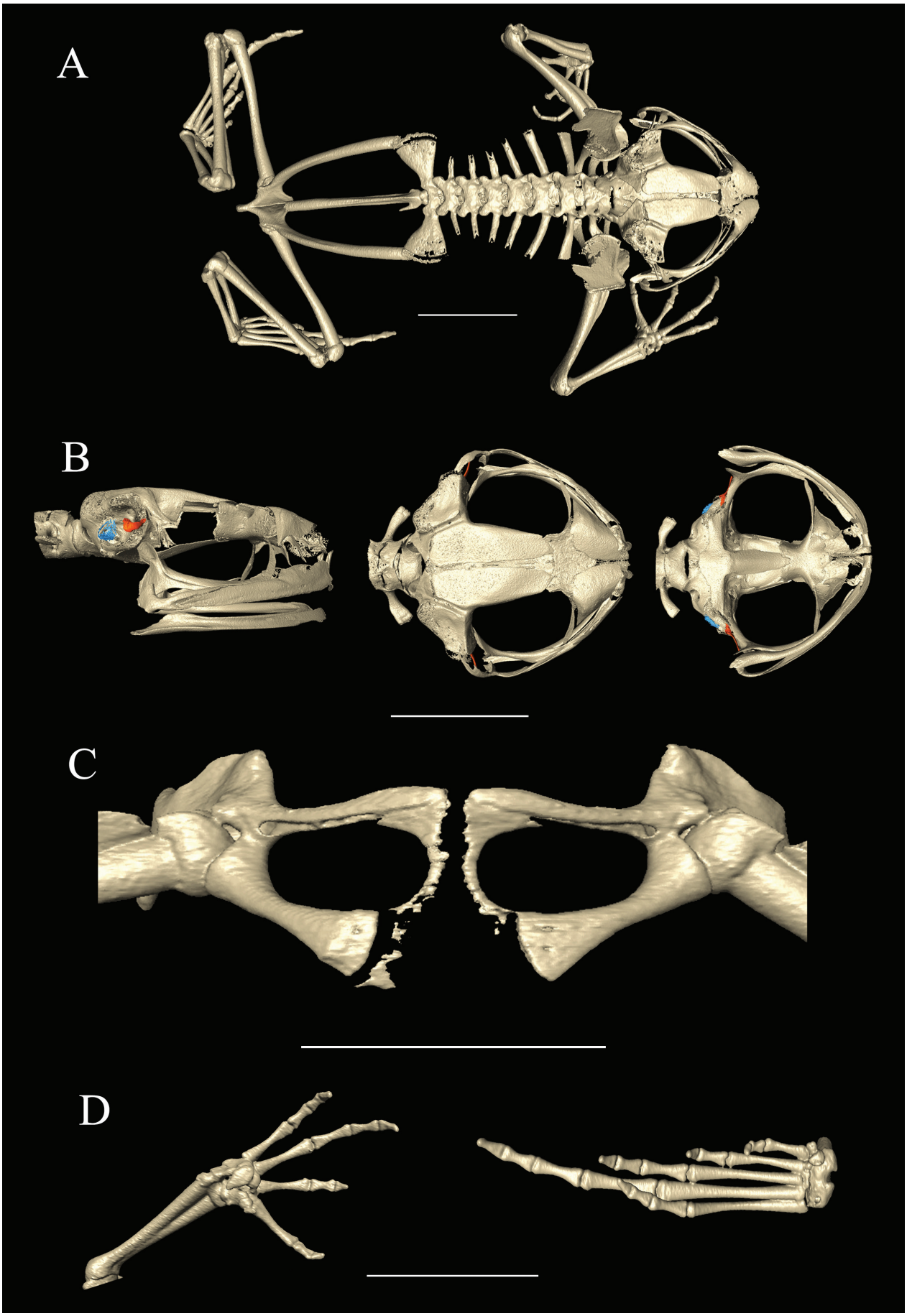

Figure 17. CT-scan of *Poyntonophrynus nambensis* **sp. nov.** holotype (ZMB 91787, female). **A** Skeleton in dorsal view. **B** Lateral, dorsal and ventral views of skull (left to right). **C** Pectoral girdle in ventral view. **D** Ventral views of right hand and right foot (left to right). Blue indicates the parotic plate, orange indicates the columella. Scale bars represent 5 mm.

Coloration varying in shades of grey, beige and brown with some traces of brick orange and dark brown (Fig. 16). Color intensity of pale dorsal blotches varied from pale grey (BMNH 2021.7538, BMNH 2021.7540, CHL 0326, FKH-0380, ZMB 91788) to very dark grey (FKH-0377–81, FKH-0457–8, FKH-0462, ZMB 91789). Ventral markings, anterior surface of forearm, posterior surface of tarsus, and palm of manus and pes with similar variation of color intensity. Except for BMNH 2021.7539, which has an immaculate venter, all individuals have dark spots placed along midline of pectoral region, and a dark line curving down in front of insertion of arm, that vary in size and form (usually more elongated antero-dorsally on males, and less elongate on females) (Fig. 16C). Dorsal hourglass-shaped blotch only absent in three out of 14 paratypes (CHL 0326, FKH-0378–9) (Fig. 16A). Soles of hands and feet from pale to very dark grey.

Humeri of male ZMB 91788 with a well-developed medial distal crest and a more discrete lateral distal crest (Fig. 7). Regular urostyle, with no pointy protrusion. Parasphenoid trifurcated anteriorly. Squamosals with reduced ventral rami. Distal element of prepollex very elongated, more than on the female holotype.

Natural history and habitat. The type series was collected in the rainy season, during the night, while breeding in small rocky pools on granite boulders, where two pairs were found in axillary amplexus (Fig. 16D). No advertisement call was heard. All specimens were caught either on moist bedrock or steep boulder faces, near forest streams or natural seepages, while the surrounding habitat included also extensive montane grasslands (Fig. 8). *Poyntonophrynus nambensis* **sp. nov.** seem to be opportunistic feeders, inferring from the stomach content of one gravid female (ZMB 91789), which had ten swarming termites, one beetle (around 1.5 mm), ten ants (nine of which very recently ingested) near 3 mm in length and all morphologically identical, the remnants of the head of a jumping spider, and other non-identified arthropod body parts. One of the females from the type series deposited 545 eggs after being captured. Eggs were arranged in a single string, had black and white poles (Fig. 16F), and a diameter of around 1.5 mm. Amphibian species found in sympatry were *Hyperolius parallelus* (Günther, 1858), *Hyperolius cinereus* Monard, 1937, *Phrynobatrachus* cf. *mababiensis* FitzSimons, 1932, *Ptychadena oxyrhynchus* (Smith, 1849), *Tomopterna tuberculosa* (Boulenger, 1882), and *P.* cf. *fernandae* (lineage A).

Distribution and conservation. This species is only known from the region of Serra da Namba, 1730–1840 m a.s.l., in the Angolan highlands. It has been recorded in various sites in relatively close proximity along the south and western slopes of the main mountain of Namba. So far, it has not been found in the escarpment zone or in other surveyed mountains in the highlands, suggesting that it may be endemic to Namba. The species appears to be locally common and its rupicolous habitat is probably not threatened, but until more research is conducted, we suggest it to be listed as Data Deficient (DD) as per IUCN Red List categories (IUCN 2022).

Etymology. The specific epithet *nambensis* (Pt.) is a reference to the Namba mountains. This is the largest and more preserved relic of Afromontane forest and montane grasslands in Angola. However, it lacks official protection. We suggest "Namba pygmy toad" and "sapo pigmeu da Namba" as English and Portuguese common names respectively.

Discussion

Amphibians are the least studied tetrapods in Angola (Marques et al. 2018; Baptista et al. 2019). During the last decade, only six new amphibian species were described from the country (Conradie et al. 2012, 2013; Ceríaco et al. 2018; 2021; Nielsen et al. 2020; Baptista et al. 2021), strikingly contrasting with reptiles, with a total of 37 new species descriptions (31 lizards and six snakes) during the same period (see Conradie et al. 2022a; Bates et al. 2023; Marques et al. 2023a, b). Thus, it can be assumed that Angola's amphibian diversity is far from completely assessed. Based on an integrative approach, including genetic, morphological, and osteological data, we herein reported on three new lineages of *Poyntonophrynus* (A–C), of which two were described as new species [*P. fernandae* **sp. nov.** (lineage B), and *P. nambensis* **sp. nov.** (lineage C)], all closely related to *P. pachnodes*. Both newly described species are endemic to Angola. Whereas the 'typical' populations are geographically isolated from each other, *P. nambensis* **sp. nov.** occurs in syntopy with *P.* cf. *fernandae* (lineage A). With the new descriptions, the number of *Poyntonophrynus* species occurring in Angola increased from four to six, and from six to eight in south-western Africa, underlining the region's importance as the genus' diversity cradle (Ceríaco et al. 2018).

Both new species showed consistent molecular divergence, with each species represented by distinct lineages, with no detected gene flow between them. Moreover, they are all morphologically distinguishable, which is remarkable in a genus characterized by such a conserved external morphology (e.g., Poynton and Broadley 1988; du Preez and Carruthers 2017; Rödel and Channing 2019; Tracy 2021). Due to their conserved morphology, it is very possible that the interspecific diversity of *Poyntonophrynus* has been underestimated, and further cryptic species propably exist. This particularly applies to populations in non-connected areas. Isolated populations, adapted to different ecotypes, may differ by lower 16S pairwise distances than reported for the genus as a whole i.e., as demonstrated in the pair *P. grindleyi* and *P. fenoulheti*, with average pairwise distances in the 16S of 3.4–3.8% (Rödel et al. 2023). *Poyntonophrynus pachnodes* is genetically more similar to *P. fernandae* sensu lato (distances ranging between 2–3.5%) than to *P. nambensis* **sp. nov.** (8.6%).

Lower pairwise distances (around 3%) for the 16S gene have been reported in several Malagasy (Vences et al. 2005; Vieites et al. 2009) and African anurans, including such distinct genera as the montane bufonid *Capensibufo*, a genus of miniaturized South African toads (Channing et al. 2017), African puddle frogs of the genus *Phrynobatrachus* (Rödel et al. 2015; Gvoždík et al. 2020), or the species rich African reed frogs genus *Hyperolius* (Bell 2016; Channing 2022). The limitations of using solely 16S distances for species delimitation have been largely discussed (e.g., Chan et al. 2022), and choosing artificial thresholds can result in under or over-estimation of diversity (Vences et al. 2022). This highlights the importance of using integrative and comprehensive taxonomical approaches. Although the genetic distances of the new Angolan populations were at the lower margin of what most authors use to test for specific differences, the integrated interpretation of all data sources (morphology, osteology, distribution, habitat requirements and genetics), supports the status of the two toad species described herein. In order to avoid taxonomic inflation and to apply a conservative approach, we herein refrain from describing lineage A as a species – at least until further data are available.

Poyntonophrynus are known to be generally associated with arid and semi-arid environments (du Preez and Carruthers 2017; Tracy 2021). Contrasting to this, recently a novel toad species has been described as an inhabitant of montane grasslands (Rödel et al. 2023), ecologically similar to *P. nambensis* **sp. nov.** We herein described a new species occurring in moist forest habitats i.e., *P. fernandae* **sp. nov.**, demonstrating that the genus is ecologically even more variable than previously thought.

The complex distributional patterns exhibited in a relatively constricted area found within Angolan *Poyntonophrynus*, with endemic species in the escarpment (*P. fernandae* **sp. nov.**), the central highlands (Namba) (*P. nambensis* **sp. nov.**), the inselberg of Serra da Neve (*P. pachnodes*), and the arid coastal plains of the Namib Desert (*P. dombensis* and *P. grandisonae*), is strikingly similar to that of other rupicolous vertebrates. Two non-related lizard genera i.e., the *Cordylus* girdled lizards and *Afroedura* geckos, comprise endemic species in these same regions (Stanley et al. 2016; Marques et al. 2019; Branch et al. 2021; Conradie et al. 2022b; Bates et al. 2023), with more ancient lineages in the highlands, and evolutionary younger lineages in other areas including Serra da Neve and the Namib Desert. The latter is another important center of endemism in Angola (Herrmann and Branch 2013; Branch et al. 2019). A linkage between the Namba mountains and the western escarpment has been proposed to interpret the speciation patterns of *Afroedura*, where the Namba endemic (*A. bogerti*) has a sister species in the escarpment (*A. pundomontana*, see Conradie et al. 2022b), and additional species present in the highlands (*A. wulfhaackei*), arid coastal plain (*A. donveae*, *A. vazpintorum*), and a strict endemic at Serra da Neve (*A. praedicta*) (Branch et al. 2021). The *Poyntonophrynus* pigmy toads and the aforementioned lizards are assumed to have low dispersal capabilities. Like many other rupicolous taxa, their ranges are highly disjunct, being completely dependent on the availability of suitable substrates (Jacobsen et al. 2014). On these they may easily become trapped in isolated remnants of suitable habitat, and consequently speciate on "rock islands" or inselbergs (Jacobsen et al. 2014; Branch et al. 2017), which may explain the detected patterns of endemism.

Poyntonophrynus fernandae **sp. nov.** sensu stricto and *P.* cf. *fernandae*, showed low pairwise distances in the mitochondrial marker 16S (2 %), but no haplotypes were shared for the RAG1 nuclear marker. Both lineages were found in association with rock boulders. *Poyntonophrynus fernandae* **sp. nov.** sensu stricto was found at lower elevation (520–1303 m a.s.l.), and mostly near moister forests in or near the escarpment, while *P.* cf. *fernandae* was found in montane grassland at higher elevations (1730 m a.s.l.). The syntopic toads from the central highlands, *P.* cf. *fernandae* and *P. nambensis* **sp. nov.**, were both collected at relatively high altitude i.e., above 1,600 m a.s.l., exclusively in the ancient mountain chain of Namba, in what is generally called the Angolan ancient massif or ancient plateau (Huntley 2019). These two toad lineages differed from each other by 8.1 % 16S pairwise distances, and shared no haplotypes.

Poyntonophrynus are often sympatric with congeners (Tracy 2021), but it is not known if and how they interact in the same ecosystem. Related co-occurring species often develop character displacement in order to reduce competition (Brown and Wilson 1956), and this is thought to be the case for *Poyntonophrynus* (Tracy 2021). Interestingly, *P. nambensis* **sp. nov.** and *P.* cf. *fernandae* were found in syntopy, with females breeding in the same rock pool. Females of both species were similar in size, but had a strikingly different ventral coloration (nearly immaculate vs. dark thick speckles, respectively), among other morphological differences. Moreover, dorsal coloration of breeding males of *P. nambensis* **sp. nov.** and of *P.* cf. *fernandae* also differed, with the first being dully-colored and found breeding at night, and the latter exhibited yellowish coloration and were found active during the day. This apparent case of different temporal breeding niches possibly allows for reproductive isolation. Color changes during breeding have been suggested to function as a sex-recognition clue to prevent mismatching attempts (e.g., Sztatecsny et al. 2010, 2012). Bright yellow coloration in breeding males is reported for many anuran species (Bell and Zamudio 2012; Bell et al. 2017; Portik et al. 2019), including other African bufonids such as *Sclerophrys kisoloensis*, *S. lemairii* or *Altiphrynoides osgoodi* (e.g., Bittencourt-Silva 2014; Rödel and Channing 2019). The relationship between visual signs (bright breeding coloration) and the occurrence or not of acoustic communication (due to ear loss) in *P.* cf. *fernandae* when comparing to *P. nambensis* **sp. nov.**, for breeding, deserves further research.

Several taxonomic questions are associated with *Poyntonophrynus*. At the species level, species distinction is problematic, and the validity of some species has been questioned e.g., *P. dombensis* vs. *P. damaranus* (see Poynton and Broadley 1988). At the generic level, the distinction between *Poyntonophrynus* and *Mertenso-*

phryne is not resolved. This confusion has genetic and osteological components. The genus, as currently understood, is non-monophyletic, with some of its species being genetically assignable to *Mertensophryne* (Liedtke et al. 2017; Ceríaco et al. 2018; Tracy 2021). From an osteological point of view, synapomorphies for the genus are also not convincingly defined yet. *Mertensophryne* is usually characterized by having a reduction of presacral vertebrae (Tihen 1960; Grandison 1978), a lack of tympanic middle ear (Tandy and Keith 1972) and phalangeal reduction. The latter feature is, however, poorly documented: Loveridge (1925) noted the reduction of the first and fourth finger, and first and fifth toes in *M. micranotis*, not specifying if phalanges were lacking; while Tandy and Keith (1972) mentioned "digits reduction" without further details and Grandison (1981) also only broadly referred to phalangeal reduction.

The two newly described species and *P.* cf. *fernandae* fit the general *Poyntonophrynus* osteology i.e., in having the shaft of the squamosal reduced or lost, and an elongate quadratojugal that attains the articulation between the maxilla and the pterygoid at its anterior extent. They also lack reduced presacral vertebrae (Poynton 1991; Graybeal and Cannatella 1995; Ceríaco et al. 2018). However, *P. fernandae* **sp. nov.** sensu lato lacks a columella, similar to *P. pachnodes*. Prior to the description of *P. pachnodes*, the absence of the tympanic middle ear was only associated with *Mertensophryne* (Ceríaco et al. 2018). Finding this character in two further species supports the conclusion that being earless is not a diagnostic feature to distinguish *Poyntonophrynus* from *Mertensophryne*, and that it varies interspecifically in *Poyntonophrynus* (Tracy 2021). One of the CT-scanned specimens of *P. dombensis* had a reduced presacral vertebrae number (seven instead of eight in one specimen), a feature that has been reported for *Mertensophryne*, but not for *Poyntonophrynus*. The potential phalangeal reduction on finger I could be in the same situation, but it is not clear from the CT scans. Osteological features that separate the two genera need further definition. We only CT-scanned two or three specimens per lineage. This is a quite small sample, and given the variability in osteological features, more specimens should be CT-scanned in the future, to allow more robust conclusions.

External morphological synapomorphies of *Poyntonophrynus* might be the lack of a tarsal fold, usually double subarticular tubercles, a distinct tympanum, and mostly indistinct parotoid glands (Poynton 1964; du Preez and Carruthers 2009; Tracy 2021). While we confirmed the first two characters in the three new lineages, the remaining two characters (tympanum and parotoid glands) varied, showing that these features should not be used as diagnostic for the genus. Due to morphological similarity between many species, some species of *Poyntonophrynus* can only be distinguished based on advertisement calls or geographic distributions (Tracy 2021). This highlights even more the morphological differences allowing the distinction of the three new Angolan lineages.

The description of two new species endemic from the western escarpment and the central highlands provides further support to recognize these regions as centers of endemism, as predicted by Clark et al. (2011) and Becker et al. (in press.). Due to their uniqueness and biogeographic relevance, these regions should become top priorities for research and conservation in Angola (Russo et al. 2019), and the entire African continent. Recommendations for the formal protection of these areas exist for almost half a century (Huntley 1974, 2017, 2023; Huntley and Matos 1994; Huntley et al. 2019), and the Angolan Government has recently commissioned studies to promulgate new protected areas designed to conserve patches of escarpment and Afromontane forests, namely at Kumbira and Mt. Moco (Russo et al. 2022). However, no *Poyntonophrynus* populations have so far been found within the limits of the proposed protected areas. Conversely, Serra da Namba, where we have recovered both new species, was not included in those efforts and remains unprotected, in spite of harboring the most extensive Afromontane forest habitats in the country (Mills et al. 2013) and renowned to contain additional strict endemic fauna (e.g., Branch et al. 2021). Our work further highlights the importance to conserve the remnant patches of escarpment forests and, in particular, the rich mosaic of habitats at Serra da Namba.

The uniqueness and importance of this region is even more evident when Angolan highlands are put in an African context (Vaz da Silva 2015; Huntley 2023). These are a part of the "Afromontane archipelago" (Powell et al. 2023), a very important speciation center. The existence of an amphibian fauna characteristic of these highlands i.e., an "Afrotemperate" fauna, has been discussed (Poynton 2000, 2013) and the occurrence of several species of grass frogs of the genus *Ptychadena* endemic to specific altitude ranges in the Ethiopian highlands support such a status (Freilich et al. 2014). The description of endemic species of dwarf toads in the Angolan highlands corroborates this for Angola, and is likely the first of many more findings to come.

Acknowledgements

We dedicate this work to the late William R. Branch, who was part of this project since the very first odd-looking toad collected in Congulo forest, and immediately suspected that we were dealing with undescribed diversity. We thank the Angolan Ministry of Environment Institute of Biodiversity (MINAMB) issuing export permits (002/INBC.MCTA/2021) for biodiversity surveys that resulted in the discovery of the new species, and in particular the Director of Instituto Nacional da Biodiversidade e Conservação (INBC), Dr. Albertina Nzuzi. Specimens were collected under permits no. 002/2015 issued by Instituto Superior de Ciências de Educação da Huíla (ISCED-Huíla). We thank Fernanda Lages from ISCED-Huíla, and Edna Azevedo and Vladimir Russo from Fundação Kissama for logistical and administrative support. We thank Luke Verburgt for having kindly contributed with critical specimens, samples, and photographs used in this study. We thank Werner Conradie for revising a preliminary version of the manuscript, and for providing sequences of *P. vertebralis* (WC-3458, WC-3460, WC-3459, WC-DNA-181). We thank Alan Channing for providing measurements and photographs of specimens of *P. jordani*, including of the holotype. We are indebted to Mr. Chiquinho and Mr. Albino, owners of two farms

at Namba and to the religious mission of Namba, for having hosted the members of the research team during various survey efforts at Namba. Funding for fieldwork in Angola and genetic analysis was provided by the National Research Foundation of South Africa (to William R. Branch). We thank NRF-SAIAB Aquatic Genomics Research Platform for the use of infrastructure and equipment, and the funding channeled through the NRF-SAIAB Institutional Support System. From ZMB we thank Frank Tillack, Felix Maier and Karla Neira-Salamea for assistance; Kristin Mahlow and Lisa Janzen for helping with CT scanning; and Marvin Schäfer for the identification of the stomach content of one pigmy toad specimen. We thank Jeffrey W. Streicher and Gabriela Bittencourt-Silva for allowing access to type material from the BMNH, and the latter for inputs on the osteological characterization. Guillaume Demare and Francisco Acosta are thanked for support with programming language and plotting in R. We thank Nguyen Thi Ngan Thanh for providing a photograph of Angolan pygmy toads and allowing its use. We thank Centro de Testagem Molecular (CTM) staff, especially Susana Lopes, Patrícia Ribeiro and Sofia Mourão for their support on genetic analysis. NLB and JLR were supported by Fundação para a Ciência e Tecnologia (FCT) contracts SFRH/PD/BD/140810/2018 and SFRH/PD/BD/140808/2018, and BIOPOLIS 2022-19 and BIOPOLIS 2022-18, respectively. Work co-funded by the project NORTE-01-0246-FEDER-000063, supported by Norte Portugal Regional Operational Programme (NORTE2020), under the PORTUGAL 2020 Partnership Agreement, through the European Regional Development Fund (ERDF), and by National Funds through FCT-Fundação para a Ciência e a Tecnologia in the scope of the project UIDP/50027/2020. Two reviewers, Jörn Köhler and Alexander Kupfer, improved the manuscript with their suggestions. All support is greatfully acknowledged.

References

American Veterinary Medical Association (2020) AVMA Guidelines for the euthanasia of animals: 2020 Edition. https://www.avma.org/sites/default/files/2020-02/Guidelines-on-Euthanasia-2020.pdf

Bandelt H-J, Forster P, Rohl A (1999) Median-joining networks for inferring intraspecific phylogenies. Molecular Biology and Evolution 16: 37–48. https://doi.org/10.1093/oxfordjournals.molbev.a026036

Baptista N, Conradie W, Vaz Pinto P, Branch WR (2019) The amphibians of Angola: Early studies and the current state of knowledge. In: Huntley BJ, Russo V, Lages F, Ferrand N (Eds) Biodiversity of Angola. Science & Conservation: A Modern Synthesis. Springer, Cham, 243–281. https://doi.org/10.1007/978-3-030-03083-4_12

Baptista NL, Vaz Pinto P, Keates C, Edwards S, Rödel M-O, Conradie W (2021) A new species of red toad, *Schismaderma* Smith, 1849 (Anura: Bufonidae), from central Angola. Zootaxa 5081: 301–332. https://doi.org/10.11646/zootaxa.5081.3.1

Bates MF, Lobón-Rovira J, Stanley EL, Branch WR, Vaz Pinto P (2023) A new species of green-eyed *Cordylus* Laurenti, 1768 from the west-central highlands of Angola, and the rediscovery of *Cordylus angolensis* (Bocage, 1895) (Squamata: Cordylidae). Vertebrate Zoology 73: 599–646. https://doi.org/10.3897/vz.73.e95639

Becker FS, Baptista NL, Vaz Pinto P, Ernst R, Conradie W (in press.) The amphibians of the highlands and escarpments of Angola and Namibia. In: Mendelsohn JM, Huntley BJ, Vaz Pinto P (Eds) Monograph on Endemism in the Highlands and Escarpments of Angola and Namibia. Namibian Journal of Environment.

Bell RC (2016) A new species of *Hyperolius* (Amphibia: Hyperoliidae) from Príncipe Island, Democratic Republic of São Tomé and Príncipe. Herpetologica 72: 343–351. https://doi.org/10.1655/Herpetologica-D-16-00008.1

Bell RC, Webster GN, Whiting MJ (2017) Breeding biology and the evolution of dynamic sexual dichromatism in frogs. Journal of Evolutionary Biology 30: 2104–2115. https://doi.org/10.1111/jeb.13170

Bell RC, Zamudio KR (2012) Sexual dichromatism in frogs: Natural selection, sexual selection and unexpected diversity. Proceedings of the Royal Society B 279: 4687–4693. https://doi.org/10.1098/rspb.2012.1609

Bittencourt-Silva G (2014) Notes on the reproductive behaviour of *Amietophrynus lemairii* (Boulenger, 1901) (Anura: Bufonidae). Herpetology Notes 7: 611–614.

Bocage JVB (1895) Sur une espèce de crapaud à ajouter à faune herpétologique d'Angola. Jornal de Sciências, Mathemáticas, Physicas e Naturaes Série 2: 51–53.

Branch WR, Baptista N, Vaz Pinto P, Conradie W (2019) The reptiles of Angola – history, diversity, endemism and hotspots. In: Huntley BJ, Ferrand N (Eds) Biodiversity of Angola. Science & Conservation: A Modern Synthesis. Springer, Cham, 283–326. https://doi.org/10.1007/978-3-030-03083-4_13

Branch WR, Haacke W, Vaz Pinto P, Conradie W, Verburgt L, Baptista N, Veríssimo L (2017) Loveridge's Angolan geckos, *Afroedura karroica bogerti* and *Pachydactylus scutatus angolensis* (Sauria, Gekkonidae): New distribution records, comments on type localities and taxonomic status. Zoosystematics and Evolution 93: 157–166. https://doi.org/10.3897/zse.93.10915

Branch WR, Schmitz A, Lobón-Rovira J, Baptista NL, António T, Conradie W (2021) Rock island melody: A revision of the *Afroedura bogerti* Loveridge, 1944 group, with descriptions of four new endemic species from Angola. Zoosystematics and Evolution 97: 55–82. https://doi.org/10.3897/zse.97.57202

Brown WLJ, Wilson EO (1956) Character displacement. Systematic Zoology 5: 49–64. https://doi.org/10.2307/2411924

Bruford MW, Hanotte M, Brookfield JFY, Burke T (1992) Single locus and multilocus DNA fingerprint. In: Hoelzel AR (Ed) Molecular Genetic Analysis of Populations: A Practical Approach. IRL Press, Oxford, 225–270.

Burgess N, D'Amico, Hales J, Underwood E, Dinerstein E, Olson D, Itoua I, Schipper J, Ricketts T, Newman K (2004) Terrestrial Ecoregions of Africa and Madagascar: A Conservation Assessment. Island Press, Washington, D.C., 524 pp.

Cáceres A, Melo M, Barlow J, De Lima RF, Mills MS (2017) Drivers of bird diversity in an understudied African centre of endemism: The Angolan central escarpment forest. Bird Conservation International 27: 256–268. https://doi.org/10.1017/S0959270917000119

Ceríaco LM, Santos BS, Marques MP, Bauer AM, Tiutenko A (2021) Citizen Science meets specimens in old formalin filled jars: A new species of banded rubber frog, genus *Phrynomantis* (Anura: Phrynomeridae) from Angola. Alytes 38: 18–48.

Ceríaco LMP, Marques MP, Bandeira S, Agarwal I, Stanley EL, Bauer AM, Heinicke MP, Blackburn DC (2018) A new earless species of *Poyntonophrynus* (Anura, Bufonidae) from the Serra da Neve inselberg, Namibe Province, Angola. ZooKeys 780: 109–136. https://doi.org/10.3897/zookeys.780.25859

Chan KO, Hertwig ST, Neokleous DN, Flury JM, Brown RM (2022) Widely used, short 16S rRNA mitochondrial gene fragments yield poor and erratic results in phylogenetic estimation and species delimitation of amphibians. BMC Ecology and Evolution 22: 1–9. https://doi.org/10.1186/s12862-022-01994-y

Channing A (2022) Color patterns to sequences: A perspective on the systematics of the *Hyperolius viridiflavus* group (Anura: Hyperoliidae) using mitochondrial DNA. Zootaxa 5134: 301–354. https://doi.org/10.11646/zootaxa.5134.3.1

Channing A, Measey GJ, De Villiers AL, Turner AA, Tolley KA (2017) Taxonomy of the *Capensibufo rosei* group (Anura: Bufonidae) from South Africa. Zootaxa 4232: 282–292. https://doi.org/10.11646/zootaxa.4232.2.11

Channing A, Rödel M-O (2019) Field Guide to the Frogs and Other Amphibians of Africa. Struik Nature, Cape Town, 408 pp.

Chernomor O, Von Haeseler A, Minh BQ (2016) Terrace aware data structure for phylogenomic inference from supermatrices. Systematic Biology 65: 997–1008. https://doi.org/10.1093/sysbio/syw037

Clark VR, Barker NP, Mucina L (2011) The Great Escarpment of southern Africa: A new frontier for biodiversity exploration. Biodiversity Conservation 20: 2543–2561. https://doi.org/10.1007/s10531-011-0103-3

Conradie W, Branch WR, Measey GJ, Tolley KA (2012) A new species of *Hyperolius* Rapp, 1842 (Anura: Hyperoliidae) from the Serra da Chela mountains, south-western Angola. Zootaxa 3269: 1–17. https://doi.org/10.11646/zootaxa.3269.1.1

Conradie W, Branch WR, Tolley KA (2013) Fifty shades of grey: Giving color to the poorly known Angolan ashy reed frog (Hyperoliidae: *Hyperolius cinereus*), with the description of a new species. Zootaxa 3635: 201–223. https://doi.org/10.11646/zootaxa.3635.3.1

Conradie W, Keates C, Verburgt L, Baptista NL, Harvey J, Júlio T, Neef G (2022a) Contributions to the herpetofauna of the Angolan Okavango-Cuando-Zambezi river drainages. Part 2: Lizards (Sauria), chelonians and crocodiles. Amphibian & Reptile Conservation 16 [General Section]: 181–214 (e322).

Conradie W, Schmitz A, Lobón-Rovira J, Becker FS, Vaz Pinto P, Hauptfleisch ML (2022b) Rock island melody remastered: Two new species in the *Afroedura bogerti* Loveridge, 1944 group from Angola and Namibia. Zoosystematics and Evolution 98: 435–453. https://doi.org/10.3897/zse.98.86299

de Queiroz K (1998) The general lineage concept of species, species criteria, and the process of speciation: A conceptual unification and terminological recommendations. In: Howard DJ, Berlocher SH (Eds) Endless Forms: Species and Speciation. Oxford University Press, Oxford, 57–75.

de Vienne DM, Giraud T, Martin OC (2007) A congruence index for testing topological similarity between trees. Bioinformatics 23: 3119–3124. https://doi.org/10.1093/bioinformatics/btm500

Deforel F, Duport-Bru AS, Rosset SD, Baldo D, Candioti FV (2021) Osteological atlas of *Melanophryniscus* (Anura, Bufonidae): A synthesis after 150 years of skeletal studies in the genus. Herpetological Monographs 35: 1–27. https://doi.org/10.1655/HERPMONOGRAPHS-D-20-00002

du Preez L, Carruthers V (2009) A Complete Guide to the Frogs of Southern Africa. Struik Nature, Cape Town, 488 pp.

du Preez L, Carruthers V (2017) Frogs of Southern Africa, a Complete Guide. Struik Nature, Cape Town, 519 pp.

Fabrezi M (2001) A survey of prepollex and prehallux variation in anuran limbs. Zoological Journal of the Linnean Society 131: 227–248. https://doi.org/10.1111/j.1096-3642.2001.tb01316.x

Freilich X, Tollis M, Boissinot S (2014) Hiding in the highlands: Evolution of a frog species complex of the genus *Ptychadena* in the Ethiopian highlands. Molecular Phylogenetics and Evolution 71: 157–169. https://doi.org/10.1016/j.ympev.2013.11.015

Frost DR (2023) Amphibian Species of the World: An Online Reference. Version 6.1 (September 22nd, 2023). Electronic Database accessible at https://amphibiansoftheworld.amnh.org/index.php. American Museum of Natural History, New York, USA. https://doi.org/10.5531/db.vz.0001

Grandison AGC (1978) The occurrence of *Nectophrynoides* (Anura: Bufonidae) in Ethiopia. A new concept of the genus with a description of a new species. Monitore Zoologico Italiano (Supplement) 11: 119–172. https://doi.org/10.1080/03749444.1978.10736579

Grandison AGC (1981) Morphology and phylogenetic position of the West African *Didynamipus sjoestedsti* Andersson, 1903 (Anura: Bufonidae). Monitore Zoologico Italiano (supplement) 15: 187–215. https://doi.org/10.1080/03749444.1981.10736635

Graybeal A, Cannatella DC (1995) A new taxon of Bufonidae from Peru, with descriptions of two new species and a review of the phylogenetic status of supraspecific bufonid taxa. Herpetologica 51: 105–131.

Gvoždík V, Nečas T, Dolinay M, Zimkus BM, Schmitz A, Fokam EB (2020) Evolutionary history of the Cameroon radiation of puddle frogs (Phrynobatrachidae: *Phrynobatrachus*), with descriptions of two critically endangered new species from the northern Cameroon Volcanic Line. PeerJ 8: e8393. https://doi.org/10.7717/peerj.8393

Hall BP (1960) The faunistic importance of the scarp of Angola. Ibis 102: 420–442. https://doi.org/10.1111/j.1474-919X.1960.tb08418.x

Hall TA (1999) BioEdit: A user-friendly biological sequence alignment editor and analysis program for Windows 95/98/NT. Nucleic Acids Symposium Series 41: 95–98.

Hayek LAC, Heyer WR, Gascon C (2001) Frog morphometrics: A cautionary tale. Alytes 18: 153–177.

Herrmann HW, Branch WR (2013) Fifty years of herpetological research in the Namib Desert and Namibia with an updated and annotated species checklist. Journal of Arid Environments 93: 94–115. https://doi.org/10.1016/j.jaridenv.2012.05.003

Hewitt J (1932) Some new species and subspecies of South African batrachians and lizards. Annals of the Natal Museum 7: 105–128.

Hoang DT, Chernomor O, Von Haeseler A, Minh BQ, Vinh LS (2018) UFBoot2: Improving the ultrafast bootstrap approximation. Molecular Biology and Evolution 35: 518–522. https://doi.org/10.1093/molbev/msx281

Huntley BJ (1974) Outlines of wildlife conservation in Angola. Journal of the Southern African Wildlife Management Association 4: 157–166.

Huntley BJ (2017) Wildlife at war in Angola: The rise and fall of an African Eden. Protea Book House, Pretoria, 432 pp.

Huntley BJ (2019) Angola in outline: Physiography, climate and patterns of biodiversity. In: Huntley BJ, Russo V, Lages F, Ferrand N (Eds) Biodiversity of Angola. Science & Conservation: A Modern Synthesis. Springer, Cham, 15–42. https://doi.org/10.1007/978-3-030-03083-4_2

Huntley (2023) Ecology of Angola. Terrestrial Biomes and Ecoregions. Springer, Cham, 460 pp. https://doi.org/10.1007/978-3-031-18923-4

Huntley BJ, Beja P, Vaz Pinto P, Russo V, Veríssimo L, Morais M (2019) Biodiversity conservation: History, protected areas and hotspots. In: Huntley BJ, Russo V, Lages F, Ferrand N (Eds) Biodiversity of Angola. Science & Conservation: A Modern Synthesis. Springer, Cham, 495–512. https://doi.org/10.1007/978-3-030-03083-4_18

Huntley BJ, Matos EM (1994) Botanical diversity and its conservation in Angola. Strelitzia 1: 53–74.

IUCN Standards and Petitions Committee (2022) Guidelines for Using the IUCN Red List Categories and Criteria. Version 15.1. (Septem-

ber 22nd, 2023) Prepared by the Standards and Petitions Committee. Downloadable from https://www.iucnredlist.org/documents/RedListGuidelines.pdf

Jacobsen NHG, Kuhn AL, Jackman TR, Bauer AM (2014) A phylogenetic analysis of the southern African gecko genus *Afroedura* Loveridge (Squamata: Gekkonidae), with the description of nine new species from Limpopo and Mpumalanga provinces of South Africa. Zootaxa 3846: 451–501. https://doi.org/10.11646/zootaxa.3846.4.1

Kalyaanamoorthy S, Minh BQ, Wong TKF, von Haeseler A, Jermiin LS (2017) ModelFinder: Fast model selection for accurate phylogenetic estimates. Nature Methods 14: 587–589. https://doi.org/10.1038/nmeth.4285

Kocher TD, Thomas WK, Meyer A, Edwards SV, Pääbo S, Villablanca FX, Wilson AC (1989) Dynamics of mitochondrial DNA evolution in animals: Amplification and sequencing with conserved primers. Proceedings of the National Academy of Sciences of the United States of America 86: 6196–6200. https://doi.org/10.1073/pnas.86.16.6196

Kumar S, Stecher G, Li M, Knyaz C, Tamura K (2018) MEGA X: Molecular Evolutionary Genetics Analysis across computing platforms. Molecular Biology and Evolution 35: 1547–1549. https://doi.org/10.1093/molbev/msy096

Kumar S, Stecher G, Tamura K (2016) MEGA7: Molecular Evolutionary Genetics Analysis version 7.0 for bigger datasets. Molecular Biology and Evolution 33: 1870–1874. https://doi.org/10.1093/molbev/msw054

Leigh JW, Bryant D (2015) POPART: A full-feature software for haplotype network construction. Methods in Ecology and Evolution 6: 1110–1116. https://doi.org/10.1111/2041-210X.12410

Liedtke HC, Muller H, Hafner J, Penner J, Gower DJ, Mazuch T, Rödel MO, Loader SP (2017) Terrestrial reproduction as an adaptation to steep terrain in African toads. Proceedings of the Royal Society B 284: 20162598. http://doi.org/10.1098/rspb.2016.2598

Linder HP, de Klerk HM, Born J, Burgess ND, Fjeldså J, Rahbek C (2012) The partitioning of Africa: Statistically defined biogeographical regions in sub-Saharan Africa. Journal of Biogeography 39: 1189–1925. https://doi.org/10.1111/j.1365-2699.2012.02728.x

Loveridge A (1925) Notes on East African batrachians, collected 1920–1923, with the description of four new species. Proceedings of the Zoological Society of London 95: 763–791. https://doi.org/10.1111/j.1096-3642.1925.tb01534.x

Marques MP, Ceríaco LMP, Blackburn DC, Bauer AM (2018) Diversity and distribution of the amphibians and terrestrial reptiles of Angola – Atlas of historical and bibliographic records (1840–2017). Proceedings of the California Academy of Sciences, Series 4, 65: 1–501.

Marques MP, Ceríaco LMP, Stanley EL, Bandeira S, Agarwal I, Bauer AM (2019) A new species of girdled lizard (Squamata: Cordylidae) from Serra da Neve inselberg, Namibe province, southwestern Angola. Zootaxa 4668: 503–524. https://doi.org/10.11646/zootaxa.4668.4.4

Marques MP, Parrinha D, Ceríaco LM, Brennan IG, Heinicke MP, Bauer AM (2023a) A new species of thick-toed gecko (*Pachydactylus*) from Serra da Neve and surrounding rocky areas of southwestern Angola (Squamata: Gekkonidae). Vertebrate Zoology 73: 325–343. https://doi.org/10.3897/vz.73.e101329

Marques MP, Parrinha D, Tiutenko A, Lopes-Lima M, Bauer AM, Ceríaco LM (2023b) A new species of African legless skink, genus *Acontias* Cuvier, 1816 "1817" (Squamata: Scincidae) from Serra da Neve inselberg, south-western Angola. African Journal of Herpetology. https://doi.org/10.1080/21564574.2023.2246487

Miller MA, Pfeiffer W, Schwartz T (2010) Creating the CIPRES science gateway for inference of large phylogenetic trees. Gateway Computing Environments Workshop 2010: 1–8. https://doi.org/10.1109/GCE.2010.5676129

Mills MS, Melo M, Vaz A (2013) The Namba mountains: New hope for Afromontane forest birds in Angola. Bird Conservation International 23: 159–167. https://doi.org/10.1017/S095927091200024X

Minh BQ, Lanfear R, Trifinopoulos J, Schrempf D, Schmidt HA (2021) IQ-TREE version 2.1.2: Tutorials and manual phylogenomic software by maximum likelihood. http://www.iqtree.org/doc/iqtree-doc.pdf

Nielsen SV, Conradie W, Ceríaco LM, Bauer AM, Heinicke MP, Stanley EL, Blackburn DC (2020) A new species of Rain Frog (Brevicipitidae, *Breviceps*) endemic to Angola. ZooKeys 979: 133–160. https://doi.org/10.3897/zookeys.979.56863

Nguyen LT, Schmidt HA, von Haeseler A, Minh BQ (2015) IQ-TREE: A fast and effective stochastic algorithm for estimating maximum-likelihood phylogenies. Molecular Biology and Evolution 32: 268–274. https://doi.org/10.1093/molbev/msu300

Olson DM, Dinerstein E, Wikramanayake ED, Burgess ND, Powell GVN, Underwood EC, D'Amico JA, Itoua I, Strand HE, Morrison JC, Loucks CJ, Allnutt TF, Ricketts TH, Kura Y, Lamoreux JF, Wettengel WW, Hedao P, Kassem KR (2001) Terrestrial ecoregions of the World: a new map of life on Earth. BioScience 51: 933–938. https://doi.org/10.1641/0006-3568(2001)051[0933:TEOTWA]2.0.CO;2

Padial JM, Miralles A, De la Riva I, Vences M (2010) The integrative future of taxonomy. Frontiers in Zoology 7: 1–14. https://doi.org/10.1186/1742-9994-7-16

Páez-Moscoso DJ, Guayasamin JM (2012) Species limits in the Andean toad genus *Osornophryne* (Bufonidae). Molecular Phylogenetics and Evolution 65: 805–822. https://doi.org/10.1016/j.ympev.2012.08.001

Palumbi SR (1996) Nucleic acids II: The polymerase chain reaction. In: Hillis DM, Moritz C, Mable BK (Eds) Molecular Systematics. Sinauer Associates, Sunderland, MA, 205–247.

Peters JA (1964) Dictionary of Herpetology. Hafner Publishing Company, New York, NY, 392 pp.

Portik DM, Bell RC, Blackburn DC, Bauer AM, Barratt CD, Branch WR, Burger M, Channing A, Colston TJ, Conradie W, Dehling JM, Drewes RC, Ernst R, Greenbaum E, Gvoždík V, Harvey J, Hillers A, Hirschfeld M, Jongsma GFM, Kielgast J, Kouete MC, Lawson LP, Leaché AD, Loader SP, Lötters S, Van Der Meijden A, Menegon M, Müller S, Nagy ZT, Ofori-Boateng C, Ohler A, Papenfuss TJ, Rößler D, Sinsch U, Rödel M-O, Veith M, Vindum J, Zassi-Boulou A-G, McGuire JA (2019) Sexual dichromatism drives diversification within a major radiation of African Amphibians. Systematic Biology 68: 859–875. https://doi.org/10.1093/sysbio/syz023

Powell LL, Vaz Pinto P, Mills M, Baptista NL, Costa K, Dijkstra K-DB, Gomes AL, Guedes P, Júlio T, Monadjem A, Palmeirim AF, Russo V, Melo M (2023) The last Afromontane forests in Angola are threatened by fires. Nature Ecology & Evolution. https://doi.org/10.1038/s41559-023-02025-9

Poynton JC (1964) Amphibia of southern Africa: A faunal study. Annals of the Natal Museum 17: 1–334.

Poynton JC (1991) Amphibians of southeastern Tanzania, with special reference to *Stephopaedes* and *Mertensophryne* (Bufonidae). Bulletin of the Museum of Comparative Zoology 152: 451–473.

Poynton, JC (2000) Evidence for an Afrotemperate amphibian fauna. African Journal of Herpetology 49: 33–41. https://doi.org/10.1080/21564574.2000.9650014

Poynton JC (2013) Afrotemperate Amphibians in southern and eastern Africa: A critical review. African Journal of Herpetology 62: 5–20. https://doi.org/10.1080/21564574.2013.794866

Poynton JC, Broadley DG (1988) Amphibia Zambesiaca 4. Bufonidae. Annals of the Natal Museum 29: 447–490.

Poynton JC, Haacke WD (1993) On a collection of amphibians from Angola, including a new species of *Bufo* Laurenti. Annals of the Transvaal Museum 36: 9–16.

R Core Team (2021) R: A language and environment for statistical computing. R Foundation for Statistical Computing, Vienna. URL https://www.R-project.org

Rambaut A (2014) FigTree. Version 1.4.2. Institute of Evolutionary Biology, University of Edinburgh, Edinburgh. http://tree.bio.ed.ac.uk/software/figtree

Rambaut A, Drummond AJ (2009) Tracer. http://beast.bio.ed.ac.uk/Tracer

Rödel M-O, Becker FS, Buiswalelo B, Conradie W, Channing A (2023) Re-evaluation of the status of *Bufo vertebralis grindleyi* and *Bufo jordani* (Anura: Bufonidae). Salamandra 59: 143–157.

Rödel M-O, Burger M, Zassi-Boulou AG, Emmrich M, Penner J, Barej MF (2015) Two new *Phrynobatrachus* species (Amphibia: Anura: Phrynobatrachidae) from the Republic of the Congo. Zootaxa 4032: 55–80. https://doi.org/10.11646/zootaxa.4032.1.3

Ronquist F, Teslenko M, van der Mark P, Ayres DL, Darling A, Hohna S, Larget B, Liu L, Suchard MA, Huelsenback JP (2012) MrBayes 3.2: Efficient Bayesian phylogenetic inference and model choice across a large model space. Systematic Biology 61: 539–542. https://doi.org/10.1093/sysbio/sys029

RStudio Team (2022) RStudio: Integrated Development Environment for R. RStudio, PBC, Boston, MA URL http://www.rstudio.com

Russo V, Huntley BJ, Lages F, Ferrand N (2019) Conclusions: Biodiversity research and conservation opportunities. In: Huntley BJ, Russo V, Lages F, Ferrand N (Eds) Biodiversity of Angola. Science & Conservation: A Modern Synthesis. Springer, Cham, 543–549. https://doi.org/10.1007/978-3-030-03083-4_20

Russo V, Vaz Pinto P, Huongo A (2022) Angola protected area network assessment. US Department of Agriculture Forest Service. Unpublished report, 74 pp.

San Mauro D, Gower DJ, Oommen OV, Wilkinson M, Zardoya R (2004) Phylogeny of caecilian amphibians (Gymnophiona) based on complete mitochondrial genomes and nuclear RAG1. Molecular Phylogenetics and Evolution 33: 413–427. https://doi.org/10.1016/j.ympev.2004.05.014

Scherz MD (2020) Diamond frogs forever: A new species of *Rhombophryne* Boettger, 1880 (Microhylidae, Cophylinae) from Montagne d'Ambre National Park, northern Madagascar. Zoosystematics and Evolution 96: 313–323. https://doi.org/10.3897/zse.96.51372

Stanley E, Ceríaco LMP, Bandeira S, Valério H, Bates MF, Branch WR (2016) A review of *Cordylus machadoi* (Squamata: Cordylidae) in southwestern Angola, with the description of a new species from the pro-Namib desert. Zootaxa 4061: 201–226. https://doi.org/10.11646/zootaxa.4061.3.1

Sztatecsny M, Preininger D, Freudmann A, Loretto MC, Maier F, Hödl W (2012) Don't get the blues: Conspicuous nuptial coloration of male moor frogs (*Rana arvalis*) supports visual mate recognition during scramble competition in large breeding aggregations. Behavioral Ecology and Sociobiology 66: 1587–1593. https://doi.org/10.1007/s00265-012-1412-6

Sztatecsny M, Strondl C, Baierl A, Ries C, Hödl W (2010) Chin up: Are the bright throats of male common frogs a condition-independent visual cue? Animal Behaviour 79: 779–786. https://doi.org/10.1016/j.anbehav.2010.01.003

Tamura K, Stecher G, Peterson D, Filipski A, Kumar S (2013) MEGA6: Molecular Evolutionary Genetics Analysis version 6.0. Molecular Biology and Evolution 30: 2725–2729. https://doi.org/10.1093/molbev/mst197

Tandy M, Keith R (1972) *Bufo* of Africa. In: Blair WF (Ed.) Evolution in the genus *Bufo*. University of Texas Press, Austin, Texas and London, 119–170.

Thermo Fisher Scientific (2020) Thermo Fisher scientific reports fourth quarter and full year 2020 results.

Tihen JA (1960) Two new genera of African bufonids, with remarks on the phylogeny of related genera. Copeia 1960: 225–233. https://doi.org/10.2307/1439662

Tracy CB (2021) Phylogenetics and comparative morphology of African dwarf toads of the genus *Poyntonophrynus*. MSc Thesis, Villanova University, Villanova, PA.

Vaz da Silva BADN (2015) Evolutionary history of the birds of the Angolan highlands — The missing piece to understand the biogeography of the Afromontane forests. MSc Thesis, Universidade do Porto, Porto, Portugal.

Vences M, Multzsch M, Gippner S, Miralles A, Crottini A, Gehring PS, Rakotoarison A, Ratsoavina FM, Glaw F, Scherz MD (2022) Integrative revision of the *Lygodactylus madagascariensis* group reveals an unexpected diversity of little brown geckos in Madagascar's rainforest. Zootaxa 5179: 1–61. https://doi.org/10.11646/zootaxa.5179.1.1

Vences M, Thomas M, van der Meijden A, Chiari Y, Vieites DR (2005) Comparative performance of the 16S rRNA gene in DNA barcoding of amphibians. Frontiers in Zoology 2: 1–12. https://doi.org/10.1186/1742-9994-2-5

Vieites DR, Wollenberg KC, Andreone F, Köhler J, Glaw F, Vences M (2009) Vast underestimation of Madagascar's biodiversity evidenced by an integrative amphibian inventory. Proceedings of the National Academy of Sciences of the United States of America 106: 8267–8272. https://doi.org/10.1073/pnas.0810821106

Xia X (2013) DAMBE5: A comprehensive software package for data analysis in molecular biology and evolution. Molecular Biology and Evolution 30: 1720–1728. https://doi.org/10.1093/molbev/mst064

Zhang J, Kapli P, Pavlidis P, Stamatakis A (2013) A general species delimitation method with applications to phylogenetic placements. Bioinformatics 29: 2869–2876. https://doi.org/10.1093/bioinformatics/btt499

Supplementary Material 1

Figure S1

Authors: Baptista NL, Vaz Pinto P, Keates C, Lobón-Rovira J, Edwards S, Rödel M-O (2023)
Data type: .jpg
Explanation note: Principal component analysis of size-corrected morphometric features of the three new *Poyntonophrynus* lineages recorded in this study, and of the other species occurring in Angola (*P. pachnodes*, *P. dombensis*, *P. grandisonae*, and *P. kavangensis*).

Link: https://doi.org/10.3897/vz.73.e103935.suppl1

Supplementary Material 2

Figure S2

Authors: Baptista NL, Vaz Pinto P, Keates C, Lobón-Rovira J, Edwards S, Rödel M-O (2023)
Data type: .jpg
Explanation note: CT-scan of *Poyntonophrynus dombensis* (FKH-406, male). **A** Skeleton in dorsal view. **B** Lateral, dorsal and ventral views of skull (left to right). **C** Pectoral girdle in ventral view. **D** Ventral views of right hand and right foot (left to right).

Link: https://doi.org/10.3897/vz.73.e103935.suppl2

Supplementary Material 3

Figure S3

Authors: Baptista NL, Vaz Pinto P, Keates C, Lobón-Rovira J, Edwards S, Rödel M-O (2023)
Data type: .jpg
Explanation note: CT-scan of *Poyntonophrynus dombensis* (ZMB 91792, female). **A** Skeleton in dorsal view. **B** Lateral, dorsal and ventral views of skull (left to right). **C** Pectoral girdle in ventral view. **D** Ventral views of right hand and right foot (left to right). Blue indicates the parotic plate, orange indicates the columella. Note malformation in spine. Scale bars represent 5 mm.

Link: https://doi.org/10.3897/vz.73.e103935.suppl3

Supplementary Material 4

Tables S1–S4

Authors: Baptista NL, Vaz Pinto P, Keates C, Lobón-Rovira J, Edwards S, Rödel M-O (2023)
Data type: .docx
Explanation note: Table S1. Vouchers of *Poyntonophrynus* spp. examined for analysis of qualitative features, comparison with literature, definition of categories, and creation of comparative table. — **Table S2.** High Resolution X-ray Computed Tomography (HRCT) parameters used to scan *Poyntonophrynus* full body scans and skulls. — **Table S3.** Measurements (in mm) of specimens of *Poyntonophrynus dombensis*, *P. kavangensis*, and *P. pachnodes* taken for this study. For abbreviations see Methods section. M—male, F—female. — **Table S4.** PCA loadings of the first three principal components, based on 11 size-corrected measurements of adult *Poyntonophrynus*. For abbreviations of measurements see Methods section. Bold highlighted loadings show the measurements that loaded most highly for each principal component.

Link: https://doi.org/10.3897/vz.73.e103935.suppl4

Supplementary Material 5

File S1

Authors: Baptista NL, Vaz Pinto P, Keates C, Lobón-Rovira J, Edwards S, Rödel M-O (2023)
Data type: .docx
Explanation note: Osteological description of *Poyntonophrynus dombensis* (Bocage, 1895).

Link: https://doi.org/10.3897/vz.73.e103935.suppl5